ASYMMETRIC TOTAL SYNTHESIS OF THE PENTACYCLIC INDOLE ALKALOID (+)-TACAMONINE

Jasmin Ferreira

Submitted in partial fulfilment of the requirements for the degree of

Master of Science

in the Department of Chemistry

UNIVERSITY OF CAPE TOWN

February 2019

DECLARATION

Asymmetric Total Synthesis of the Pentacyclic Indole Alkaloid (+)-Tacamonine

I, Jasmin Ferreira, declare the following:

1. That the above-titled report is my own work, both in concept and execution, apart from the normal guidance of my supervisor;

2. That in cases where others' work has been cited, this has been acknowledged and referenced;

3. That no part of this work has been, is being, or is to be submitted for another degree at this or any other university;

4. That I grant the University of Cape Town free licence to reproduce this work, in whole or in part, for the purpose of research.

I hereby present this report in partial fulfillment of the requirements for the degree of Master of Science in the Department of Chemistry at the University of Cape Town.

Signed by candidate

February 2019

In loving memory of my grandmother

ACKNOWLEDGEMENTS

My sincerest thanks go out, first and foremost, to my incredible supervisor Professor Roger Hunter, for his endless enthusiasm, unwavering support, and encouragement. Thank you for inspiring me, for seeing the potential in me, and for carefully nurturing my talents over the years, ultimately molding me into the synthetic chemist that I am today. Most of all, thank you for your patience, for your kind, caring approach, and for instilling in me an unyielding passion for organic chemistry.

To the members of the Hunter group, thank you for making all the gruelling time spent in the lab enjoyable. In particular, to Dr. Myles Smith, thank you for your guidance and friendship over the years and for pushing me, sometimes even to an annoying degree, to attain the highest possible standard of research. Secondly, to Dr. Sophie Rees-Jones, thank you for always being willing to assist wherever necessary, from the running of the HPLC machine to searching for misplaced chemicals, your contribution to the efficiency of the Hunter group is invaluable.

In addition, I would like to express my gratitude to Dr. Gerhard Venter for his assistance in the computational analysis, to Dr. Hong Su for the X-ray crystallographic structure determination, and to Pete Roberts for the countless 2D NMR spectra. To the chemistry department as a whole, thank you for providing such a pleasant, community-like working environment.

Outside of chemistry, my eternal thanks go out to my parents for their love, and most importantly, for supporting my decision to leave home to pursue undergraduate study at UCT. Furthermore, I would like to acknowledge two particularly special individuals. To Court, your seemingly infinite well of positivity and optimism has guided me through some of my darkest times. Thank you for believing in me and for always managing to put a smile on my face regardless of the circumstances. Finally, to Chris, thank you for struggling through this with me and for reminding me that I was not alone even when it felt that way. The impact that your companionship, support and encouragement has had on my life simply cannot be overstated. I can only hope to be able to return the favour to you someday.

ABSTRACT

(+)-Tacamonine, a natural product isolated from the Central African plant *Tabernaemontana eglandulosa*, belongs to the relatively new *tacaman* class of pentacyclic monoterpenoid indole alkaloids. Its close structural similarity to the potent cerebral vasodilator (-)-vincamone has promoted several efforts towards its synthesis, culminating in the appearance of two asymmetric and seven racemic syntheses in the literature.

This dissertation details the successful execution of our strategy for the concise, highly-efficient, asymmetric total synthesis of (+)-tacamonine. Chapter 1 serves as an introduction to the *tacaman* class, including the proposed biosynthesis for members of this class, followed by a review of the reported synthetic approaches to tacamonine. Chapter 2 details the evolution of our approach based on the use of key radical cyclization methodology to ultimately accomplish a total synthesis of the target. An investigation of the diastereoselectivity displayed in the radical cyclization step is also described through computational methods.

Our route followed a novel ABC to ABCD to ABCDE ring-construction strategy, which first involved the synthesis of 3,4-dihydro-β-carboline as well as a chiral acid ester fragment that was acquired through Evans' auxiliary-controlled alkylation chemistry. The latter set the absolute configuration at C-20 bearing the ethyl group in the D-ring, and thereafter, the two fragments were coupled together before being advanced to the radical cyclization precursor. Radical cyclization then led to the formation of the desired *cis* D/E-ring junction in a diastereomeric ratio of 10:1, the major diastereomer displaying the required C-3/C-14 to C-20 *anti*-diastereoselectivity. Subsequent global reduction and oxidation/E-ring formation processes afforded the target in 8 steps over 10 operations in 25% overall yield and in 96% enantiomeric excess. X-Ray crystallographic structure determination provided conclusive evidence for the formation of the target.

TABLE OF CONTENTS

LIST OF ABBREVIATIONS

Ac	acetyl, acetate
ACCN	1,1'-azobis(cyclohexanecarbonitrile)
AIBN	2,2'-azobis(2-methylpropionitrile)
Bn	benzyl
Boc	*tert*-butyloxycarbonyl
br	broad
Bu	butyl
c	concentration
calcd	calculated
COSY	correlation spectroscopy
Cp	cyclopentadienyl
DCC	*N,N'*-dicyclohexylcarbodiimide
DCM	dichloromethane
DCU	dicyclohexylurea
dd	doublet of doublets
ddd	doublet of doublet of doublets
ddt	doublet of doublet of triplets
dil	dilute
DMAP	4-(*N,N'*-dimethylamino)pyridine
DMF	*N,N*-dimethylformamide
DMSO	dimethyl sulfoxide
dr	diastereomeric ratio
dtt	doublet of triplet of triplets
EDCI	*N*-(3-dimethylaminopropyl)-*N'*-ethylcarbodiimide
ee	enantiomeric excess
equiv	equivalents

Et	ethyl
EtOAc	ethyl acetate
ΔG	Gibbs free energy
Glc	glycoside
h	hour(s)
ΔH	enthalpy
HOBt	1-hydroxybenzotriazole
HPLC	high-performance liquid chromatography
HRMS	high-resolution mass spectrometry
HSQC	heteronuclear single quantum coherence spectroscopy
***i*-PrOH**	isopropanol
IR	infrared
J	coupling constant
k	rate constant
LAH	lithium aluminium hydride
m	multiplet
Me	methyl
MeOH	methanol
min	minutes
mp	melting point
Ms	methanesulfonyl
NaHMDS	sodium bis(trimethylsilyl)amide
NIS	*N*-iodosuccinimide
NMO	4-methylmorpholine *N*-oxide
NMR	nuclear magnetic resonance
PCC	pyridinium chlorochromate
Ph	phenyl

PhMe	toluene
PhOMe	anisole
PPL	porcine pancreatic lipase
ppm	parts per million
rac	racemate
RaNi	Raney nickel
rt	room temperature
s	singlet
ΔS	entropy
t	triplet
T	temperature
TBDMS	*tert*-butyldimethylsilyl
TBSOTf	*tert*-butyldimethylsilyl trifluoromethanesulfonate
***t*-Bu**	*tert*-butyl
TDCI	1,1'-thiocarbonyldiimidazole
TFA	trifluoroacetic acid
THF	tetrahydrofuran
TLC	thin layer chromatography
TMS	trimethylsilyl
TPAP	tetrapropylammonium perruthenate
Ts	p-toluenesulfonyl
UV	ultraviolet

C H A P T E R 1

Introduction and Literature Review

1.1 Introduction and Biological Importance

Indole alkaloids have been a topic of synthetic interest for decades as a result of the important pharmacological properties and complex structural variation that exists within this class of natural products.[1] These alkaloids, containing the indole structural moiety (Figure 1), are further divided into two main types, namely, non-isoprenoid and isoprenoid indole alkaloids.[2,3] Members of the non-isoprenoid type include simple derivatives of indole (**1**) and β-carboline (**2**) amongst others. In contrast, the isoprenoid indole alkaloids incorporate terpenoid structural elements (isoprene groups) in addition to the indole subunit (**3**,**4**).[2,3]

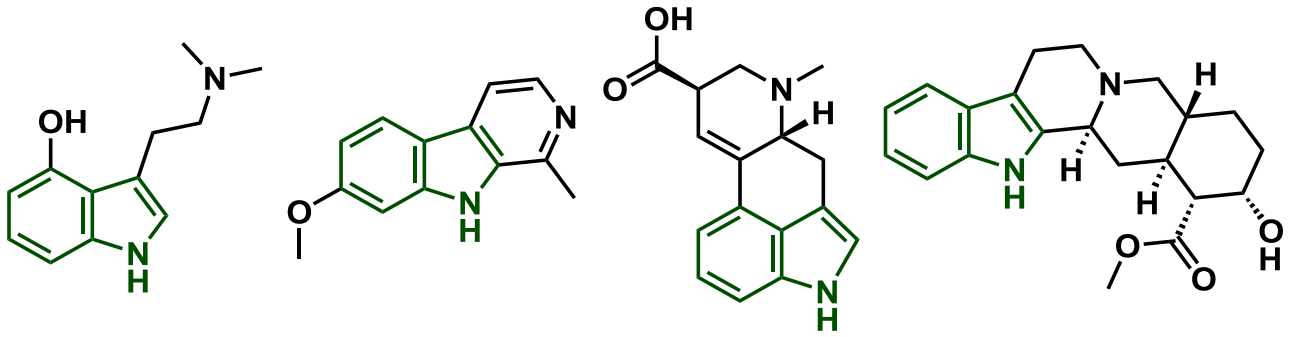

1: psilocin **2: harmine** **3: lysergic acid** **4: yohimbine**

Figure 1. An assortment of well-known biologically active indole alkaloids.

Monoterpenoid indole alkaloids are also referred to as secologanin tryptamine alkaloids stemming from the identification of a tryptamine portion as well as a C_9 or C_{10} fragment derived from secologanin in their core frameworks (Figure 2).[2,3] These alkaloids have generally been rationalized in terms of their biosynthetic origins and have consequently been subdivided into three main structural types. These are termed the *Corynanthe* type, as in ajmalicine (**5**), the *Iboga* type, as in catharanthine (**6**), and the *Aspidosperma* type, exemplified by tabersonine (**7**).[2,3]

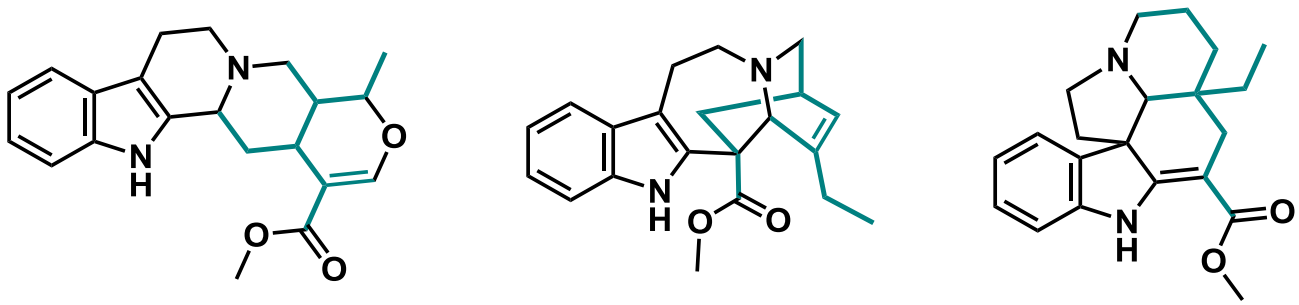

5: ajmalicine **6: catharanthine** **7: tabersonine**

Figure 2. Representative monoterpenoid indole alkaloids.

The multifarious structural nature of these types has resulted in the further identification of classes or families.[2,3] The focus of this work, in particular, is based on two closely related classes of the *Aspidosperma* type, namely, the *vinca* and *tacaman* classes,[2,3] exemplified by key representatives of these classes in Figure 3.

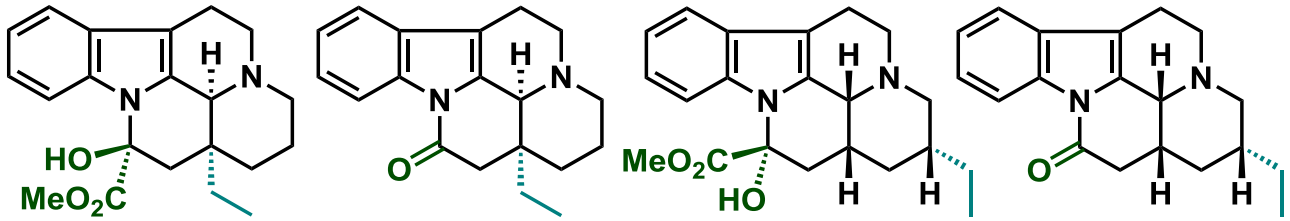

8: vincamine **9: vincamone** **10: tacamine** **11: tacamonine**

Figure 3. Key members of the *vinca* and *tacaman* families respectively.

Tacamonine (**11**), the target of this work, belongs to the *tacaman* class of monoterpene indole alkaloids.[1] It was first synthesised in 1982 as a racemate by Massiot *et al*.[4] prior to its isolation, known then as pseudovincamone I, making it one of the exceptional cases where a natural product has been synthetically prepared before being found in Nature.[5,6] Thereafter, it was isolated in 1984 by Van Beek and co-workers[7] from the leaves and twigs of *Tabernaemontana eglandulosa*, a small liane plant widely distributed in forests in Central Africa that occurs usually as solitary plants, flowering during the night.[7] Traditionally, the roots of *Tabernaemontana eglandulosa* have been used for the treatment of snake bite in the Democratic Republic of Congo, most likely stimulating these early investigations.[8] In this pioneering work, a total of eight alkaloids belonging to the new *tacaman* class were isolated, with tacamine (**10**), tacamonine (**11**), 16-*epi*-tacamine (**12**) as the three most abundant components (Figure 4).[7] Structurally, these indole alkaloids are all pentacyclic in that they contain an ABCDE five-ring system which is in turn made up of the nitrogen-containing indole structural moiety and an isoprene subunit (**13**, Figure 5).[1]

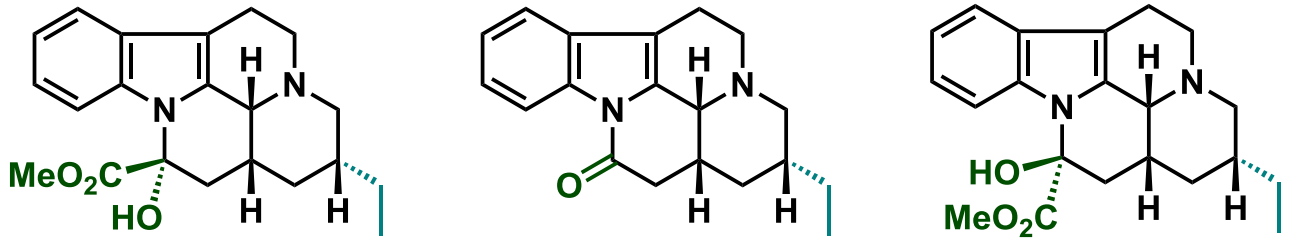

10: tacamine **11: tacamonine** **12: 16-*epi*-tacamine**

Figure 4. The three most abundant *tacaman* alkaloids isolated by Van Beek *et al*. in 1984.[7]

In terms of its biological significance, tacamonine (**11**) bears a close relation to vincamone (**9**), belonging to the *vinca* class, differing only in the position of the ethyl group (Figure 5).[9] Members of the *vinca* family have long since been known to exhibit potent cerebral vasodilator and hypotensive activities.[1,5,8,9] This close structural similarity has thus promoted several efforts towards the synthesis of tacamonine and other members of the *tacaman* family.[1,9]

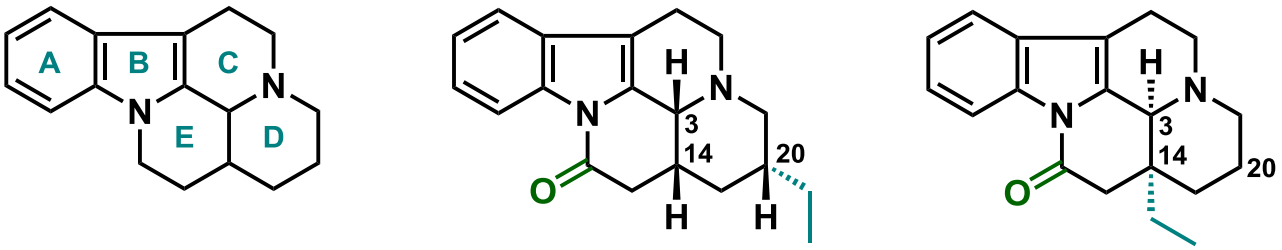

13: generic framework **11: (+)-tacamonine** **9: (-)-vincamone**

Figure 5. Structural similarities and differences between tacamonine and vincamone.

Synthetically, attachment of the ethyl group at C-20 away from the D/E-ring junction adds an additional stereocenter and thus provides a further degree of complexity to its synthesis since all three methine hydrogens at C-3, C-14 and C-20 have to be positioned *cis* relative to each other.

1.2 Biosynthesis

In terms of biosynthetic considerations, the exact biosynthetic pathways resulting in the derivation of the *tacaman* class remain unknown.[7] As previously mentioned in the introductory section, monoterpenoid indole alkaloids of the *Aspidosperma* type such as tabersonine (**7**) are derived from tryptamine (**14**) and secologanin (**15**) as shown in Scheme 1.[3] Tabersonine (**7**) is then used in the derivation of the *vinca* family as exemplified by vincamine (**8**), the mechanism of which was recently confirmed in 2015 by Kellner *et al*.[10] The *tacaman* family is thus thought to be derived in a similar manner from pseudotabersonine (**16**), though this remains to be confirmed.[7]

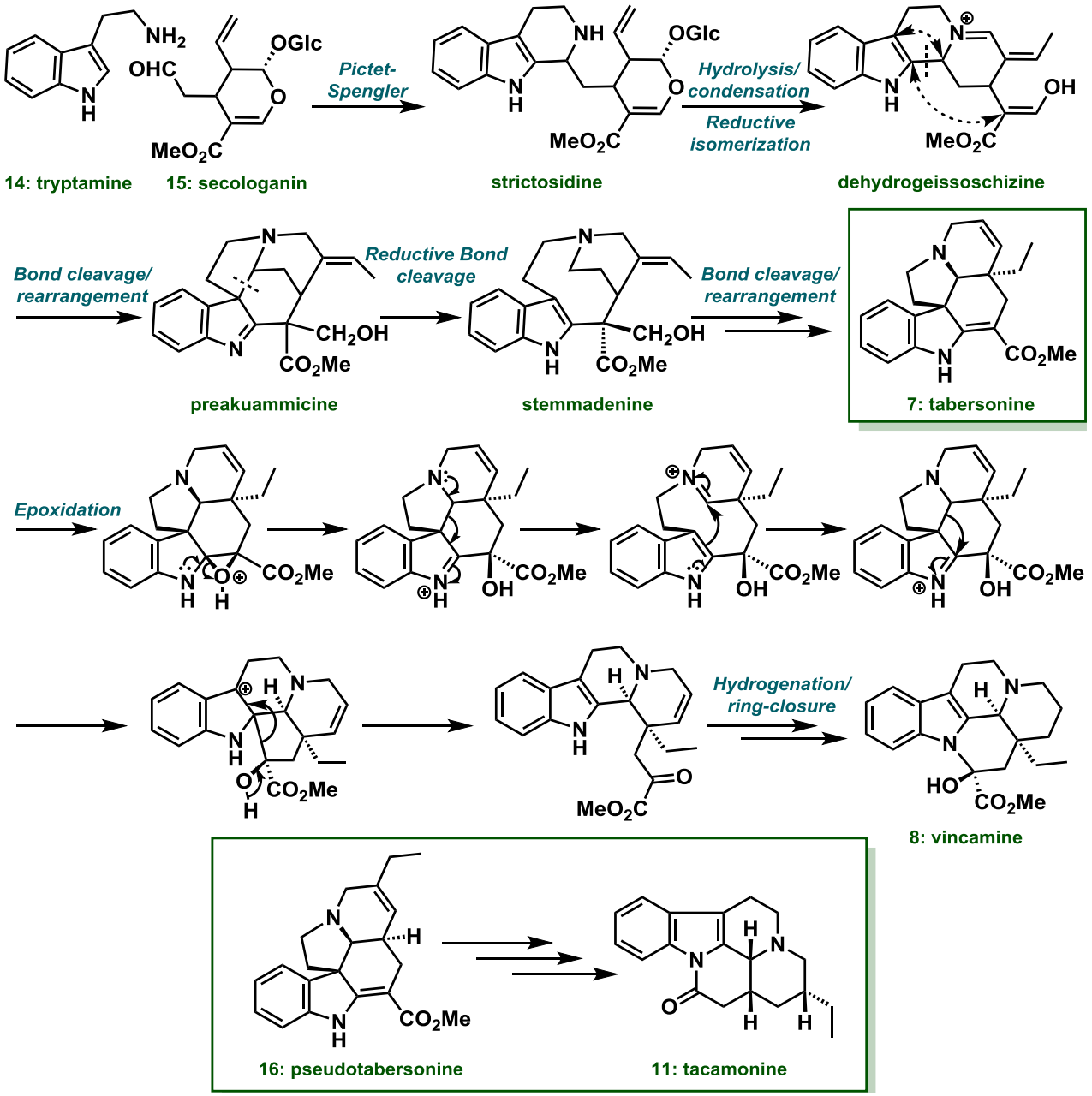

Scheme 1. Proposed biosynthesis for the *vinca* and *tacaman* classes.[3,10]

1.3 Synthetic Studies in the Tacaman Class

1.3.1 Syntheses of (±)-Tacamonine

In the years following the isolation of natural (+)-tacamomine, two asymmetric total syntheses (discussed later on) as well as a total of seven racemic syntheses have been reported in the literature, three of which are formal syntheses. As will be seen in the upcoming section, the A-B indole ring system (**13**, Figure 5) is generally introduced through coupling of a tryptamine fragment, while in most cases the C-ring is constructed via a Bischler-Napieralski cyclization.

In general, the fundamental differences in the synthetic approaches lie in the method used to construct the D-ring fragment, the method used to generate the *cis* D/E-ring junction, as well as the order in which the pentacyclic core is constructed. Classically, most syntheses construct the framework using an AB**D** to AB**C**D to ABCD**E** ring strategy, with a single ABC to ABC**DE** strategy known in the literature.[1]

1.3.1.1 Convergent ABD to ABCD approaches

In 1998 Lounasmaa *et al*.[11] published a stereoselective racemic total synthesis of tacamonine which involved a more efficient approach based on their prior work.[5,6] In this approach they relied on the development of the D-ring component from a substituted pyridine and made use of epimerization to form the required *cis* D/E-ring junction. They began with the synthesis of ester intermediate **20** which was achieved over three steps (Scheme 2). This involved the alkylation of pyridine **17** with tryptophyl bromide, followed by catalytic Wenkert hydrogenation of **18** in the presence of base. Acid-induced cyclization of **19** afforded the kinetically favoured *trans* D/E ester intermediate **20** as a single diastereomer.

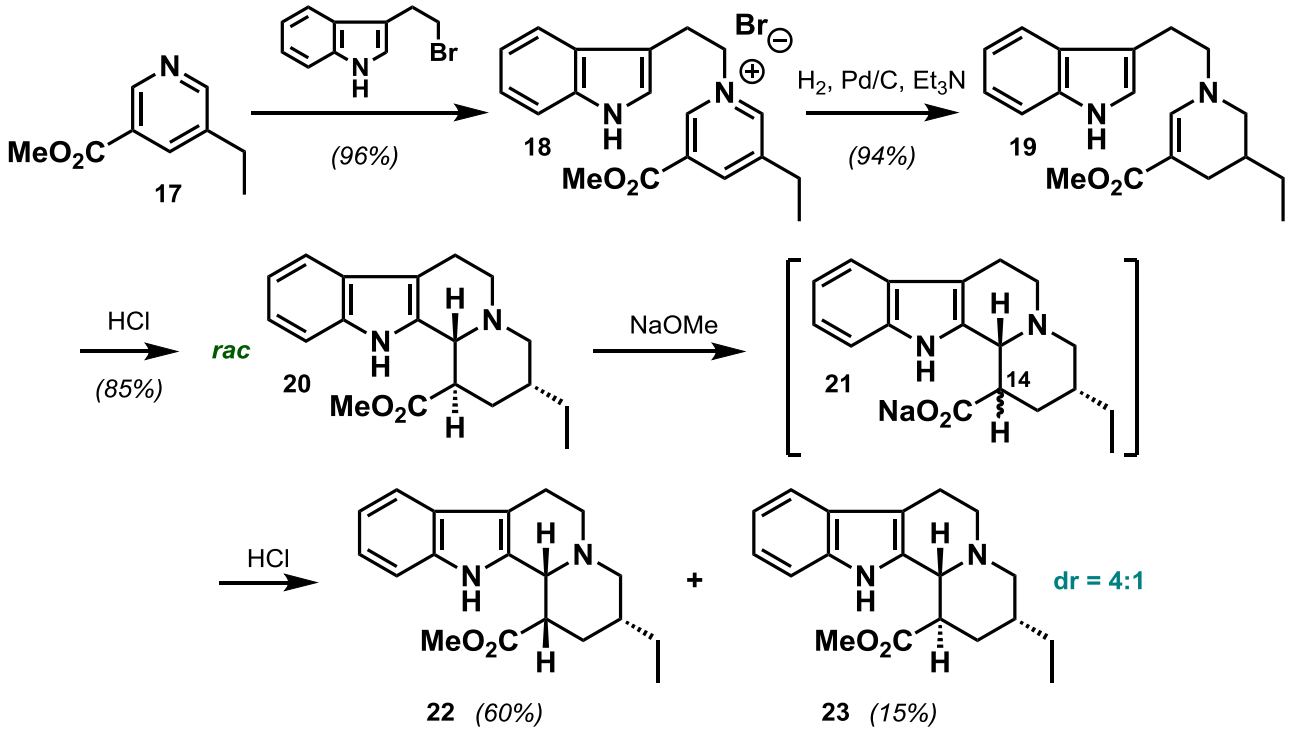

Scheme 2. The initial stages of the Lounasmaa group's approach, including epimerization for the formation of the *cis* D/E-ring junction.[11]

Interestingly, the group found that treatment of **20** with sodium methoxide in methanol followed by reesterification in methanol saturated with hydrogen chloride led to the formation of products **22** and **23** in a 4:1 ratio. They postulated that this process occurs through the sodium salt intermediate **21**, since the corresponding acid could be isolated, and rationalised that the C-14 proton could be exchanged with base leading to the more thermodynamically favourable epimer **22** with the original ethyl group now in the equatorial position (more on these conformational aspects later).

With ester **22** in hand, possessing the required all *cis*-H stereocentres, the final ring of the pentacyclic core could be constructed (Scheme 3). Reduction of ester **22** produced alcohol **24**, which was then converted to nitrile **25** via the tosylate. Finally, consecutive acid and base treatments of nitrile **25** allowed for the two-step, one-pot conversion to racemic tacamonine (**11**) in high yield.

As a whole, the route involves 10 operations over 7 steps providing the target in 23% overall yield, making it one of the more efficient racemic syntheses of tacamonine developed to date. The only drawback being the laborious one-carbon extension in the end-game for completing the E-ring.

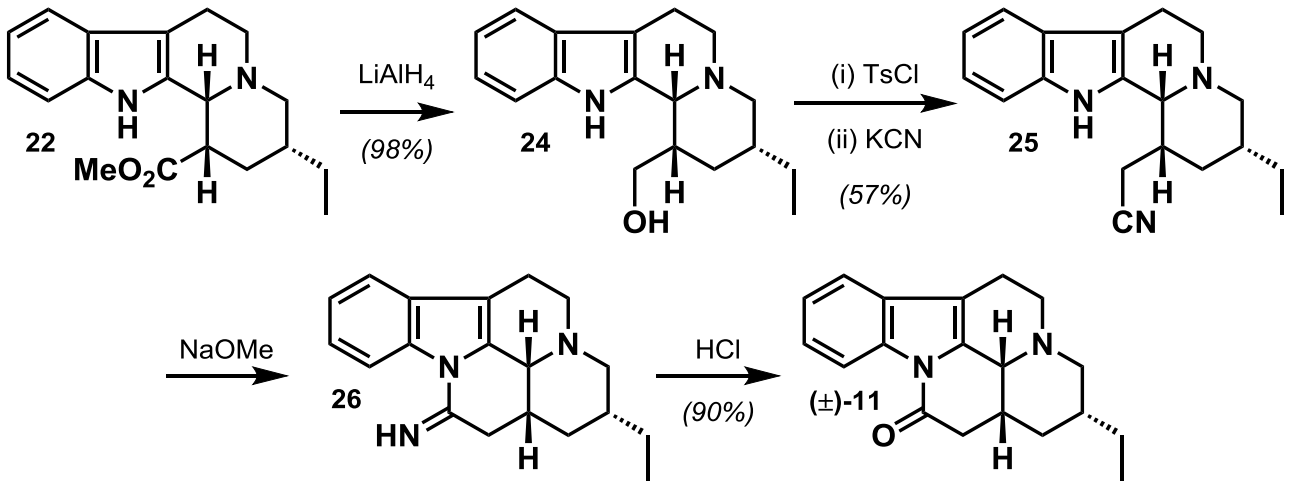

Scheme 3. The concluding steps in the stereoselective racemic total synthesis of tacamonine by Lounasmaa *et al*.[11]

A few years later a somewhat unique stereoselective but still racemic total synthesis was developed by Lavilla *et al*. and published in 2001.[12] Unlike any of the other methods that follow in this discussion, the group used a non-biomimetic oxidative halocyclization of a 1,4-dihydropyridine for the formation of the C-ring following the same ABD to ABCD strategy. Furthermore, the group made use of radical addition of the resulting halo derivative to an activated alkene to install the requisite *cis* D/E-ring junction.

Their approach (Scheme 4) began with the synthesis of the desired 1,4-dihydropyridine **27** which was obtained through literature procedures involving quaternization of 3-acetylpyridine with tryptophyl bromide and concomitant reduction of the pyridinium salt with sodium dithionite (not shown).[13] In a previous work,[14] the group had shown that iodo derivative **29** could be obtained stereoselectively as a result of the non-biomimetic oxidative halocyclization of **27** via **28** owing the more nucleophilic character of the enamine in contrast to the vinylogous amide. In addition, they found that radical Zn-mediated conjugate addition of **29** and α-chloroacrylonitrile led to the formation of the *cis* indoloquinolizidine **30** as a mixture of C-16 epimers. This stereochemical outcome implied a clean inversion of configuration at the pro-radical centre leading to the thermodynamically more stable *cis* product. This result was supported by further theoretical calculations that suggested conformational control at the radical level leading to the preferred facial selectivity. The selective formation of the *cis* D/E-ring relieves steric strain between the bulky indole substituent in the pseudoequatorial position and the D-ring side chain in the axial position as depicted in **31**.

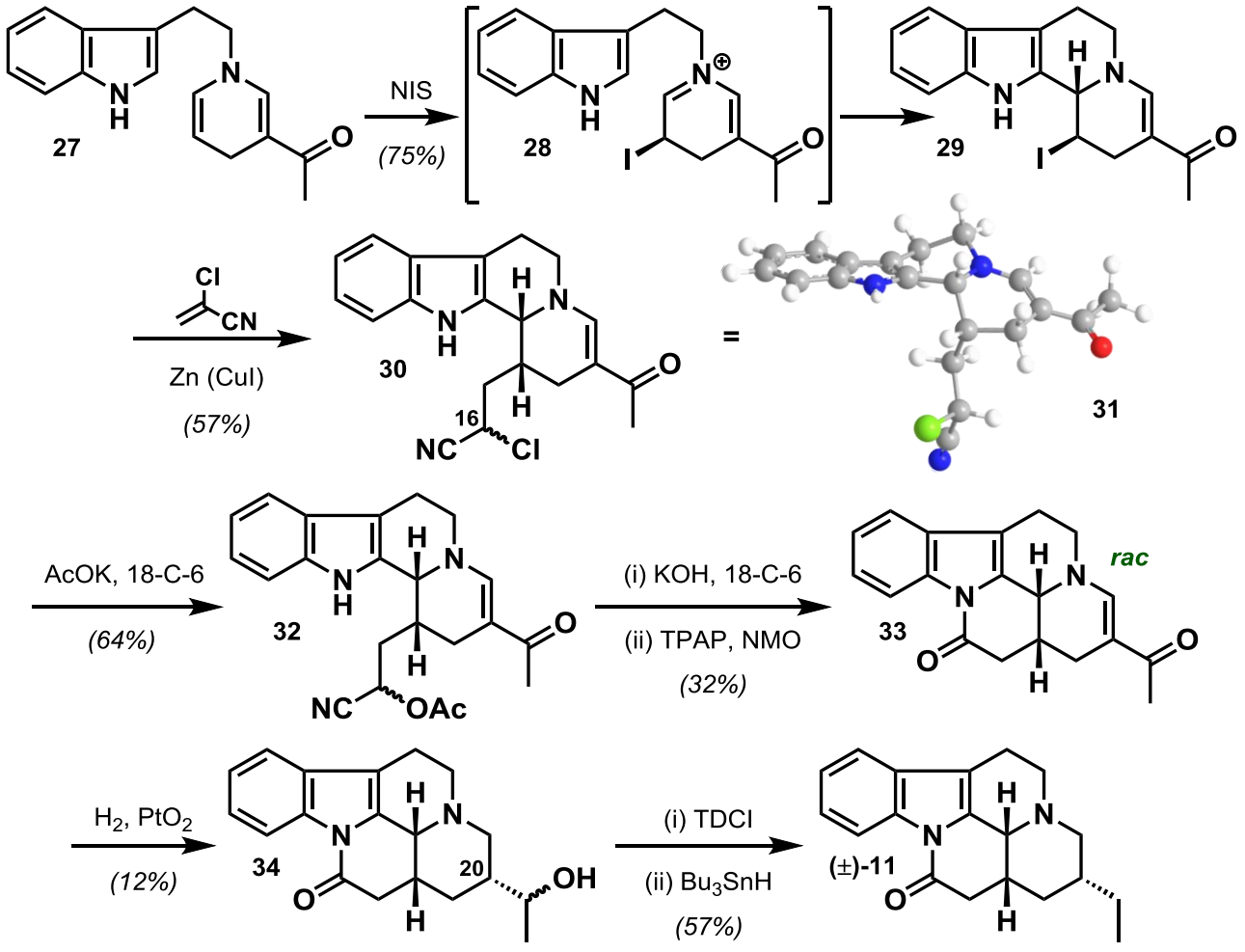

Scheme 4. Stereoselective racemic total synthesis of tacamonine by Lavilla *et al.*[12]

Once the *cis* D/E-ring junction had been established the group moved on to prime the E-ring precursor for cyclization. Chloronitrile **30** was advanced to acetoxynitrile **32** as an epimeric mixture under phase-transfer catalysis (18-C-6) conditions. Further hydrolysis and spontaneous cyclization of the aldehyde product resulted in the formation a mixture of C-16 *N,O*-hemiacetal epimers which were immediately oxidized to yield acylindole **33**.

The group then moved on to generate the C-20 stereocentre and establish the all *cis*-H framework. Pleasingly, they found that simultaneous reduction of the olefin and carbonyl moieties took place with stereocontrol via *syn*-addition from the least-hindered face to afford epimeric alcohol mixture **34**, which was advanced to racemic tacamonine (**11**) following Barton-McCombie deoxygenation of the corresponding thioimidazolide. Though this route highlights several interesting aspects of stereocontrol and encompasses only 6 steps from **27** over 8 operations, it is unfortunately highly inefficient, boasting an overall yield of less than 1% from **27**.

In 2008, Ho and co-workers reported another stereoselective racemic total synthesis of tacamonine.[15] Conceptually, the group aimed to make use of a bridged D-ring precursor to direct the *cis* D/E-ring junction formation during the imine reduction stage of the Bischler-Napieralski cyclization. These efforts began with the synthesis of the requisite D-ring precursor (Scheme 5). Bridged **35**, acquired through a literature acyloin condensation procedure (not shown),[16] was subsequently oxidised to diketone **36**. Stereoselective *exo* borohydride reduction and concomitant acetylation produced **37** which was then subjected to aggressive oxidative cleavage to afford diacid **38**.

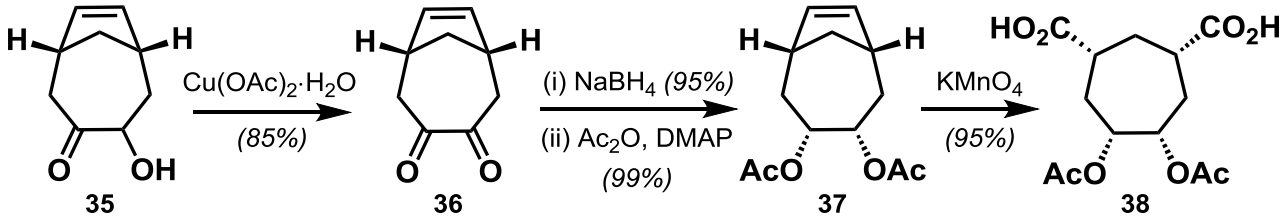

Scheme 5. The Ho group's synthesis of D-ring precursor **38**.[15]

With diacid **38** in hand, the stage was now set to attach the tryptamine moiety and assemble the desired bridged D-ring precursor, containing all the carbon atoms of the non-tryptamine fragment (Scheme 6). This conversion to glutarimide **39** was carried out in a one-pot, two-step reaction procedure involving initial amide formation and subsequent ring closure. Glutarimide **39** was then advanced to lactam **41** through a series of functional group manipulations, namely, treatment with Lawesson's reagent to provide the monothio derivative **40** and subsequent reductive desulfurization with Raney nickel.

At this point the C-ring was assembled under Bischler-Napieralski conditions and advanced to diol **42** by global reduction of the iminium salt and acetyl groups. The observed *cis* stereoselectivity was rationalised on steric and stereoelectronic grounds in favour of hydride attack from the β-face of a bridge-locked iminium salt as previously anticipated.

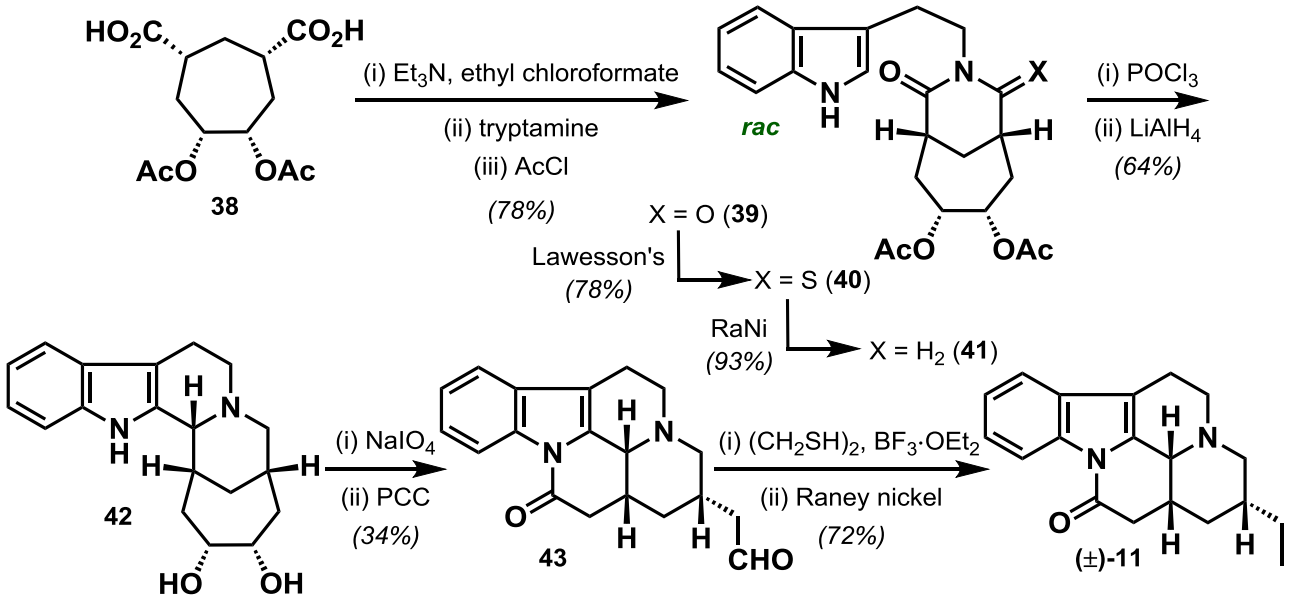

Scheme 6. Completion of the racemic total synthesis of tacamonine by Ho *et al*.[15]

Moving on to the E-ring assembly, oxidative periodate cleavage of the vicinal diol in **42** proceeded with spontaneous cyclization to afford a mixture of unstable epimeric *N,O*-hemiacetals which were immediately oxidised to lactam aldehyde **43**. Finally, deoxygenation of the remaining formyl group via its ethylenedithioacetal afforded racemic tacamonine (**11**) in 7% overall yield from **35** in 10 steps over 14 operations. Though this synthesis embraced some elegant chemical manipulations, it is unfortunately rather lengthy as a result.

1.3.1.2 Linear D-ring construction strategies

As is evident from the discussion of these more classical approaches, in general we see that the D-ring fragment is constructed prior to the addition of the tryptamine fragment in a convergent approach to furnish an ABD construct. In more recent years, various approaches have emerged that allow for the construction of the D-ring in the presence of the tryptamine fragment as part of a more linear approach, while still falling under the general ABD to ABCD ring-construction strategy.

One such method was published by Chen *et al*. in 2003, thereby securing a formal, entry towards the synthesis of racemic tacamonine.[17] Their investigations centred on the use of a regioselective reduction for the conversion of an *N*-alkyl-3-sulfonyl glutarimide, generated through their previously developed [3 + 3] annulation strategy,[18] into a lactam. In this work (Scheme 7), they envisaged target **47** as a product of this new procedure and rationalised that it could be converted to lactam **48**, which could subsequently be converted to racemic tacamonine (**11**) according to literature precedents.[19] Indeed, they established that reaction of Baylis-Hillman adduct **45** with the appropriate sulfonylacetamide **44** afforded target **46** in a one-pot stepwise [3 + 3] annulation process using sodium hydride as a base promoter.

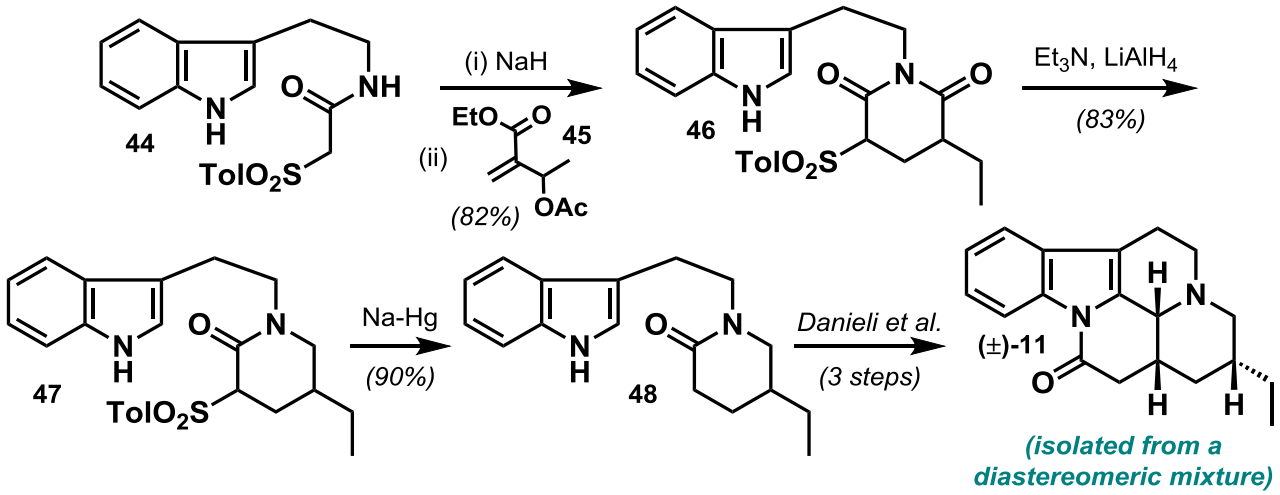

Scheme 7. Formal non-stereoselective racemic synthesis of tacamonine by Chen *et al*.[17]

The mechanism of this reaction was postulated to proceed through 1,4-Michael addition, intramolecular cyclization and elimination as depicted in Scheme 8.

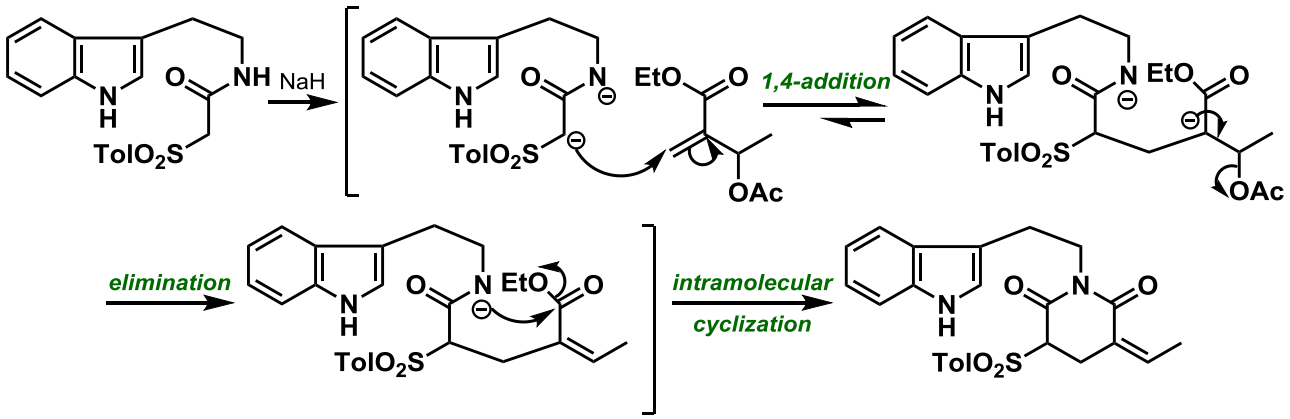

Scheme 8. The Ho group's proposed mechanism for the [3 + 3] annulation strategy.[17]

In the subsequent step (Scheme 7) glutarimide **46** was selectively reduced at the more electrophilic carbonyl group (due to the electron-withdrawing sulfonyl group invoking a greater resonance stabilisation by nitrogen of its adjacent carbonyl) to yield lactam **47**.

Subsequent reductive desulfonation afforded **48**, thus constituting a non-stereoselective racemic formal entry via literature procedures.[19]

In 2005, Ihara *et al*. developed another non-stereoselective racemic formal entry via a linear ABD to ABCD strategy through application of their newly developed intermolecular tandem aza-Michael/C-Michael procedure.[20] Using this methodology[21] (Scheme 9), the group was able to furnish piperidinone **50** in high yield through the intermolecular dimerization reaction of acrylamide **49** using *tert*-butyldimethylsilyl triflate as a Lewis acid promoter, followed by global *N*-Boc protection of the product. This intermolecular reaction presumably proceeds via azaenol silyl ether formation (of the secondary amide) of one of the partners, followed by aza-Michael addition on to the other, thereby setting up a closure opportunity via a C-Michael. In the subsequent step, treatment of **50** with sodium methoxide resulted in the simultaneous removal of the *N*-Boc indole group to afford methyl ester **51**. Finally, selective reduction of the ester with lithium borohydride afforded target alcohol **52** which has been previously converted to tacamonine in the literature[19] via lactam **48** as with the Chen group's synthesis previously.

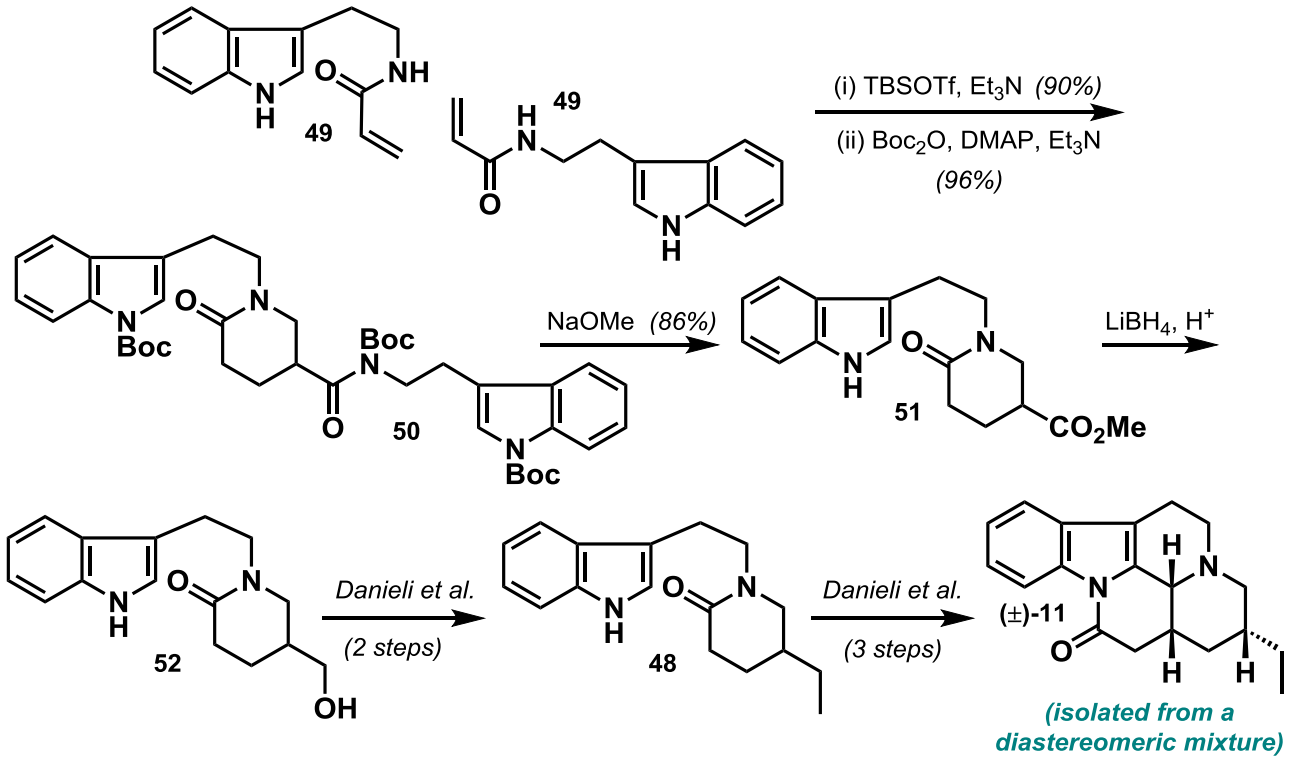

Scheme 9. Formal non-stereoselective racemic synthesis of tacamonine by Ihara *et al*.[20]

In 2006, Deiters *et al*. also reported a linear strategy for the formation of the D-ring, which was achieved through a ring-closing metathesis/1,4-addition process in order to achieve the usual ABD to ABCD strategy (Scheme 10).[22]

Their efforts began with the EDCI-mediated amide coupling between readily available **53** and diallylamine to form the desired metathesis substrate **54**. Their novel one-pot, two-step procedure transformed **54** into **56** via sequential ring-closing metathesis and zirconocene-catalyzed carbomagnesium reactions.

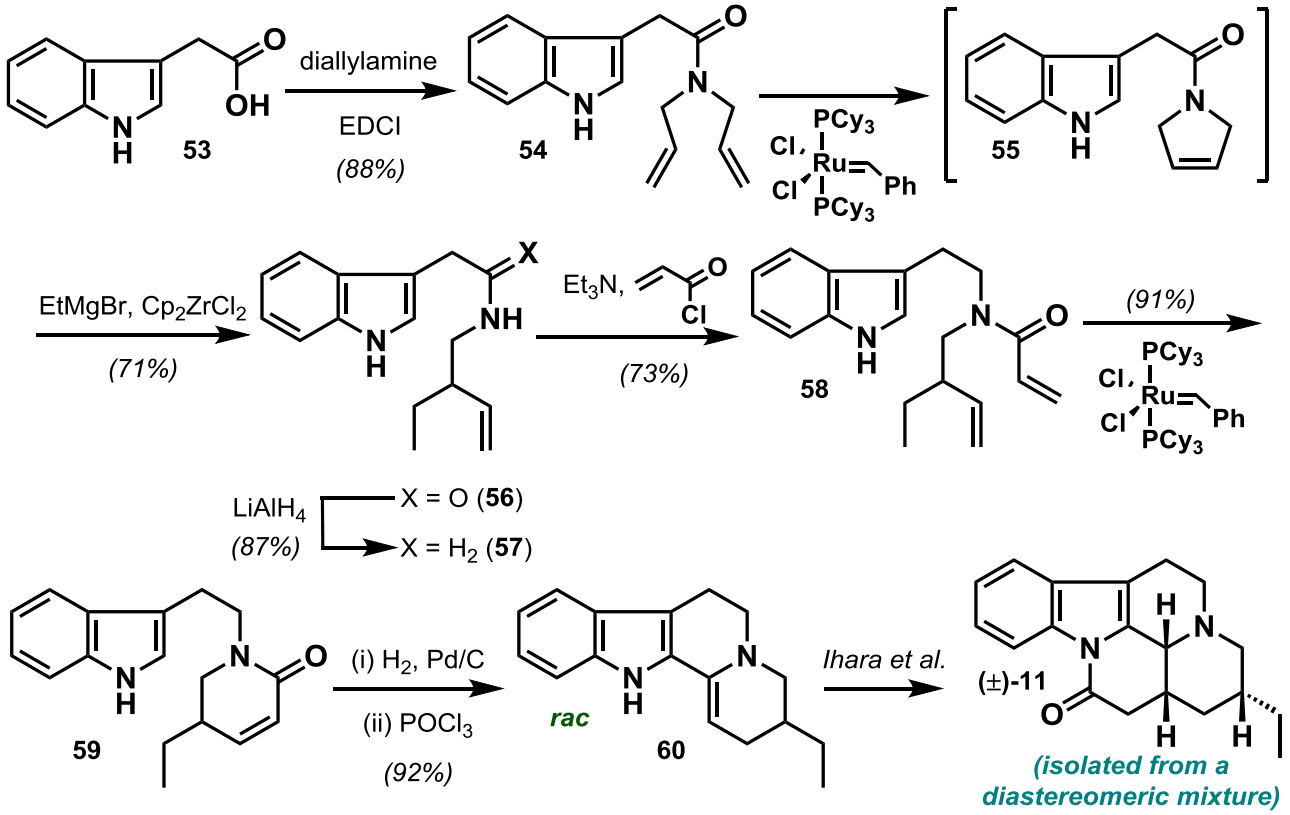

Scheme 10. Formal non-stereoselective racemic synthesis of tacamonine by Deiters *et al*.[22]

The postulated mechanism of this fascinating organometallic reaction from **55** to **56** (Scheme 11), investigated by Hoveyda *et al*. in similar works,[23,24] proceeds via the initial formation of zirconocene (**61**) followed by insertion of the alkene **55** to give **62**. Subsequent cleavage of the zirconacyclopentane by ethylmagnesium bromide via **63** and **64** results in the formation of **56** as depicted in Scheme 11.

In the remaining steps (Scheme 10), reduction of the amide group in **56** and treatment with acryloyl chloride to introduce the requisite side chain afforded **58**, thereby installing the fragments necessary for the second ring-closing metathesis step. Indeed, the D-ring was generated smoothly when subjected to metathesis conditions. In the final operations, **59** was subjected to catalytic hydrogenation and elaborated via the familiar Bischler-Napieralski cyclization. This process led selectively to **60**, which had already been reported as an advanced intermediate, thus constituting a formal racemic synthesis of tacamonine via the method of Ihara *et al*.[8]

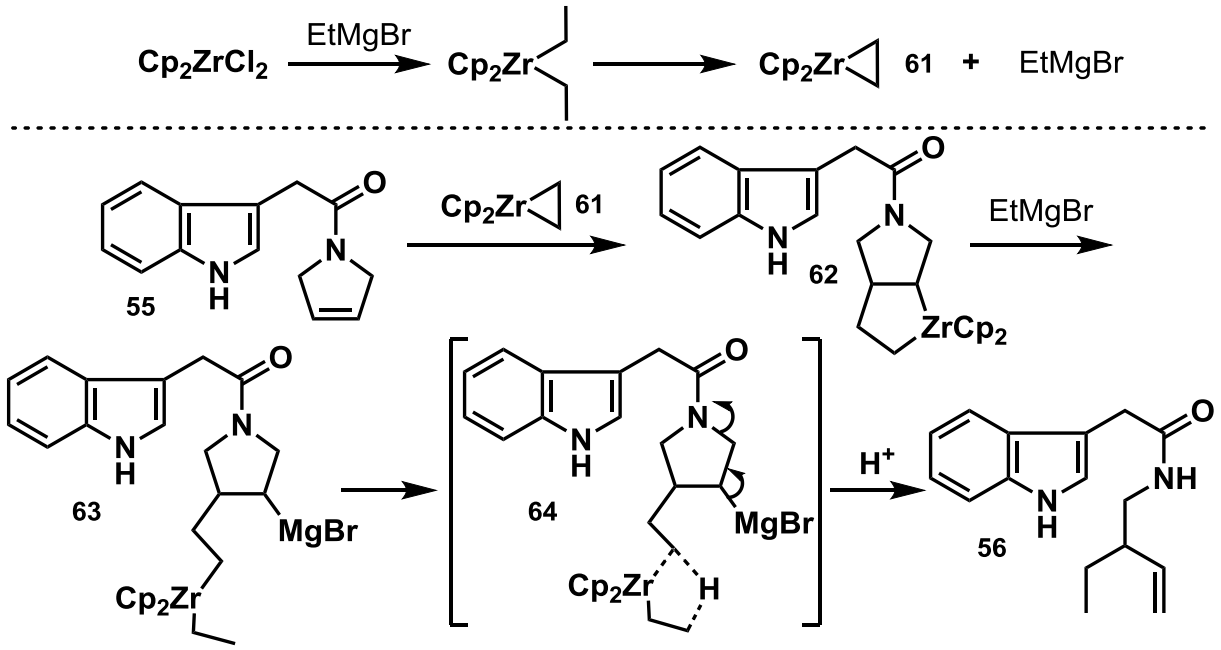

Scheme 11. Postulated mechanism of the zirconocene-catalyzed carbomagnesium reaction.[23,24]

Certainly one of the more innovative approaches to the pentacyclic *tacaman* skeleton was reported by Padwa *et al*. in 2008.[1] Their approach differs to the more conventional methods previously discussed as the C-ring is assembled prior to the D-ring in an ABC to ABCDE strategy, in which the D- and E-rings are constructed simultaneously through a novel Rh(II)-catalyzed cyclization/cycloaddition cascade.

More specifically (Scheme 12), these efforts commenced through treatment of carboline **65** with the associated acid chloride to form **66**, which was then advanced to cycloaddition precursor **67** via indole *N*-acylation with ethyl 2-diazomalonyl chloride using sodium hydride to generate the anion. They postulated that heating **67** with a catalytic amount of rhodium(II) acetate would generate a rhodium carbenoid intermediate that would react with the lactam carbonyl to generate an oxonium-ion ylide intermediate **68**, which in turn would react in an intramolecular 1,3-dipolar cycloaddition. Pleasingly, they found that subjecting α-diazoindoloamide **67** to their Rh(II) cascade conditions gave the desired intramolecular [4 + 2] cycloadduct **69** in high yield and as a single diastereomer, the latter due to the tight stereocontrol operating in the cycloaddition step.

At this stage, bearing in mind the need to generate an all *cis*-H stereochemical requirement between H-3/14 and H-20 ultimately, they envisioned a catalytic enamine hydrogenation strategy to deliver the desired D/E-ring junction resulting from *syn*-addition from the least hindered face.

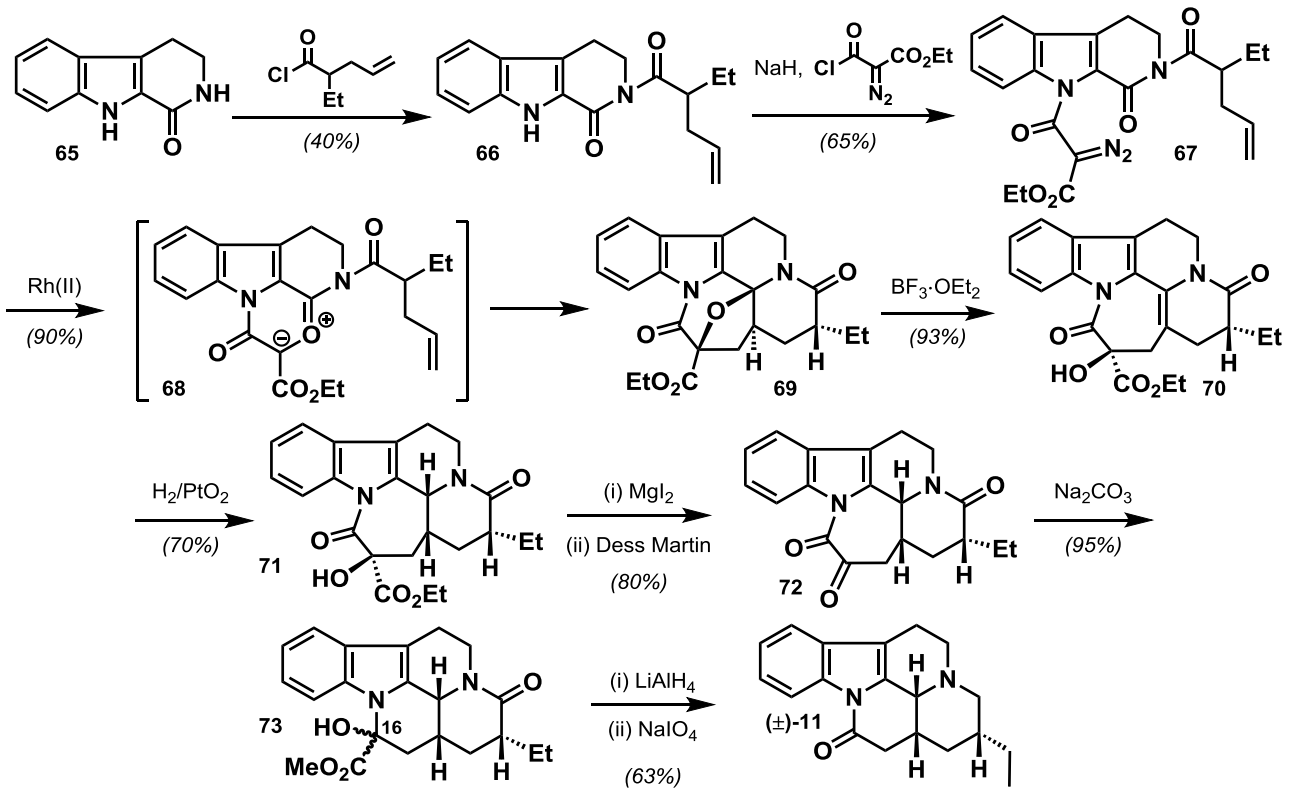

Scheme 12. Stereoselective racemic total synthesis of tacamonine by Padwa *et al*.[1]

To this end, enamine **70** was synthesized via oxabicyclic eliminative ring opening with boron trifluoride diethyl etherate from **69** in high yield. With the enamine in place, catalytic hydrogenation of **70** forged the requisite *cis*-fused ring system as a single diastereomer **71**, as anticipated.

Thereafter, the group focused on the preparation of the six-membered E-ring, which they envisaged as accessible through ring-contraction of a keto-amide. In this process, removal of the carbethoxy group was achieved following decarboxylation of **71** with magnesium iodide to afford a secondary alcohol which was immediately oxidized to the requisite keto-amide **72.** Further advancement to hydroxy ester **73** as a mixture of C-16 diastereomers was achieved under base-induced ring-contraction conditions. With the *tacaman* framework now firmly in place, global reduction of both the ester and lactam carbonyl functionalities was achieved through treatment of **73** with excess lithium aluminium hydride to deliver the diol, which was then immediately subjected to sodium periodate oxidative cleavage to yield racemic tacamonine (**11**) as a single diastereomer in 7% overall yield from **65** over 8 steps consisting of 10 total operations in an elegant synthesis, but one with an over-elaborate endgame.

1.3.2 Asymmetric Total Syntheses of (+)-Tacamonine

Since its isolation in 1984, only two asymmetric total syntheses of (+)-tacamonine have emerged in the literature, the first of which was achieved by Ihara *et al*. in 1994.[8] These syntheses still rely on certain diastereoselective reaction steps, but generate only the (+)-enantiomer by beginning with a suitable chiral, non-racemic precursor. The Ihara group's approach (Scheme 13), was thus based on the synthesis of a chiral, non-racemic propane-1,3-diol intermediate **74** to install the requisite homochiral C-20 stereocentre, from which the other stereocentres were derived diastereoselectively. In terms of what has been described before, the synthesis pursued a linear AB to ABD strategy and in which radical cyclization was used as the key step. Thereafter, a Bischler-Napieralski cyclization was used as the key step. Thereafter, a Bischler-Napieralski cyclization was used to afford an ABCD intermediate, followed by consecutive reduction and E-ring closure processes. A retrosynthetic analysis of their synthesis is shown in Scheme 13.

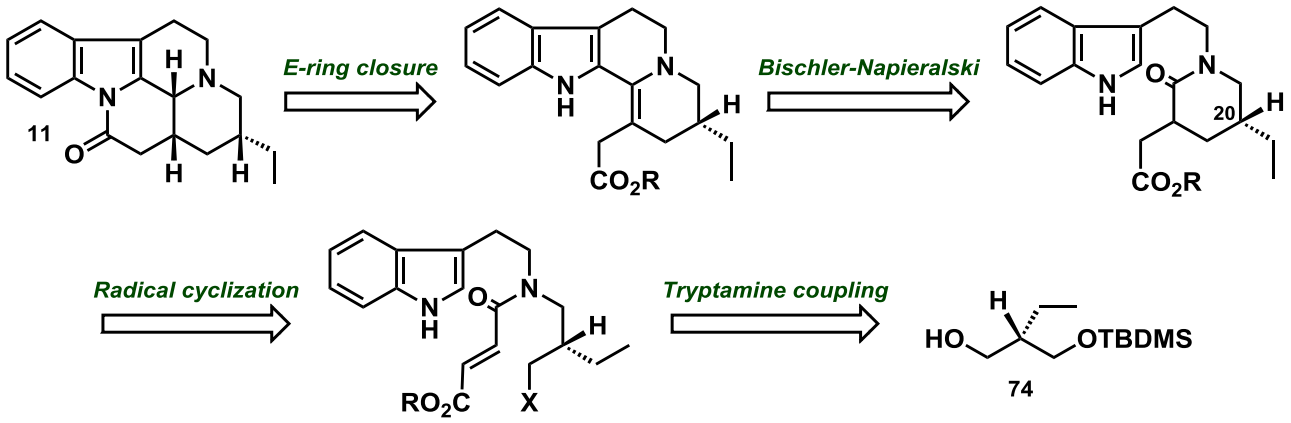

Scheme 13. Retrosynthetic analysis of the Ihara group's asymmetric approach.[8]

Thus, these efforts commenced with the synthesis and modification of the chiral precursor **74** shown in Scheme 14, in which readily available chiral oxazolidinone **75** was advanced to **76** through standard Evans methodology.[25] Compound **76** was then diastereoselectively hydroxymethylated to **77** when subjected to titanium(IV) chloride, triethylamine and *s*-trioxane followed by protection of the hydroxyl group of the product. Though **77** was obtained in high diastereomeric excess, it was unfortunately synthesized in only 48% yield. Subsequent reductive auxiliary deprotection of **77** with lithium borohydride in the presence of one equivalent of water provided the desired chiral precursor **74** in high optical purity (~100% ee) and in good yield. Mesylation and concomitant bromination of **74** afforded the chiral bromo-intermediate **78** necessary for the ensuing tryptamine coupling step.

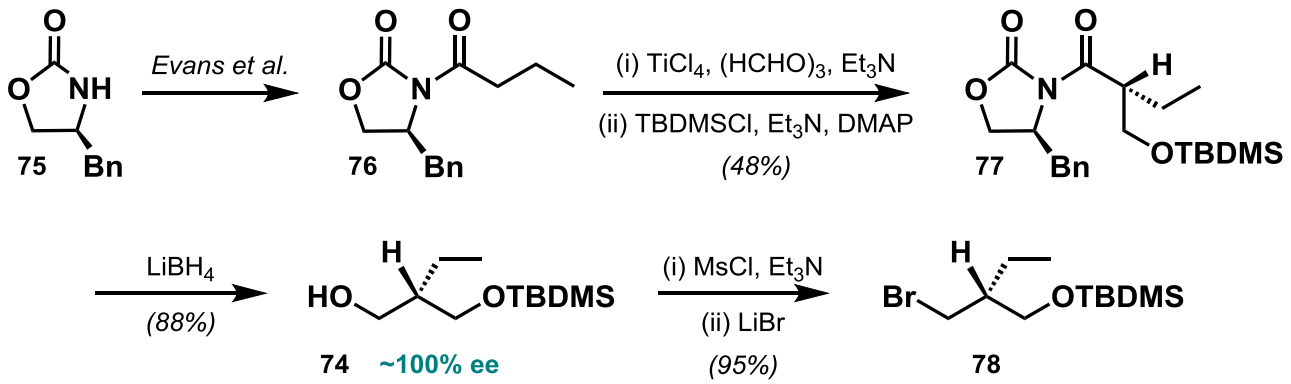

Scheme 14. Synthesis and modification of the chiral precursor **74** by Ihara *et al*.[8]

With **78** in hand, the group then sought to combine all of the required fragments together (Scheme 15). This was achieved through a simple S_N2 substitution reaction of bromide **78** with tryptamine followed by DCC coupling of the product in the presence of DMAP with fumaric acid monoethyl ester to afford amide **79** in a fair 64% yield overall. In order to prepare the radical cyclization precursor **81**, **79** was first subjected to deprotection conditions for the removal of the silyl group followed by mesylation and bromination of the product **80**.

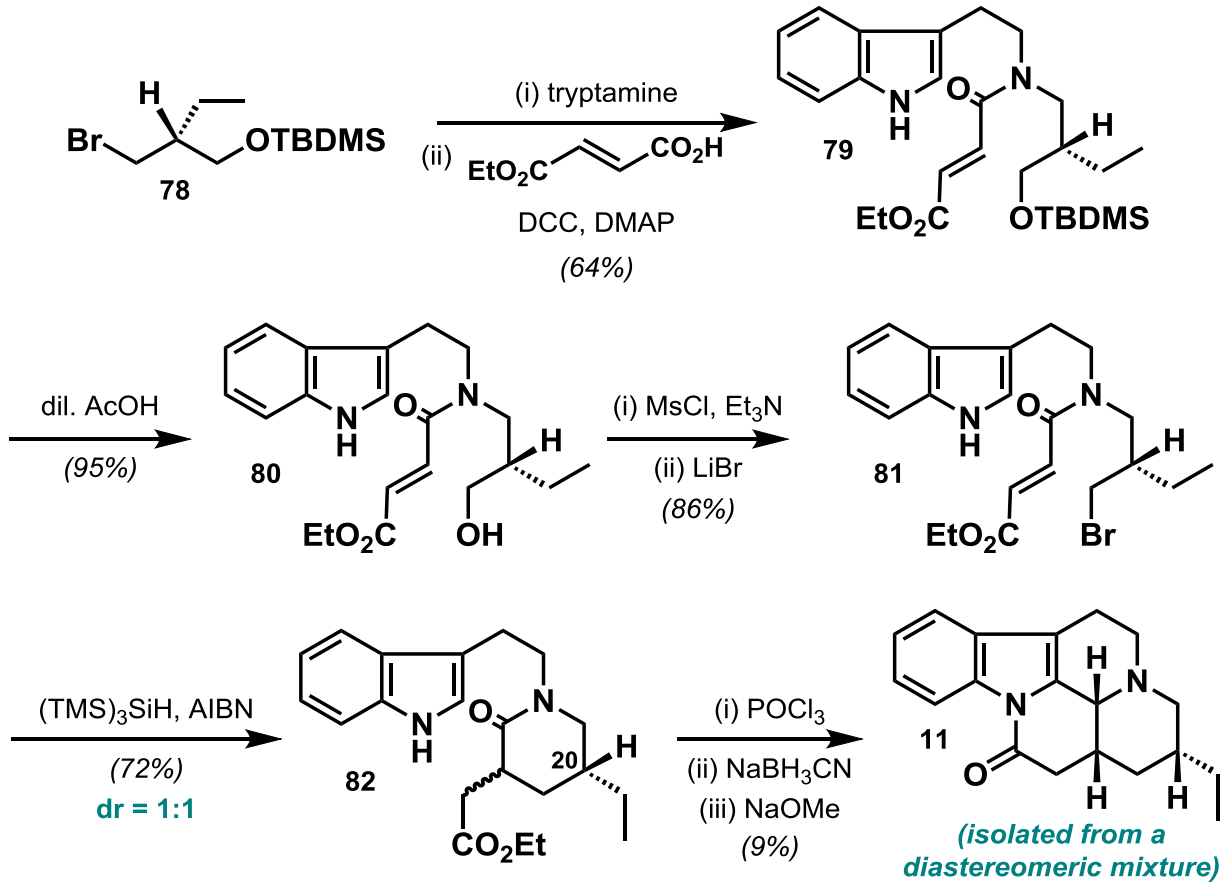

Scheme 15. Completion of the first asymmetric total synthesis of (+)-tacamonine by Ihara *et al*.[8]

The key step in this synthesis, involving the formation of the D-ring, was achieved through radical cyclization of **81** using tris(trimethylsilyl)silane in the presence of AIBN, which proceeded via a 6-*exo*-*trig* stereomode to afford product **82**. However, this was obtained in a suboptimal yield and unfortunately as a 1:1 mixture of diastereomers (relative to C-20) which were carried over into the remaining steps.

With advanced intermediate **82** in hand, the synthesis was completed in a three-step procedure through Bischler-Napieralski C-ring formation, reduction of the product in the presence of the ester with sodium cyanoborohydride, and finally, E-ring formation through nucleophilic acyl substitution with sodium methoxide. These concluding steps resulted in the formation of the target **11** as a diastereoisomeric mixture from which the correct all *cis*-H diastereomer was isolated in a meagre 9% yield.

In summary, the group was able to synthesize (+)-tacamonine in only 1% overall yield from oxazolidinone **75** involving a total of 15 operations over 9 distinct steps. Although asymmetric, this synthesis was highly inefficient and produced tacamonine as a diastereoisomeric mixture from which the correct all *cis*-H diastereomer **11** had to be isolated in the final step.

In 2001, Danieli and co-workers published the only other asymmetric total synthesis of (+)-tacamonine known in the literature, this time avoiding the task of tedious diastereoisomeric separation in the final step.[9] The key disconnections in their approach were similar to those of the Ihara group (Scheme 13), following an ABD to ABCD to ABCDE ring construction strategy, also involving a linear D-ring construction. Their work relied on the use of an optically pure 2-substituted propane-1,3-diol intermediate which was in this case obtained through selective enzymatic acylation of an enantiotopic group instead of using a chiral auxiliary approach. Furthermore, similar to the previously mentioned strategy of the Padwa group (Scheme 12), a stereocontrolled reduction procedure was utilized in order to generate the requisite D/E-ring junction.

The group began with readily available tosyloxybutyne **83** which was advanced to diol **84** through standard procedures (Scheme 16). In the following step, desymmetrization of diol **84** was achieved via enzymatic PPL transesterification providing monoacetate **85** in good yield and in high enantiomeric excess (98% yield, >99% ee). Subsequent ozonization of **85** afforded chiral lactone **86** in high 97% yield as desired.

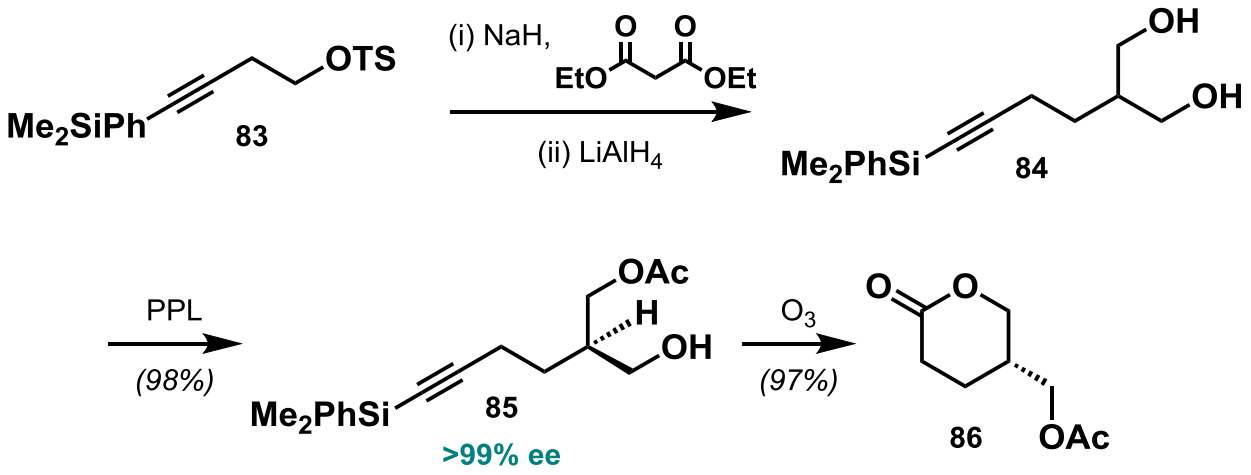

Scheme 16. Synthesis of the chiral precursor **86** by Danieli *et al*.[9]

With chiral lactone intermediate **86** in hand, the group was able to couple with the tryptamine fragment through chemoselective nucleophilic acyl substitution producing alcohol **87** in a good 76% yield (Scheme 17). The D-ring component was then formed in two further steps involving mesylate formation to afford **88**, followed by cyclization under basic conditions to give the desired cyclization product **89**. Lactam **89** was then easily converted to enamine **90** under standard Bischler-Napieralski conditions.

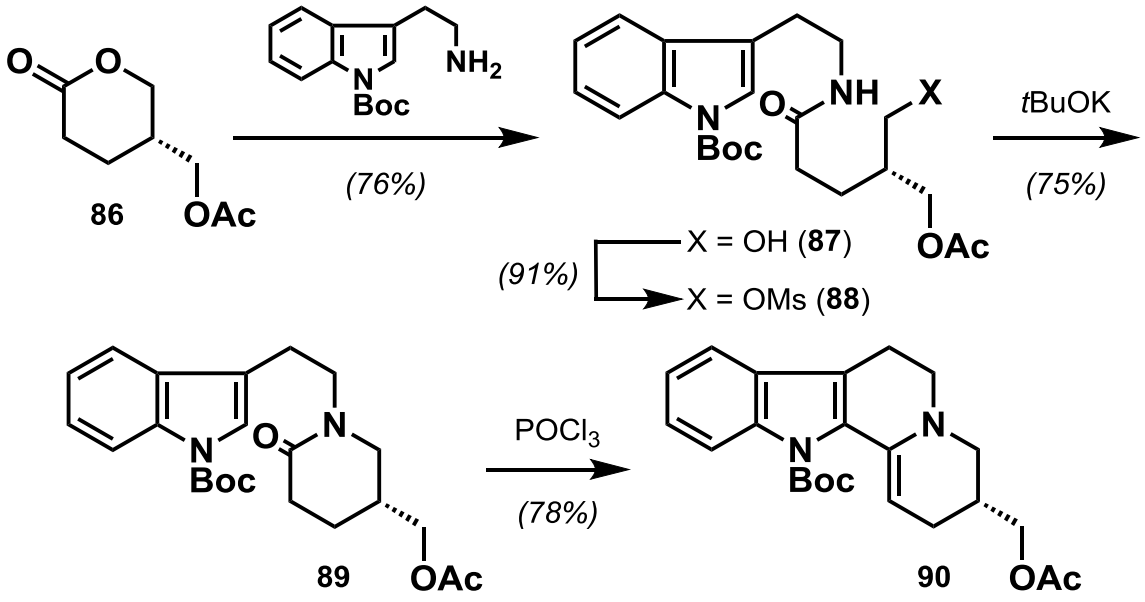

Scheme 17. Coupling of the tryptamine fragment and C-ring formation by Danieli *et al*.[9]

Through prior experience the group was aware that enamines such as **90** could be advanced to pentacyclic compounds embodying an oxazepinoindoloquinolizine skeleton (**91**, Scheme 18) through reaction with formaldehyde followed by sodium borohydride.

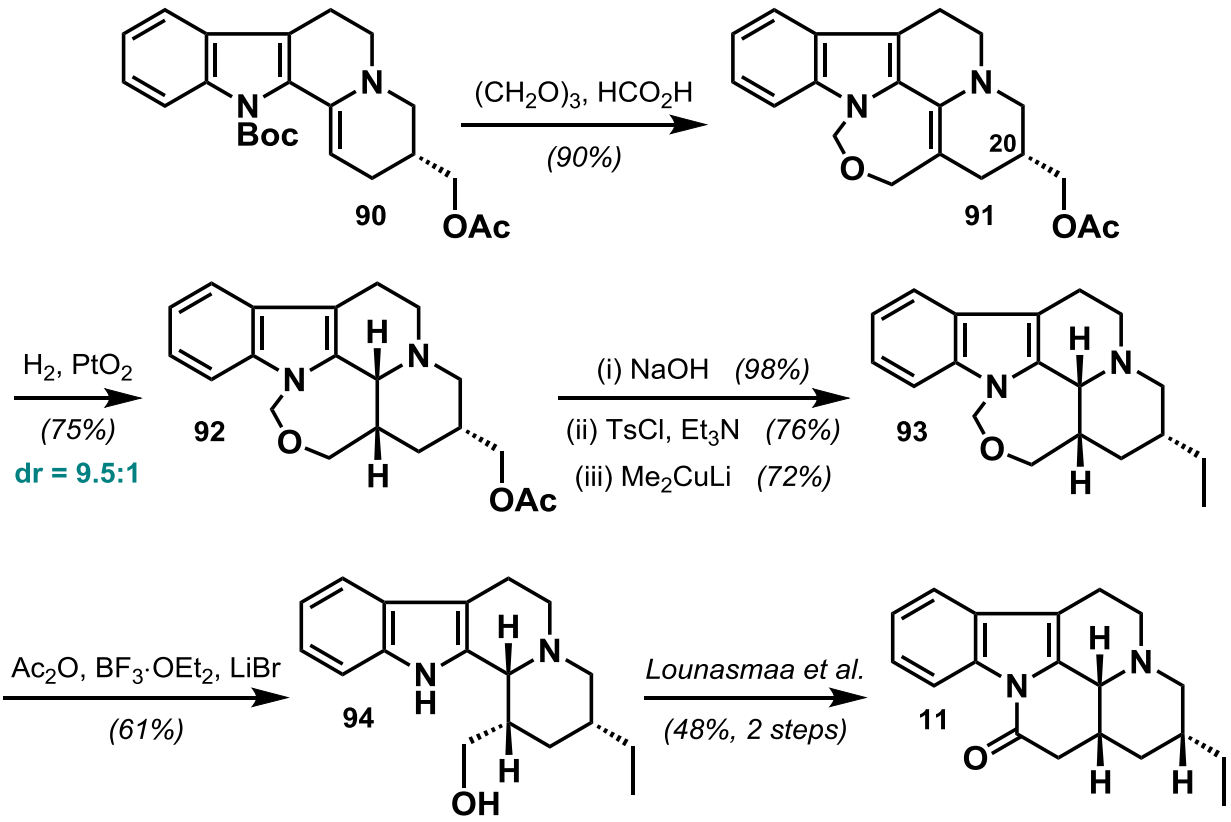

Scheme 18. Completion of the final known asymmetric total synthesis of (+)-tacamonine by Danieli *et al*.[9]

In the event, successful formation of pentacycle **91** still containing the C-3/C-14 double bond set the stage for the diastereoselective addition of hydrogen, on the basis that approach from the concave α-face of the molecule would be severely hindered by the pseudoaxial oriented C-20 group, as before. This process afforded **92** in high diastereomeric excess (9.5:1 dr) and in satisfactory yield (75%). Subsequent homologation of the C-20 acetoxymethyl side chain in **92** was achieved in a three-step sequence involving acetate hydrolysis, tosylation and displacement of the tosylate with lithium dimethyl cuprate (54% over 3 steps) to afford **93**. In the penultimate operation the group employed Sundberg's deprotection protocol to form alcohol **94**, which was followed by the concluding E-ring formation according to the Lounasmaa group's procedure[11] in suboptimal yields of 61% and 48% respectively.

Overall, the route encompasses a lengthy 17 operations over 15 steps from commercially available starting materials, providing enantiopure (+)-tacamonine (**11**) in only 4% overall yield.

1.4 Conclusions

As is evident from the discussion of these two reported asymmetric routes, there is much room for improvement in terms of the overall number of steps, as well as the efficiency of these steps, since the Ihara and Danieli groups were able to synthesise (+)-tacamonine in only 1% and 4% overall yields respectively from readily available starting materials.[8,9] Though the Ihara group's strategy proceeded over a reasonable 9 steps in comparison to the Danieli group's lengthy 15 step route, the major drawback was the lack of diastereoselectivity in the radical cyclization which ultimately had a significant impact on the overall yield and efficiency of the route as a whole.

Furthermore, these asymmetric routes both followed the standard linear ABD to ABCD ring-construction strategy beginning with a chiral, non-racemic precursor, obtained via chiral auxiliary-based methodology in the Ihara group, and enzymatic monoacetylation in the case of the Danieli group. In both cases this allowed for the pre-installation of the requisite homochiral C-20 stereocentre, from which the other stereocentres were successfully derived diastereoselectively by the Danieli group.

In view of these reports, we aimed to develop a concise, efficient, asymmetric total synthesis strategy following a novel ABC to ABCD approach, the full extent of which will be presented and discussed in Chapter 2.

1.5 References

1. D. B. England and A. Padwa, *J. Org. Chem.*, 2008, **73**, 2792-2802.
2. T. Aniszewski, in *Alkaloids – Secrets of Life*, Elsevier, Amsterdam, 1st edn, 2007, ch. 2, pp. 111-119.
3. P. M. Dewick, in *Medicinal Natural Products*, John Wiley & Sons Ltd, England, 2nd edn, 2002, ch. 6, pp. 346-359.
4. G. Massiot, F. S. Oliveira and J. Lévy, *Bull. Soc. Chim. Fr. II*, **1982**, 185-190.
5. D. Din Belle, A. Tolvanen and M. Lounasmaa, *Tetrahedron*, 1996, **52**, 11361-11378.
6. M. Lounasmaa, D. Din Belle and A. Tolvanen, *Tetrahedron Lett.*, 1995, **36**, 7141-7144.
7. T. A. van Beek, R. Verpoorte and A. B. Svendsen, *Tetrahedron*, 1984, **40**, 737-748.
8. M. Ihara, F. Setsu, M. Shohda, N. Taniguchi, Y. Tokunaga and K. Fukumoto, *J. Org. Chem.*, 1994, **59**, 5317-5323.
9. B. Danieli, G. Lesma, D. Passarella, A. Sacchetti and A. Silvani, *Tetrahedron Lett.*, 2001, **42**, 7237-7240.
10. F. Kellner, F. Geu-Flores, N. H. Sherden, S. Brown, E. Foureau, V. Courdavault and S. E. O'Connor, *Chem. Commun.*, 2015, **51**, 7626-7628.
11. M. Lounasmaa, K. Karinen, D. Din Belle and A. Tolvanen, *Tetrahedron*, 1998, **54**, 157-164.
12. R. Lavilla, O. Coll, J. Bosch, M. Orozco and F. J. Luque, *Eur. J. Org. Chem.*, **2001**, 3719-3729.
13. M. Lounasmaa and M. Puhakka, *Acta Chem. Scand.*, *Ser. B*, 1978, **32**, 77-78.
14. R. Lavilla, O. Coll, M. Nicolàs, B. A. Sufi, J. A. Torrents and J. Bosch, *Eur. J. Org. Chem.*, **1999**, 2997-3003.
15. T. Ho and Q. Lin, *Tetrahedron*, 2008, **64**, 10401-10405.
16. P. G. Gassman and X. Creary, *J. Chem. Soc. Chem. Commun.*, **1972**, 1214-1215.
17. C. Chen, B. Chang, M. Tsai, M. Chang and N. Chang, *Tetrahedron*, 2003, **59**, 9383-9387.

18. C. Chen, M. Chang, R. Hsu, S. Chen and N. Chang, *Tetrahedron Lett.*, 2003, **44**, 8627-8630.

19. B. Danieli, G. Lesma, S. Macecchini, D. Passarella and A. Silvani, *Tetrahedron: Asymmetry*, 1999, **10**, 4057-4064.

20. K. Takasu, N. Nishida, A. Tomimura and M. Ihara, *J. Org. Chem.*, 2005, **70**, 3957-3962.

21. M. Ihara, *Chem. Pharm. Bull.*, 2006, **54**, 765-774.

22. A. Deiters, M. Pettersson and S. F. Martin, *J. Org. Chem.*, 2006, **71**, 6547-6561.

23. A. H. Hoveyda and Z. Xu, *J. Am. Chem. Soc.*, 1991, **113**, 5080-5082.

24. J. P. Morken, M. T. Didiuk and A. H. Hoveyda, *J. Am. Chem. Soc.*, 1993, **115**, 6997-6998.

25. D. A. Evans, K.T. Chapman, D. T. Huang and A. T. Kawaguchi, *Angew. Chem.*, *Int. Ed. Engl.*, 1987, **26**, 1184-1186.

C H A P T E R 2

Results and Discussion

2.1 Background

2.1.1 Introduction

Natural (+)-tacamonine has been a long-standing synthetic target in our laboratory, with initial studies dating as far back as 1997.[1] These model studies, which will be discussed in detail shortly, were based on the generation of the *tacaman* skeleton through cyclization of an α-acylamino radical.[1-3] The aim of this work was thus to extend this methodology to a modified system in order to complete an asymmetric total synthesis of (+)-tacamonine (**1**, Figure 1).

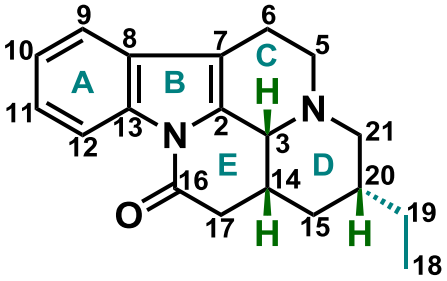

1: (+)-tacamonine

Figure 1. A depiction of the natural (+)-tacamonine numbering convention used in the literature.[4]

When considering the structure of (+)-tacamonine (**1**, Figure 1), the two significant synthetic challenges that needed to be addressed, in addition to the construction of the pentacyclic core itself, were the control of both the C-3/C-14 D/E *cis*-ring junction diastereoselectivity as well as the C/D to C-20 (ethyl) *anti*-diastereoselectivity, since all the C-3, C-14, and C-20 methine hydrogens had to be positioned *cis* relative to each other. Our approach to these intricate synthetic challenges will be discussed later on. At this stage, however, it should be noted that all the structures presented in this chapter are numbered relative to the natural (+)-tacamonine numbering convention as shown in Figure 1 (ring designations A to E also shown).[4]

2.1.2 Previous Work: Stereoselective Model D-Ring Construction Strategies

In 1997 our group developed a moderately stereoselective benzylic α-acylamino radical cyclization strategy for addressing the chemistry of generating the *tacaman* D/E-ring junction, in which a phthalimide template was used to model the ABC ring system.[1] In this (Scheme 1), it was found that cyclization of the ribose-derived **2** could be achieved under normal radical cyclization conditions (via radical intermediate **3**) leading predominantly to the undesired *trans*-H C-3/C-14 junction in **4** in a 4:1 diastereomeric ratio.

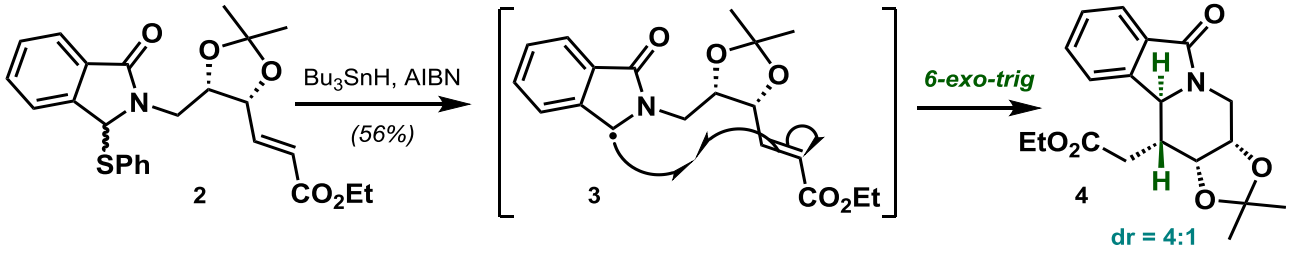

Scheme 1. *Reagents and conditions:* Bu_3SnH (1.5 equiv), AIBN (0.1 equiv), benzene, reflux, 4 h, 56%, dr = 4:1.

Although it gave the wrong target D/E ring-junction relative stereochemistry, as well as having a five-membered modelling for the C-ring, nevertheless, it suggested that a benzylic radical could be generated and utilised for the purpose of forming the target's C3-C14 D/E bond, as well as suggesting that an adjacent allylic centre to C-14 might be able to satisfactorily direct the diastereoselectivity of ring junction formation.

This notion was tested in a subsequent 2000 work (Scheme 2), where a modified precursor **5** derived from (*S*)-malic acid was subjected to the same radical cyclization conditions.[2] This led to the formation of the desired major *cis*-H diastereomer **6** in a 4:2:1 diastereomeric ratio following silyl group removal, providing support in favour of directing the diastereoselectivity, this time through the use of a bulky silyloxy group at the allylic position to achieve the correct *cis*-D/E-diastereoselectivity.

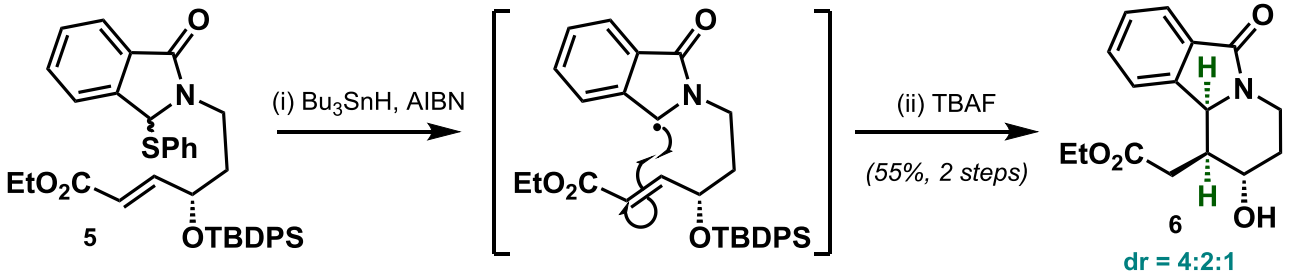

Scheme 2. *Reagents and conditions:* (i) Bu_3SnH (3 equiv), AIBN (0.1 equiv), PhMe, reflux; (ii) TBAF, THF, 55% (as major diastereomer, over 2 steps), dr = 4:2:1.

In a more recent work published in 2009, the same radical cyclization methodology was applied to a substrate more closely related to the *tacaman* skeleton; namely, that of 2-acyl-1-phenyl-thiotetrahydro-β-carboline (**9**, Scheme 3).[3] This model precursor **9** was synthesized through *N*-acylation/iminium ion trapping of an acid (**7**) and 3,4-dihydro-β-carboline (**8**) under mild conditions, designed to accommodate sensitive acids bearing α-stereocentres (as is the case of the target).

It was found that this could be achieved in one-pot through initial DCC/HOBt-activation of the acid **7** followed by *N*-acylation with the highly nucleophilic β-carboline **8**.

Concomitant low-temperature boron trifluoride diethyl etherate-mediated interception of the resultant iminium ion with thiophenol provided **9** in high yield.

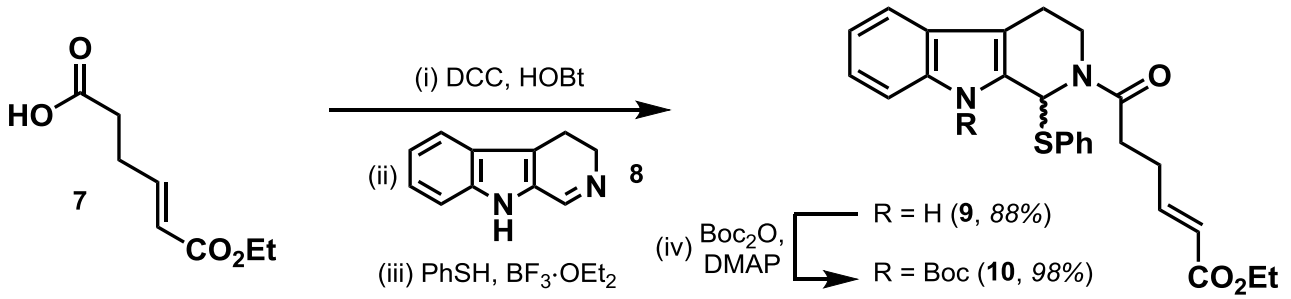

Scheme 3. *Reagents and conditions:* (i) **7** (1.2 equiv), DCC (1.2 equiv), HOBt (1.2 equiv),CH_2Cl_2, 0 °C; (ii) 3,4-dihydro-β-carboline (1.0 equiv); (iii) PhSH (1.3 equiv), $BF_3{\cdot}OEt_2$ (1.3 equiv), –78 °C, 88% (one-pot); (iv) Boc_2O (1.3 equiv), DMAP (0.1 equiv), THF, rt, 98%.

Subsequent indole *N*-Boc protection afforded the requisite precursor **10**, which was then subjected to the standard radical cyclization conditions (Scheme 4). Much to our group's delight, the desired *cis*-H diastereomer **11** was formed as the major product in 81% yield in addition to the minor *trans*-H diastereomer **12** and radical reduction product **13** in 12% and 6% yields respectively (dr = 6.5:1), **11** and **12** both as racemic products.

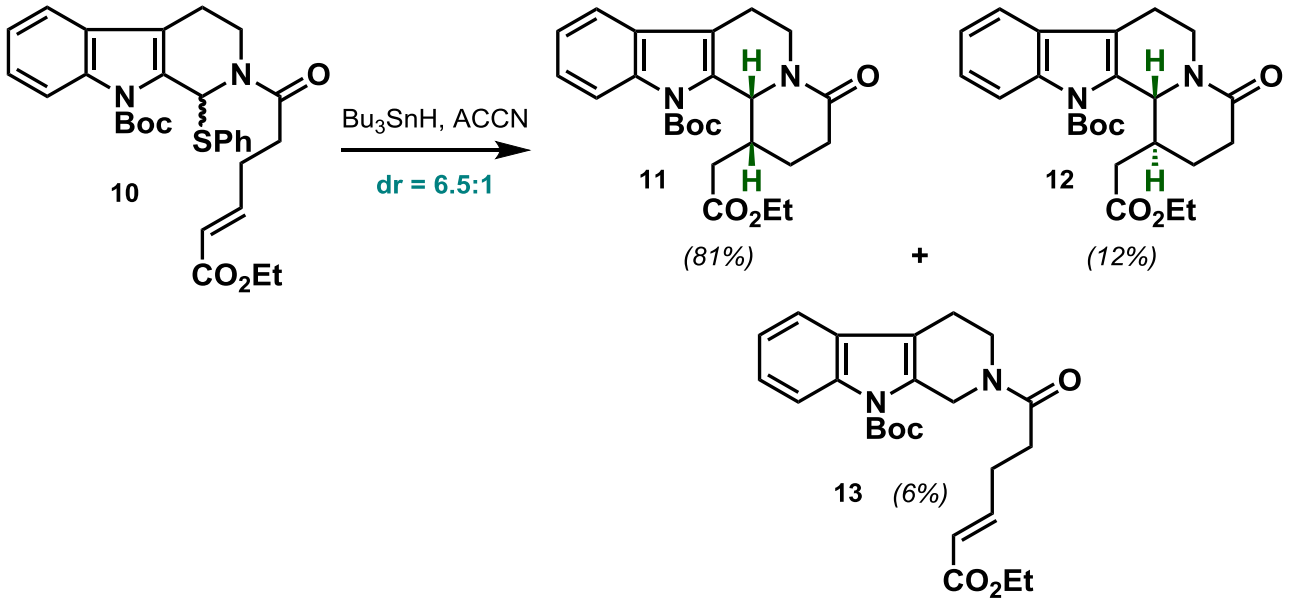

Scheme 4. *Reagents and conditions:* Bu_3SnH (1.5 equiv), ACCN (0.1 equiv), PhMe, reflux, 81% (**11**), 12% (**12**), 6% (**13**), dr = 6.5:1.

Further evidence for the formation of the desired *cis*-H diastereomer was provided in the form of an X-ray crystal structure determination. To this end, major lactam **11** (isolated as a gum) was subjected to standard saponification conditions to afford the crystalline acid. The X-ray structure of the acid **14** obtained (shown in Figure 2) clearly confirmed the desired *cis* arrangement of H-3 and H-14.

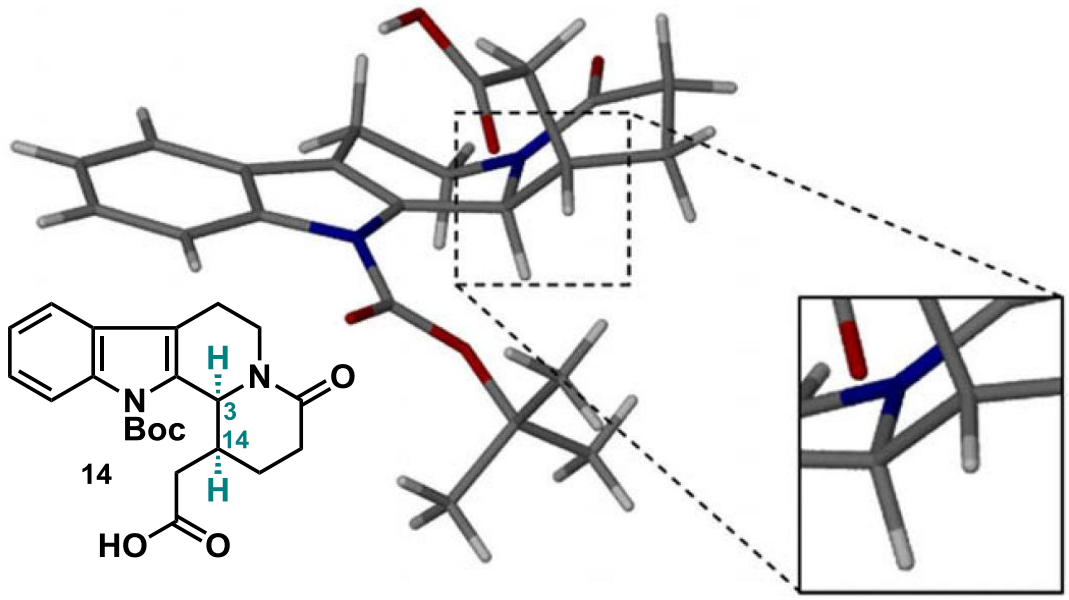

Figure 2. X-ray crystal structure of acid **14** displaying the correct *cis* arrangement of H-3 and H-14 by Smith *et al*.[3]

The proposed transition states for the formation of the *cis*-H (**11**) and *trans*-H (**12**) products are shown in Figure 3 as **TS-1** and **TS-2** respectively. In this model, which was based on the assumption that the larger indole substituent adopts a pseudoequatorial position, **TS-1** showed that the *cis*-H product would arise from the enoate ester adopting a pseudoaxial orientation, while in **TS-2**, the ester in a pseudoequatorial orientation would afford the *trans*-H product. In the case of the latter, non-bonded steric interaction of the ester with the bulky *N-tert*-butoxycarbonyl group causes significant destabilization, thus favouring the formation of the *cis* product.

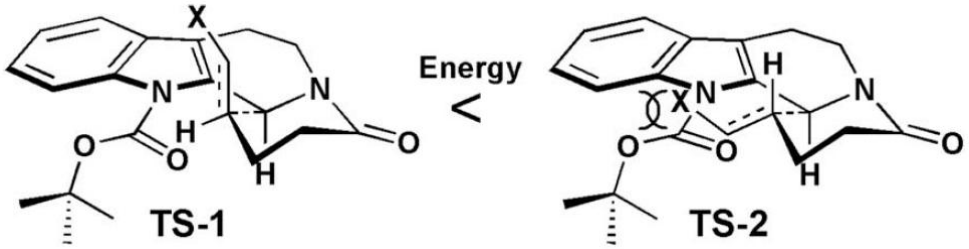

Figure 3. Proposed transition state model for the observed stereoselectivity (X = CO_2Et) by Smith *et al*.[3]

This encouraging result in favour of the generation of the *cis*-H (D/E) diastereomer propelled us to attempt the radical cyclization on the tacamonine precursor itself, with the C-20 ethyl group already in place, in the hope of achieving the correct C-3/14 to C-20 diastereoselectivity.

2.1.3 Retrosynthetic Analysis of (+)-Tacamonine

Our approach using this radical cyclization disconnection strategy is thus outlined retrosynthetically in Scheme 5. In the forward sense, using coupling methodology shown in Scheme 3, we envisaged the synthesis of the radical cyclization precursor **17** through coupling/trapping of a chiral acid ester fragment (**15**) and 3,4-dihydro-β-carboline (**8**) followed by *N*-Boc protection. We postulated that concomitant radical cyclization should then result in the stereoselective formation of the desired all *cis*-H diastereomer **18**. Additionally, the initial end-game strategy perceived for the subsequent conversion of the cyclization product **18** to (+)-tacamonine (**1**) involved *N*-Boc deprotection, base-mediated E-ring formation and chemoselective reduction processes respectively.

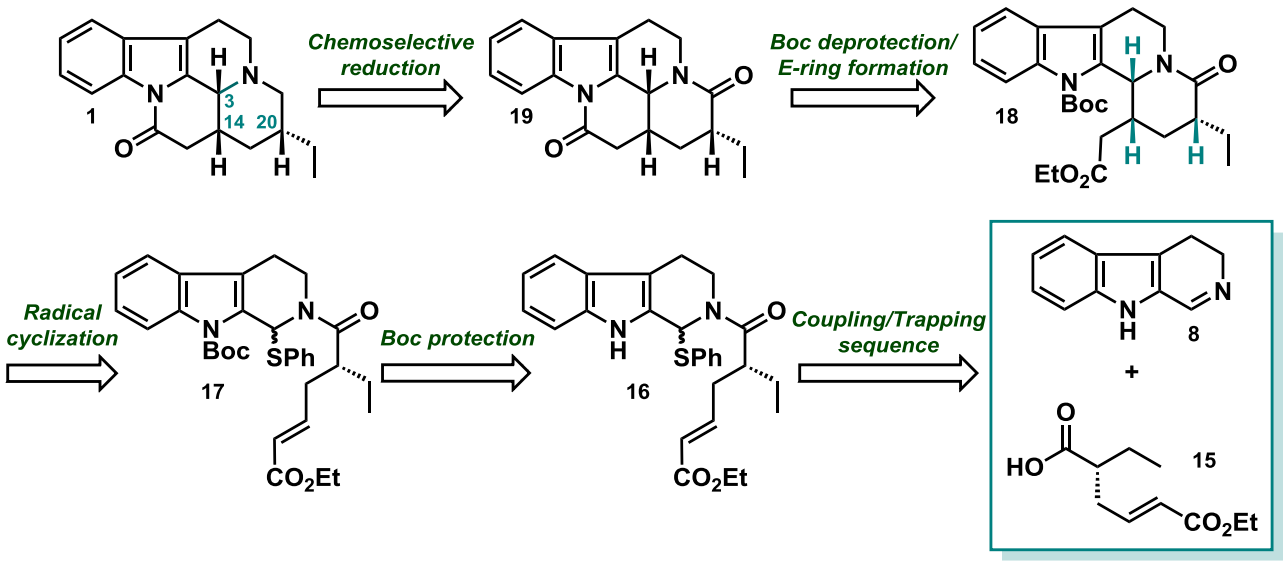

Scheme 5. Our retrosynthetic analysis of (+)-tacamonine.

Our retrosynthetic approaches to each of the identified coupling fragments **15** and **8** are in turn shown in Scheme 6. In the forward sense, we envisaged the synthesis of the chiral acid ester fragment **15** through diastereoselective auxiliary-controlled allylation followed by auxiliary cleavage and attachment of the ester moiety via olefin metathesis. In the case of the carboline fragment **8**, we envisaged *N*-formylation of tryptamine and subsequent Bischler-Napieralski cyclization of the product.

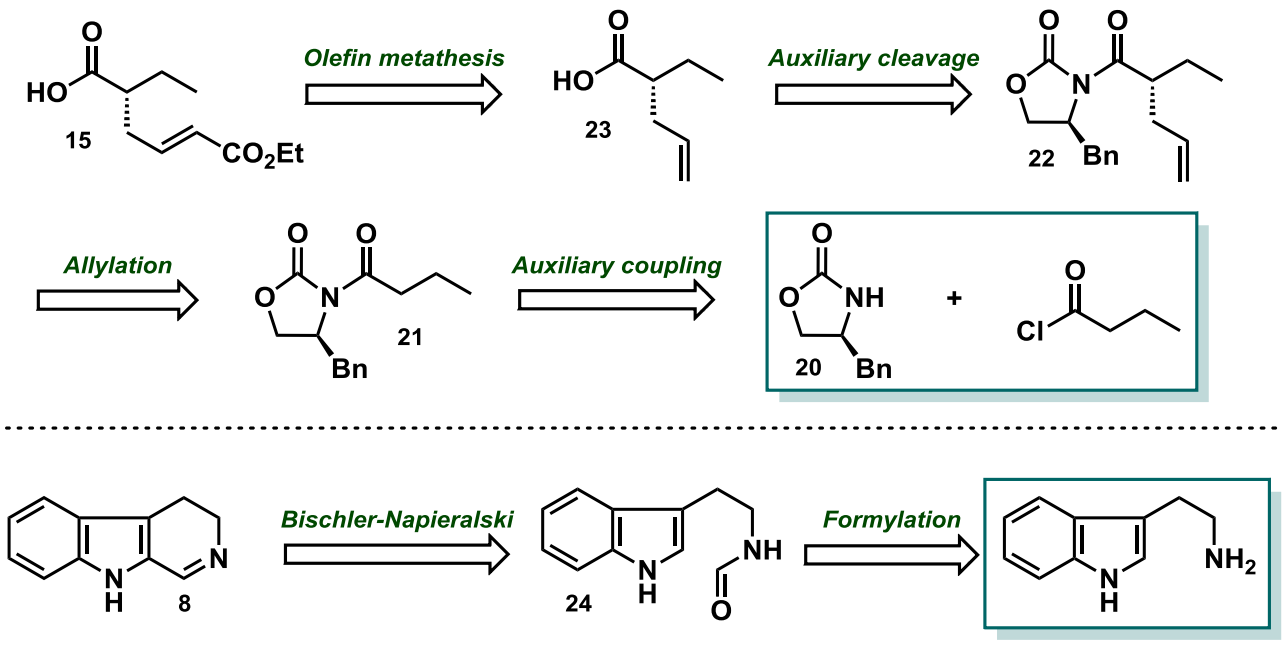

Scheme 6. Retrosynthetic analysis of the acid ester (**15**) and carboline (**8**) fragments respectively.

Naturally, we expected various challenges to arise along the way, particularly in the case of the radical cyclization step, although we believed that the same controlling factors would hold leading to the required D/E stereoselectivity as for the model (Figure 3). What was not apparent, however, was the question of the *anti* C-3/C-14 (D/E) to C-20 diastereoselectivity, that is, to obtain the D/E-ring junction as having the hydrogens both 'up' in absolute stereochemical terms, as in (+)-tacamonine (**1**, Scheme 5 for numbering). Before carrying out the synthesis it is true to say that we did not have any firm mechanistic basis for confidently believing that the radical cyclization would result in achieving this stereo-outcome, other than the fact that generating a *cis* D/E-ring junction with the hydrogens 'up' would secure a pseudoequatorial configuration for the C-20 'down' ethyl group (see later). Similarly, a level of concern existed for achieving an appropriate chemical efficiency in the final chemoselective reduction.

A discussion of our results now follows, and any modifications made to the initial strategy and justifications thereof will be presented.

2.2 Asymmetric Total Synthesis of (+)-Tacamonine

2.2.1 Synthesis of the Chiral Acid Ester and Carboline Fragments

We began our asymmetric total synthesis of (+)-tacamonine by first synthesizing each of the previously identified coupling fragments, namely, 3,4-dihydro-β-carboline (**8**) and the chiral acid ester **15**.

In the case of the former, the procedure of Whittaker[5] was adopted in a classical Bischler-Napieralski reaction as shown in Scheme 7, proceeding via an electrophilic aromatic substitution based cyclization involving an iminium species (not shown).

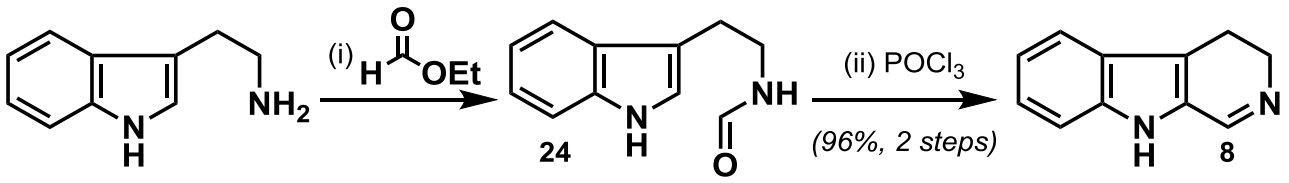

Scheme 7. *Reagents and conditions:* (i) ethyl formate (excess), 70 °C, 17 h; (ii) $POCl_3$ (excess), 0 °C to rt, 1.5 h, 96% (over 2 steps).

To that end, a suspension of tryptamine in excess ethyl formate was heated overnight and left to cool to room temperature after 17 h. The remaining ethyl formate was then removed *in vacuo* to afford crude *N*-formyltryptamine **24** as a brown oil,[6] which was immediately used in the next step without further purification. Advancement to 3,4-dihydro-β-carboline was achieved through treatment of **24** with excess phosphoryl chloride at 0 °C, followed by stirring at room temperature. After 1.5 h excess phosphoryl chloride was removed by distillation. The target carboline fragment **8** was then isolated in 96% crude yield over two steps in gram quantities (~10 g scale) following quenching with water and basic work-up. ^{1}H NMR spectroscopy of the resulting crude pale yellow micro-crystalline product showed all the characteristic peaks along with line broadening as a result of 3,4-dihydro-β-carboline existing in equilibrium with its dimeric form.**7** The ^{1}H NMR spectral and melting point data obtained were in agreement with the literature,[5,6] which indicated that the crude material could be used without further purification.

With 3,4-dihydro-β-carboline in hand we focused our efforts toward the synthesis of chiral acid ester fragment **15**. Using the method of Evans[8] (Scheme 8), (*S*)-4-benzyl-2-oxazolidinone **20** (~1 g scale) was treated with *n*-butyllithium at low temperature followed by the addition of butyryl chloride after 30 min and allowing the solution to warm to room temperature. TLC analysis showed the clean conversion of the starting material to a less polar spot as expected. After 4 h the solution was quenched, extracted and purified by flash chromatography to afford the known butylated oxazolidinone **21** in 98% yield and in high enantiomeric excess (98%) as ascertained by chiral HPLC on a chiral OD column. The ^{1}H NMR, ^{13}C, IR, HRMS and optical rotation data of **21** were all in agreement with the literature data (see Chapter 3 section 3.1).[8,9]

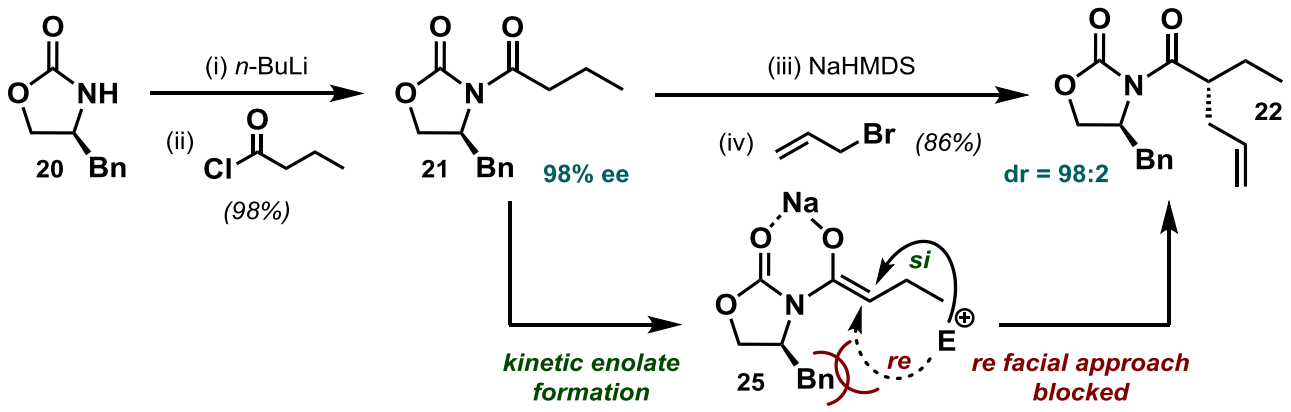

Scheme 8. *Reagents and conditions:* (i) *n*-BuLi (1.1 equiv), THF, –78 °C, 30 min; (ii) butyryl chloride (1.4 equiv), –78 °C to rt, 4 h, 98%, 98% ee; (iii) NaHMDS (1.1 equiv), THF, –78 °C, 30 min; (iv) allyl bromide (2.5 equiv), –78 °C to –20 °C, 5 h, 86%, dr = 98:2.

In the following step, oxazolidinone **21** (~1 g scale) was treated with sodium hexamethyldisilazide at –78 °C to allow for the formation of the (*Z*)-kinetic enolate as depicted in Scheme 8 as **25**, followed by the addition of allyl bromide after 30 min. The reaction mixture was then left to warm slowly to –20 °C over 5 h after which it was quenched, extracted and purified by flash chromatography to afford the known allylated oxazolidinone **22** in 86% yield and in a diastereomeric ratio of 98:2 as ascertained by HPLC on a C-18 column. The diastereoselectivity manifested in this step is as a result of steric blockage of *re* facial approach of the electrophile by the chiral auxiliary, which is locked in place through sodium ion chelation, all in accordance with the model proposed by Evans in his original work.[10] Furthermore, full characterization data obtained was once again in complete agreement with the literature data for **22**.[11]

Advancement to the desired chiral acid ester fragment **15** was achieved in two further steps, involving auxiliary cleavage and olefin metathesis (Scheme 9). In the case of the former, allylated auxiliary **22** (~1 g scale) was treated with lithium hydroperoxide at 0 °C for 2 h for the chemoselective hydrolysis of the exocyclic carbonyl group, followed by the addition of sodium sulfite for the reduction of the peracid intermediate and the consumption of unreacted lithium hydroperoxide.[12] TLC analysis showed the clean conversion of the non-polar starting material to the characteristic polar acid spot. A subsequent extraction process allowed for 96% recovery of the chiral auxiliary. Further acidification, re-extraction and concentration *in vacuo* processes afforded crude acid **23** in quantitative yield and in high purity.

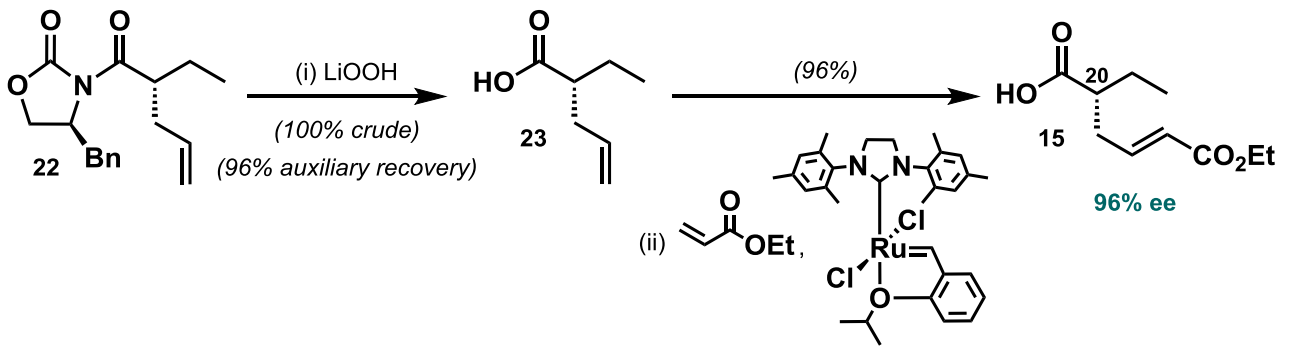

Scheme 9. *Reagents and conditions:* (i) $LiOH{\cdot}H_2O$ (2 equiv), H_2O_2 (5 equiv), Na_2SO_3, THF/H_2O, 0 °C, 2 h, 100% (crude yield), 96% (auxiliary recovery); (ii) ethyl acrylate (5 equiv), Hoveyda-Grubbs 2nd generation cat. (0.01 equiv), CH_2Cl_2, rt to 50 °C, 2 h, 96%, 96% ee.

This auxiliary cleavage procedure, pioneered by Evans, was selected as it is known to allow for the chemoselective detachment of the exocyclic carbonyl group without racemization of the newly installed chiral centre at C-20.[12] It thus allowed for the swift formation of the desired chiral acid **23** under mild conditions at low temperature with no further purification deemed necessary.

The ^{1}H NMR spectrum of the chiral acid **23** obtained contained all the requisite peaks as shown in Figure 4, most notably the newly installed vinyl system (H-14/H-17).

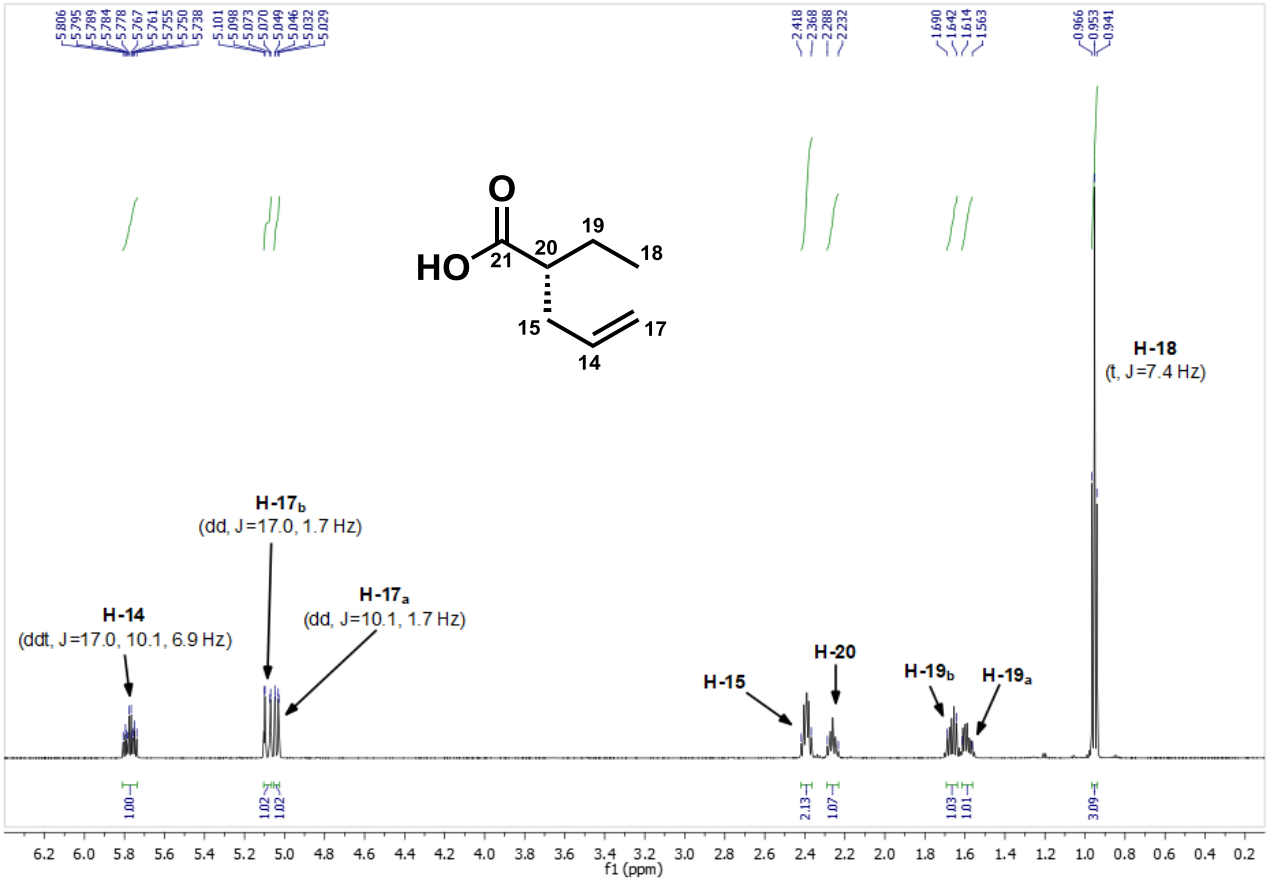

Figure 4. Crude ^{1}H NMR spectrum of chiral acid **23**.

The H-14 signal was seen resonating at 5.77 ppm as well as the H-17 protons which were each seen as a doublet of doublets resonating at 5.09 and 5.04 ppm respectively with the appropriate geminal (1.7 Hz), *cis*-vinyl (10.1 Hz) and *trans*-vinyl (17.0 Hz) couplings. The H-20 proton was observed as a single multiplet resonating at 2.21 ppm along with the diastereotopic and hence magnetically non-equivalent H-19 protons seen as two multiplets at 1.66 and 1.59 ppm respectively.

In the concluding operation (Scheme 9), acid **23** (~1 g scale) was subjected to olefin metathesis conditions involving reflux with excess ethyl acrylate in the presence of the Hoveyda-Grubbs 2nd generation catalyst for 2 h. This catalyst, in particular, was selected as it is known to favour the generation of the *trans*-alkene product in accordance with our target requirements.[13] Following subsequent cooling, concentration *in vacuo* and purification by flash chromatography the desired acid ester fragment **15** was isolated in high 96% yield. Chiral HPLC analysis on an IC column verified that the loss of optical purity over these two steps was minimal as the enantiomeric excess remained virtually unchanged (98% to 96% ee), thus confirming that negligible racemization had occurred in the auxiliary cleavage process, as expected. Furthermore, our somewhat unusual decision to process the acid **23** itself in this way, instead of making use of any other potential surrogate group, was due to the need for chemoselectivity differentiation in the ensuing coupling step with the ester group already in place.

The ^{1}H NMR spectrum of the acid ester fragment **15** (Figure 5) revealed the appearance of the newly installed ethoxycarbonyl group. Evidence for the formation of the *trans*-alkene was provided by the H-17 signal, which was now seen as a doublet at 5.87 ppm, with an appropriate *trans*-vicinal coupling of 15.6 Hz. Similarly, the ^{13}C NMR spectrum (Figure 5) showed the presence of the downfield acid carbonyl group (C-21) at 180.7 ppm as well as the newly installed ester carbonyl group (C-16) at 166.5 ppm. The vinyl carbon signals were seen at 145.4 and 123.6 ppm respectively, with the C-14 signal more deshielded than the C-17 signal as expected due to resonance considerations. The tertiary C-20 signal appeared at 60.5 ppm, followed by the two secondary C-15 and C-19 carbon signals appearing at 33.7 and 24.8 ppm respectively (C-15 is deshielded relative to C-19 due to being allylic to the vinylic carbethoxy system). The secondary and primary carbon signals of the ethoxy group appeared at 45.7 and 14.4 ppm and are highlighted in Figure 5. Finally, the primary C-18 signal was seen at 11.5 ppm and was shielded relative to the primary ethoxy carbon as expected. Overall, a total of 10 carbon resonances were seen in the spectrum corresponding to all 10 carbon atoms in the acid ester structure.

Other evidence in support of the formation of the acid ester fragment **15** was obtained in the form of HRMS.

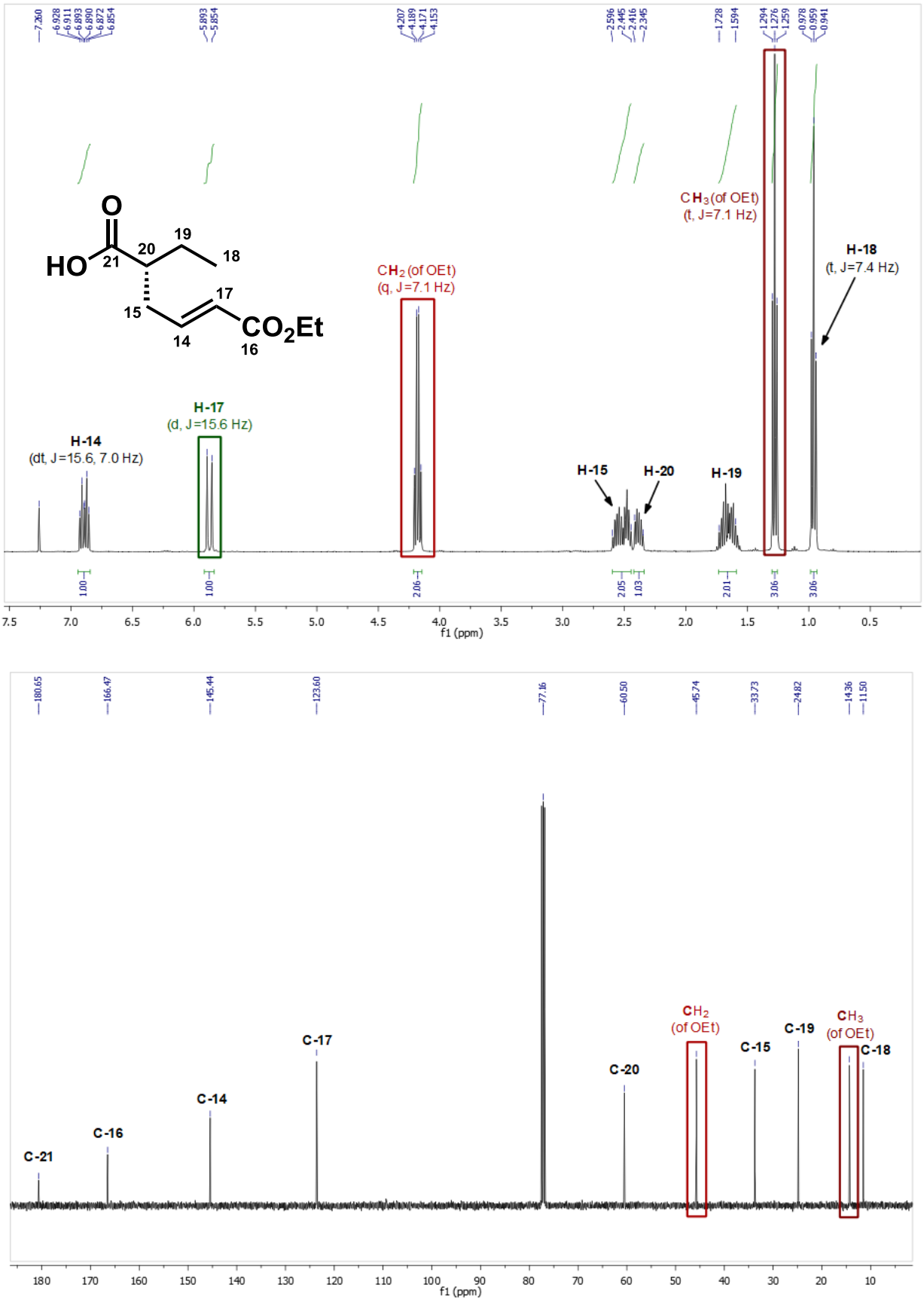

Figure 5. ^{1}H (top) and ^{13}C (bottom) NMR spectrum of the acid ester fragment **15**.

2.2.2 Synthesis of the Radical Cyclization Precursor

At this stage, with both the requisite carboline **8** and acid ester **15** fragments in hand, we envisaged the formation of the desired radical precursor **17** through our one-pot DCC coupling/thiophenol trapping sequence, followed by indole *N*-Boc protection of the product.[3] There are recent alternatives for this type of coupling such as propylphosphonic anhydride[14] (T3P, Figure 6), but we elected to go ahead with our method.

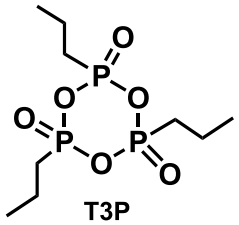

Figure 6. Alternative amide coupling reagent T3P.

To this end (Scheme 10), acid ester **15** was cooled to 0 °C and treated with *N,N*'-dicyclohexylcarbodiimide, 1-hydroxybenzotriazole and 3,4-dihydro-β-carboline (**8**) with stirring for 1 h. During this time TLC analysis showed a full conversion of the starting material to more polar spots as expected. The reaction mixture was then cooled to –78 °C followed by the addition of boron trifluoride diethyl etherate and then thiophenol, and the mixture left to warm slowly to –50 °C over a 1 h period; TLC analysis now indicating the conversion to two less polar spots. Following subsequent quenching, multiple extraction and filtration processes (for the removal of the urea by-product), and purification by flash chromatography, the desired sulfanyl amides **16** were isolated in 91% yield as a mixture of two diastereomers, with two amide rotamers each (see NMR analysis later). The scrambling at the sulfanyl C-3 stereocentre diastereomers was seen to be inconsequential at this stage since its stereogenicity would be lost upon formation of the radical species in the ensuing cyclization step.

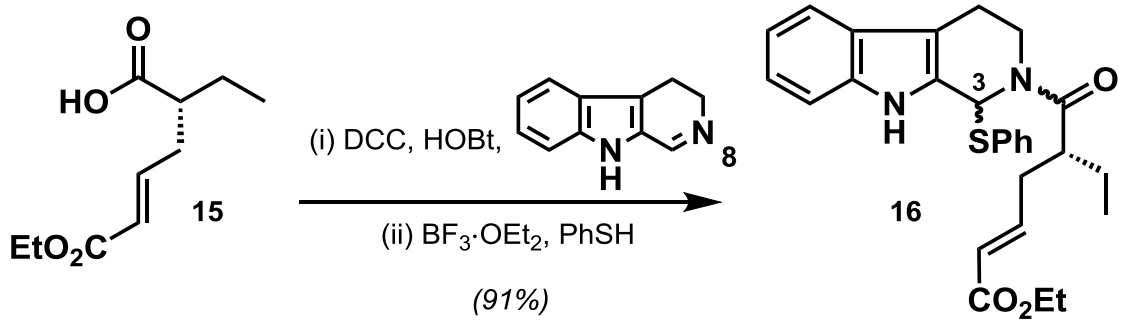

Scheme 10. *Reagents and conditions:* (i) DCC (1.1 equiv), HOBt (1.1 equiv), 3,4-dihydro-β-carboline (1.2 equiv), CH_2Cl_2, 0 °C, 1 h; (ii) $BF_3{\cdot}OEt_2$ (1.3 equiv), PhSH (1.3 equiv), –78 °C to –50 °C, 1 h, 91%.

The postulated mechanism of this one-pot *N*-acylation/iminium ion trapping procedure is shown in Scheme 11.

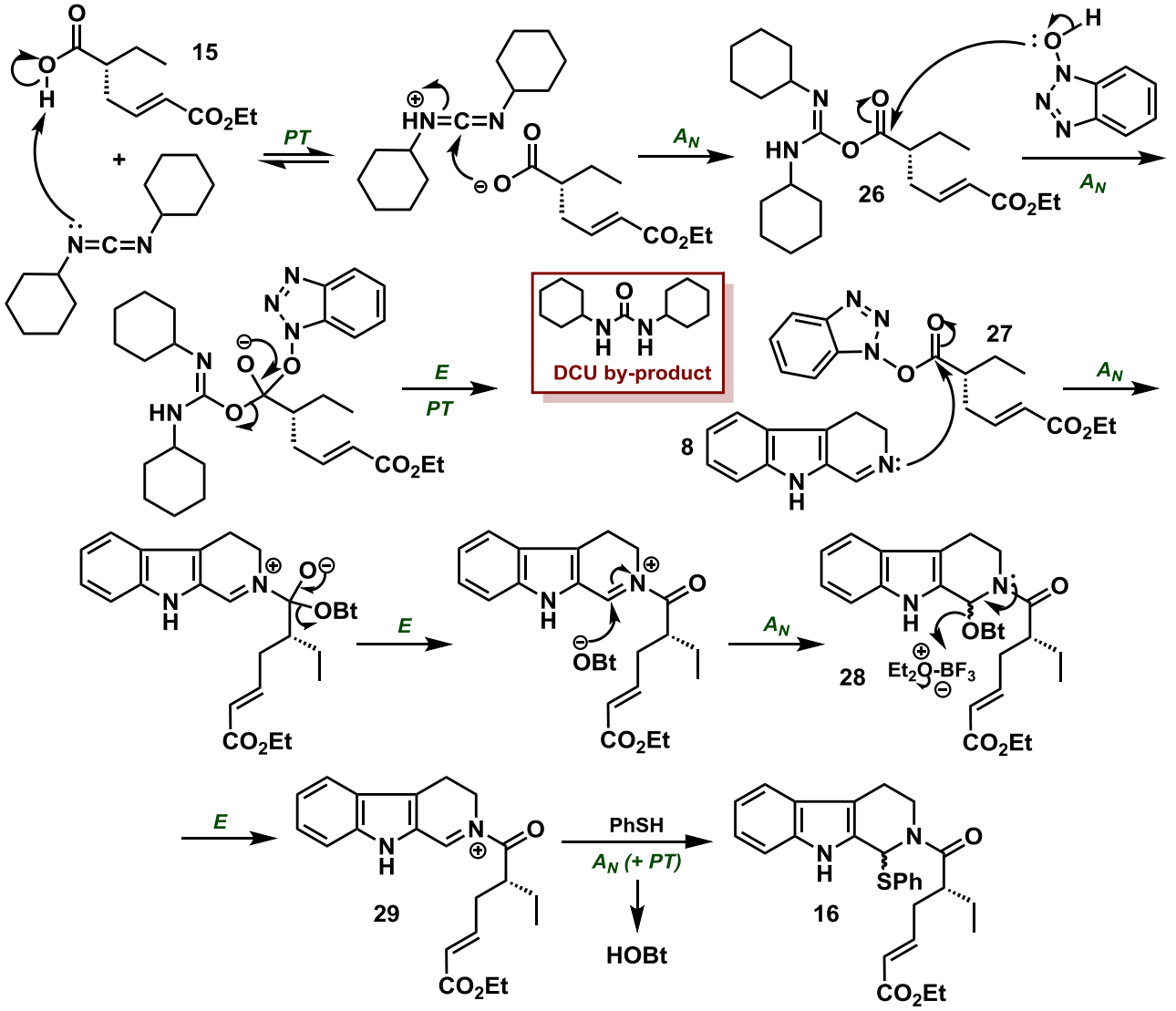

Scheme 11. Mechanism of the *N*-acylation/iminium ion trapping of acid ester **15** and 3,4-dihydro-β-carboline (**8**).

The first step involves the reaction of the acid ester **15** and *N,N'*-dicyclohexylcarbodiimide to form the O-acylurea **26**. 1-Hydroxybenzotriazole then substitutes O-acylurea **26** to give the BtO-active ester **27** and the dicyclohexylurea by-product. The presence of the BtO group enhances the reactivity of the activated ester by encouraging/stabilising the approach of 3,4-dihydro-β-carboline in the following step via hydrogen bonding,[15] which acylates to form the iminium ion, which presumably then gets intercepted by the BtO leaving group to form α-alkoxy amide **28**. Subsequent boron trifluoride diethyl etherate-mediated elimination via an S_N1 dissociative process promotes dissociative cleavage back to the iminium ion **29**, which then adds thiophenol to form the much more stable α-sulfanyl amides **16**.

For purposes of the NMR discussion that follows it should be noted that both the ^{1}H and ^{13}C NMR spectra obtained for the sulfanyl amides **16** have been divided into two parts due to their complex nature. The ^{1}H NMR spectrum is shown over the 0 to 5 ppm range in Figure 8 while the 5 to 9 ppm range is shown in Figure 9. Similarly, the ^{13}C spectrum is shown over the 0 to 75 ppm and 100 to 180 ppm ranges in Figure 10 respectively. Moreover, the peaks belonging to the ethoxycarbonyl system have from this point onwards been labelled as 'OEt' for simplicity. Finally, these spectra would have been impossible to assign without the assistance of COSY (not shown) and HSQC analysis. In view of this, the corresponding HSQC data is shown below the ^{1}H NMR spectra in Figures 8 and 9.

The ^{1}H NMR spectrum of the sulfanyl amides **16** (Figure 8, Figure 9) revealed the appearance of 4 signals for each magnetically equivalent aliphatic and vinyl proton environment due to the presence of 2 diastereomers with 2 amide rotamers each as shown in Figure 7. They were found to exist in an 8:6:3:2 ratio, as estimated by ^{1}H NMR, and have been grouped together for assignment purposes since the assignment of all the individual peaks for each diastereomer and each amide rotamer was beyond the scope of this work. Furthermore, integration of the individual peaks have been omitted for simplicity.

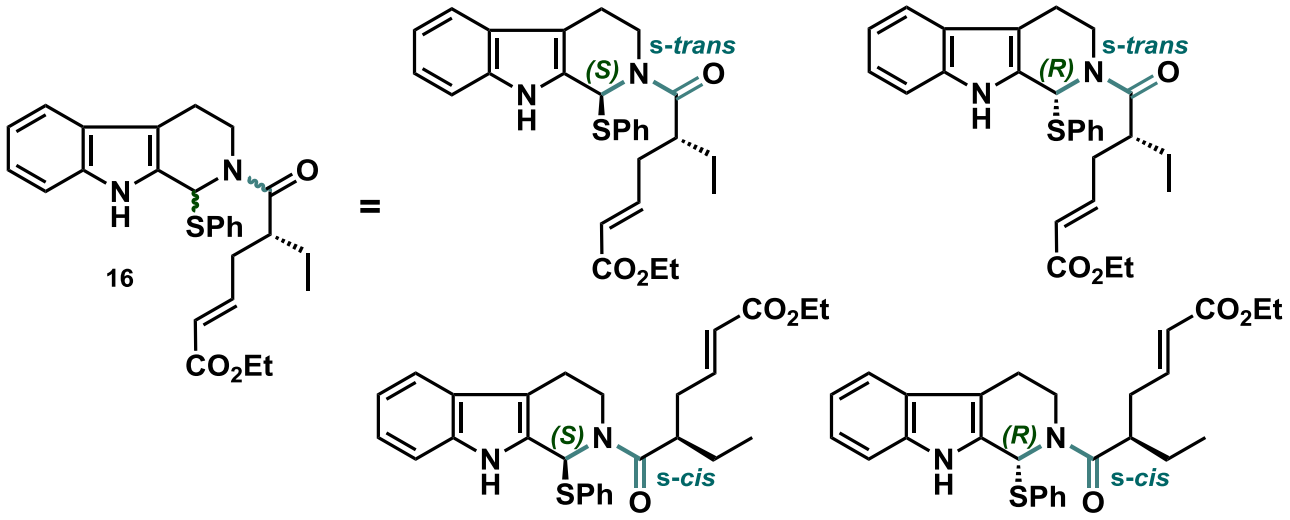

Figure 7. A depiction of the amide rotamers and diastereomers present in the NMR spectra of the sulfanyl amide **16**.

Analysis of the ^{1}H NMR spectrum for the 0 to 5 ppm range (Figure 8) revealed four distinct triplets resonating in the 0.7 ppm range corresponding to the magnetically equivalent H-18 protons (Me of the Et group). Similarly, four triplets (two overlapping) were seen in the 1.2 ppm range for the protons attached to the primary carbon of the ethoxy group and were deshielded relative to the H-18 signals as expected. The diastereotopic and thus magnetically non-equivalent H-19 protons were similarly seen as four multiplets in the 1.5 ppm region while the diastereotopic H-15 protons were deshielded resonating in the 2.3 ppm region as expected. The H-20 proton was observed as four multiplets, with two overlapping at 2.21 and 2.78 ppm respectively, while the H-6 protons were seen overlapping at 2.82 ppm. The proton signals for the secondary carbon of the ethoxy group were dispersed over 3.22 to 4.23 ppm. The H-5 protons were seen as four signals at 3.31, 3.83, 4.09 and 4.92 ppm, interestingly displaying a large 1.61 ppm separation between the first and last signal.

In the remainder of the spectrum shown in Figure 9 (5-10 pm range), four distinct doublets for the H-17 proton of the vinyl system were seen resonating in the 5.7 ppm region while the vinyl H-14 signals were deshielded relative to H-17 in the 6.5 to 6.9 ppm range as expected, but also appearing as four distinct doublets. The H-3 proton was seen as four singlets at 6.34, 6.44, 7.38 and 7.42 ppm, once again displaying a significant 1.08 ppm separation between the first and last signals similar to H-5. A possible explanation for this is that the s-*cis* amide rotamer has its carbonyl group deshielding zone facing towards H-3. A similar effect could thus be present for H-5 due to the close proximity of H-5 to the amide bond. Finally, the proton of the secondary amine was seen as four distinct singlets in the reasonable 8.2 ppm region. Aromatic protons were clumped as a range.

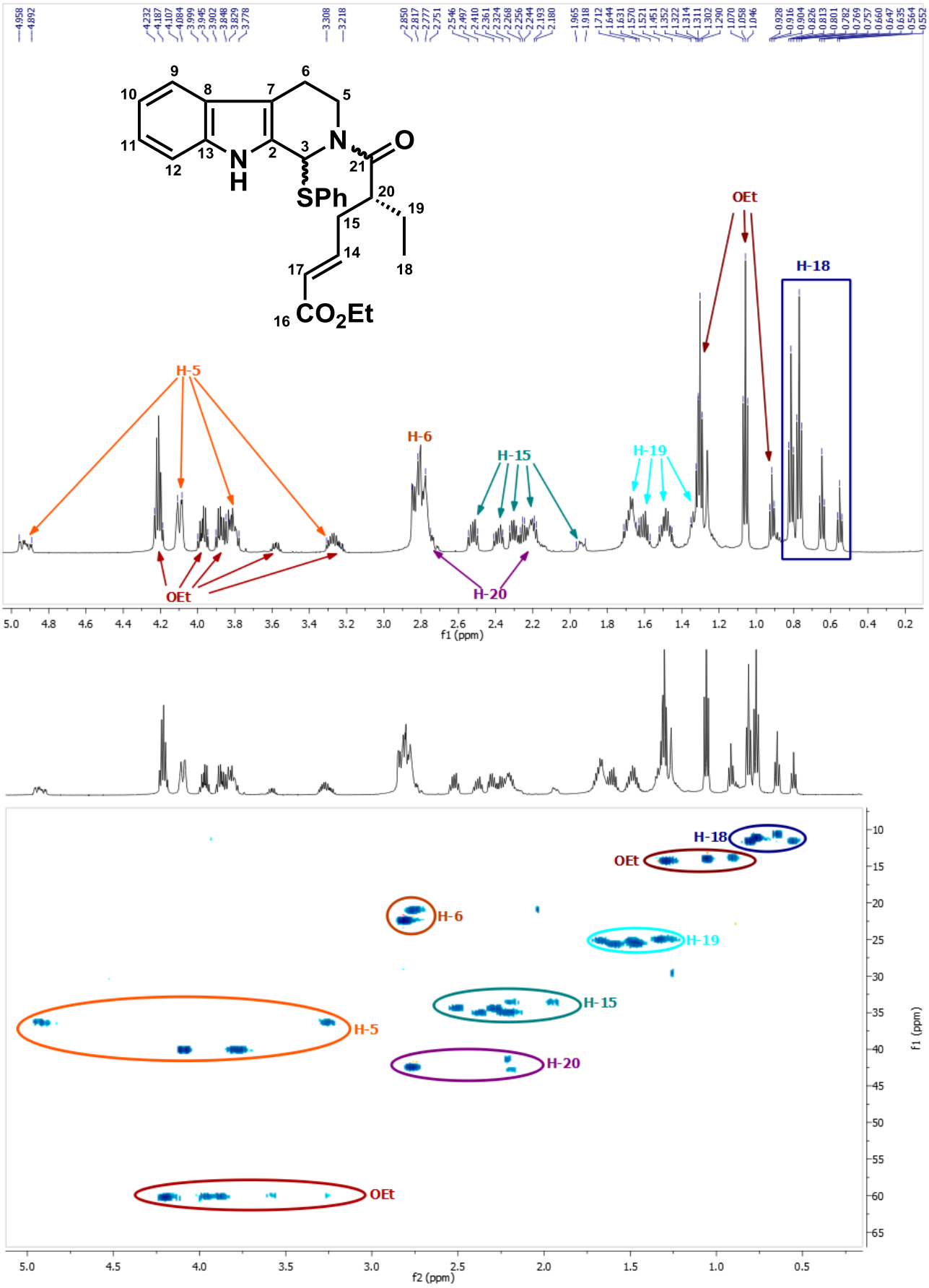

Figure 8. ^{1}H NMR (top) and HSQC (bottom) spectra of the sulfanyl amides **16** shown over the 0 to 5 ppm range.

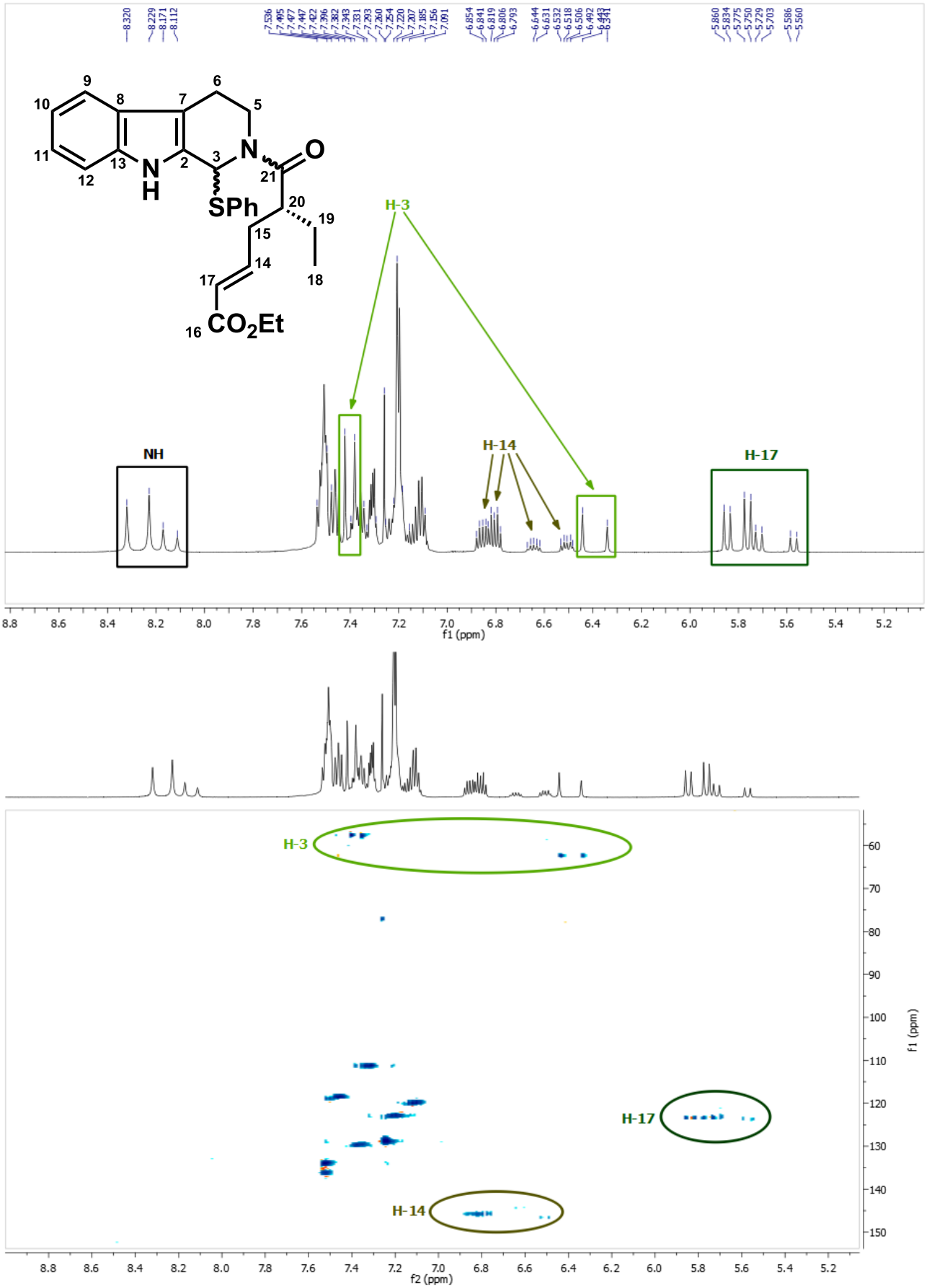

Figure 9. ^{1}H NMR (top) and HSQC (bottom) spectra of the sulfanyl amides **16** shown over the 5 to 9 ppm range.

Further observation of the ^{13}C spectrum (Figure 10) once again showed 4 peaks for each magnetically equivalent aliphatic and vinyl carbon environment which were seen to overlap in some cases. The C-18, primary ethoxy carbon, C-19 and C-15 signals were all seen in regions similar to those in the ^{13}C NMR spectrum of the acid ester precursor **15** (Figure 5). The C-20 signals were shielded and appeared in the 42 ppm region while the secondary ethoxy carbon signals were deshielded and appeared in the 60 ppm region. The new C-6 resonances emerged around a reasonable 22 ppm, while the C-5 signals were once again seen to be separated over a 3.5 ppm range around 38 ppm. The vinyl (C-17 and C-14) as well as the α,β-unsaturated ester carbonyl resonances were all found in similar positions to those for the acid ester **15** (Figure 5). Finally, the newly formed amide carbonyl signals were found around 173 ppm and were shielded relative to the acid carbonyl resonance of the starting material, as expected.

At this stage it should be noted that the formation of the two amide rotamers in addition to the two diastereomers was also seen as inconsequential, since the amide bond was expected to interconvert between the s-*cis* and s-*trans* amide at the temperature of the ensuing radical cyclization (refluxing toluene, 110 °C).[16] We postulated that this interconversion would therefore allow cyclization to complete at full conversion via the s-*trans* amide diastereomers following *N*-Boc protection (Scheme 12).

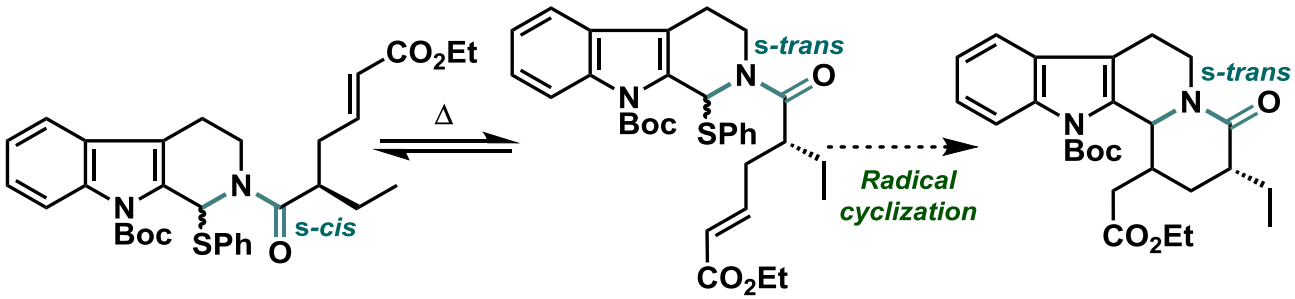

Scheme 12. Expected interconversion of the s-*cis* amide at high temperature to the s-*trans* amide able to undergo radical cyclization.

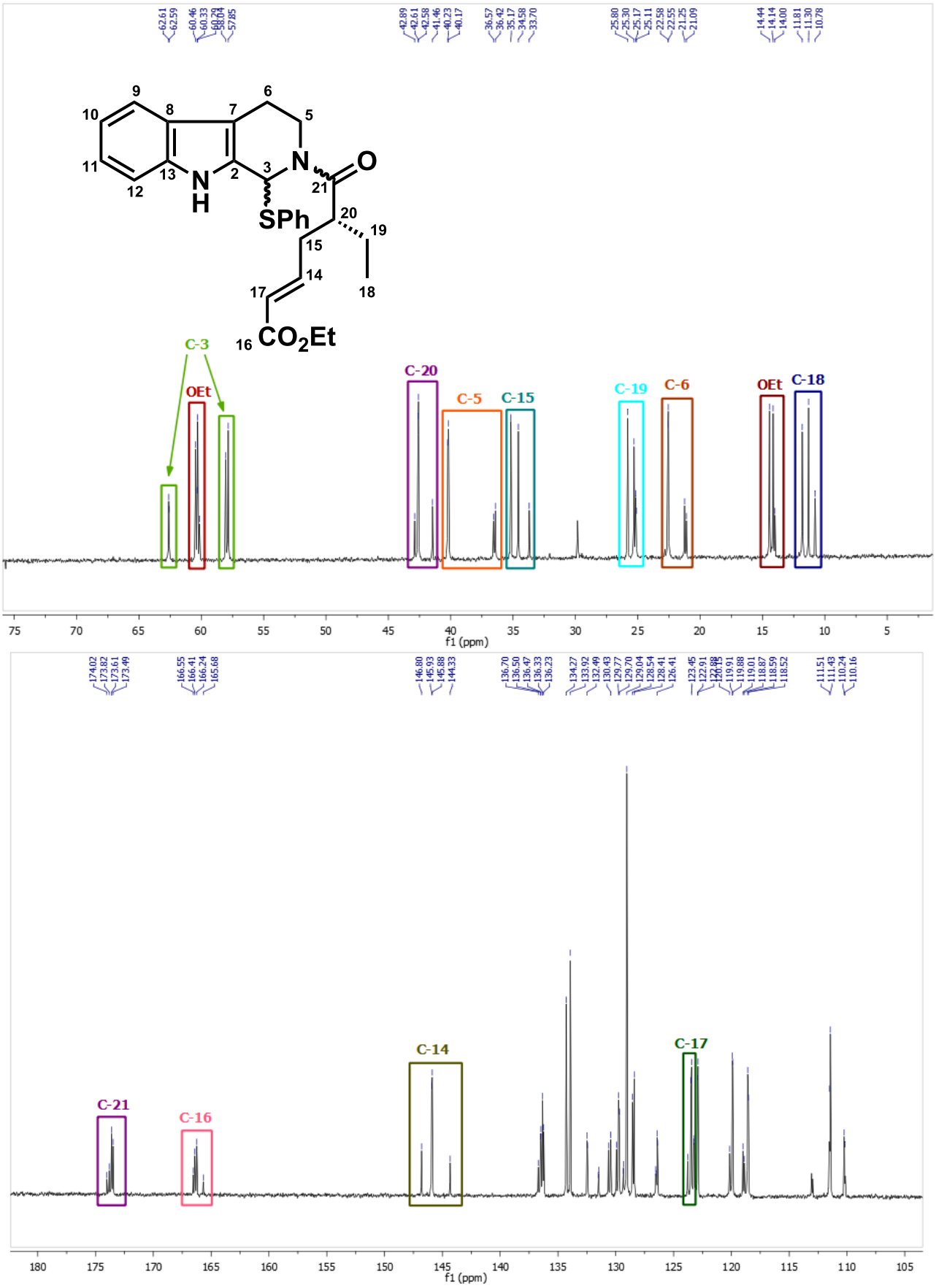

Figure 10. ^{13}C NMR spectrum of the sulfanyl amides **16** shown over the 0 to 75 ppm (top) and 100 to 180 ppm (bottom) ranges respectively.

With the requisite sulfanyl amides **16** in hand, the final operation that remained in the synthesis of the radical cyclization precursor **17** was *N*-Boc protection of the indole moiety.

This was achieved through treatment of sulfanyl amides **16** (~3 g scale) with di-*tert*-butyl dicarbonate followed by 4-dimethylaminopyridine at room temperature for 2 h (Scheme 13). TLC analysis once again showed the clean conversion of the starting material to two less polar spots as expected. The desired *N*-Boc-protected sulfanyl amides **17** were isolated in quantitative yield following subsequent concentration *in vacuo* and flash chromatography processes.

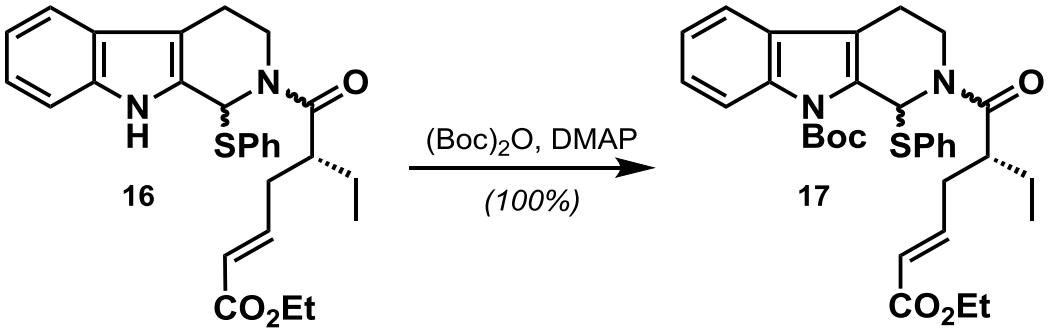

Scheme 13. *Reagents and conditions:* $(Boc)_2O$ (1.3 equiv), DMAP (0.05 equiv), THF, rt, 2 h, 100%.

^1H and ^{13}C NMR spectroscopy provided evidence for the successful installation of the *N*-Boc group (Figure 11). The ^1H NMR spectrum of **17** showed the four requisite diastereomer/rotamer *N*-Boc singlets at 1.69, 1.70, 1.79 and 1.81 ppm which indicated that the *N*-Boc group adopted a single conformation, most likely as the *cis* amide with the carbamate carbonyl group pointing towards H-3 on steric grounds (see calculations later in section 2.3). The relevant *N*-Boc ester signals were also seen in the ^{13}C NMR spectrum around 29, 85 and 150 ppm for the primary, quaternary and carbamate carbons respectively. Deshielding of the H-3 singlet resonances from the prior 6.4 and 7.4 ppm regions (Figure 9) to the 7.2 and 8.0 ppm regions was also observed, with the corresponding ^{13}C resonances also shown to be slightly deshielded. Furthermore, all the other resonances in both the ^1H and ^{13}C NMR spectra remained mostly unchanged and for simplicity have not been labelled in Figure 11. Finally, HRMS data gave a molecular ion $[M - SPh]^+$ at 453.2396 in which $C_{26}H_{33}N_2O_5^+$ requires 453.2389, thus offering conclusive evidence for the formation of the desired precursor **17**.

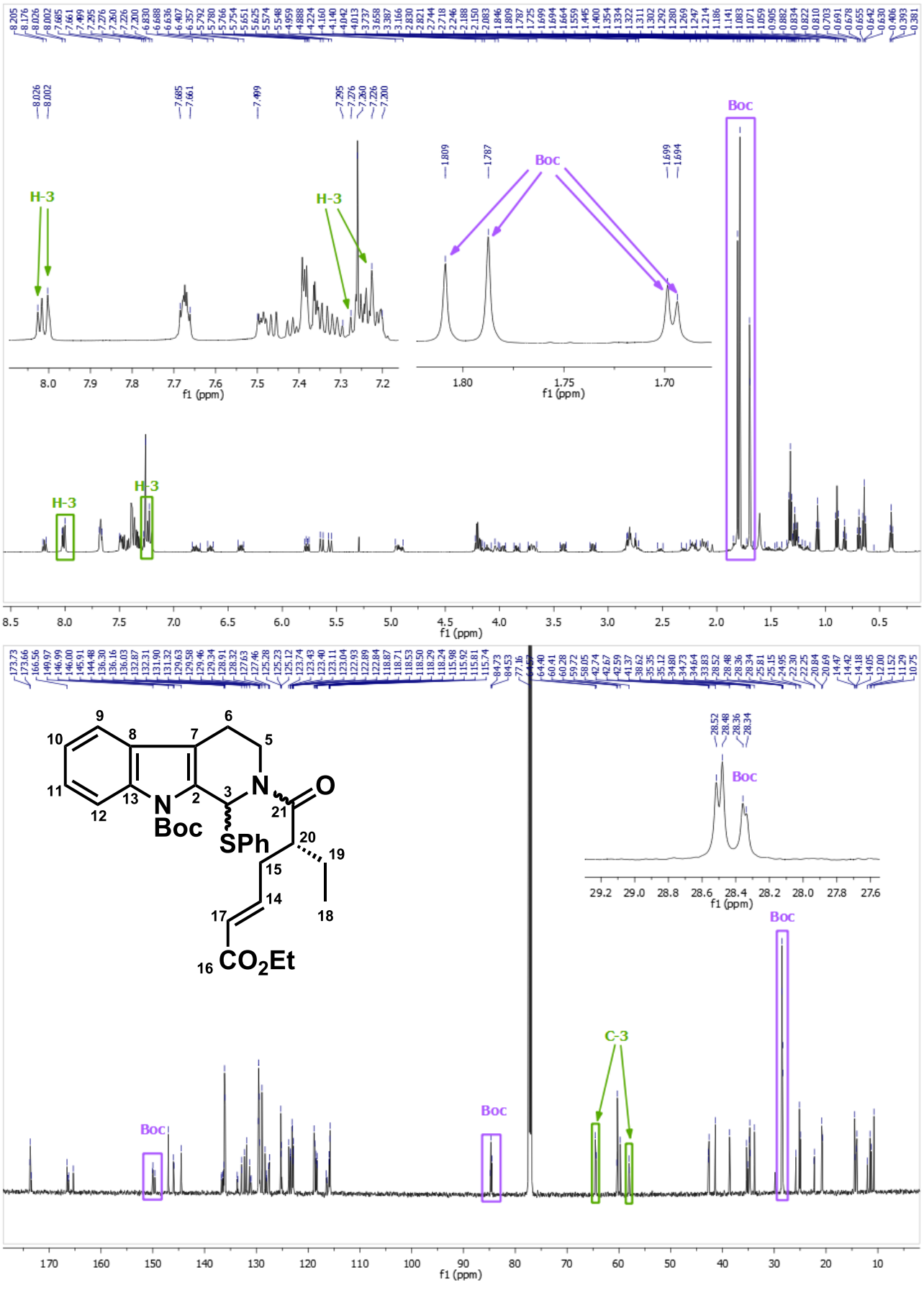

Figure 11. ^{1}H (top) and ^{13}C (bottom) NMR spectra of the *N*-Boc protected sulfanyl amides **17**.

2.2.3 D-Ring Construction via Radical Cyclization

The successful synthesis of the radical cyclization precursor **17** meant that the key radical cyclization step could finally be attempted. Overall, this step was repeated several times in order to determine the optimal reaction conditions, in which it was found that the slow addition of the radical initiator under dilute conditions (0.01 M) and lowering the equivalents of tributyltin hydride from 1.5 to 1.3 equivalents minimized the formation of the radical reduction product as well as increased the yield and diastereoselectivity.

Making use of these optimized conditions (Scheme 14), the *N*-Boc protected sulfanyl amides (**17**, ~3 g scale) were treated with tributyltin hydride in deoxygenated toluene at room temperature and then immediately heated to reflux. The radical initiator 1,1'-azobis(cyclohexanecarbonitrile) was then slowly added over a 1 h period and the solution refluxed (110 °C) for a further 2 h. Meticulous TLC analysis showed the disappearance of the starting material after this time and the formation of one major and one minor closely running, slightly more polar spot, as well as several smaller, slightly more polar spots. The reaction mixture was then left to cool to room temperature and concentrated *in vacuo*. Careful chromatography of the resulting residue did not, however, allow for the complete separation of the major and minor isomers. In view of this, the yields were corrected via ^{1}H NMR estimation and were found to be 85% (corrected, major-**18**) and 8% (corrected, minor-**18**) respectively in a diastereomeric ratio of 10:1.

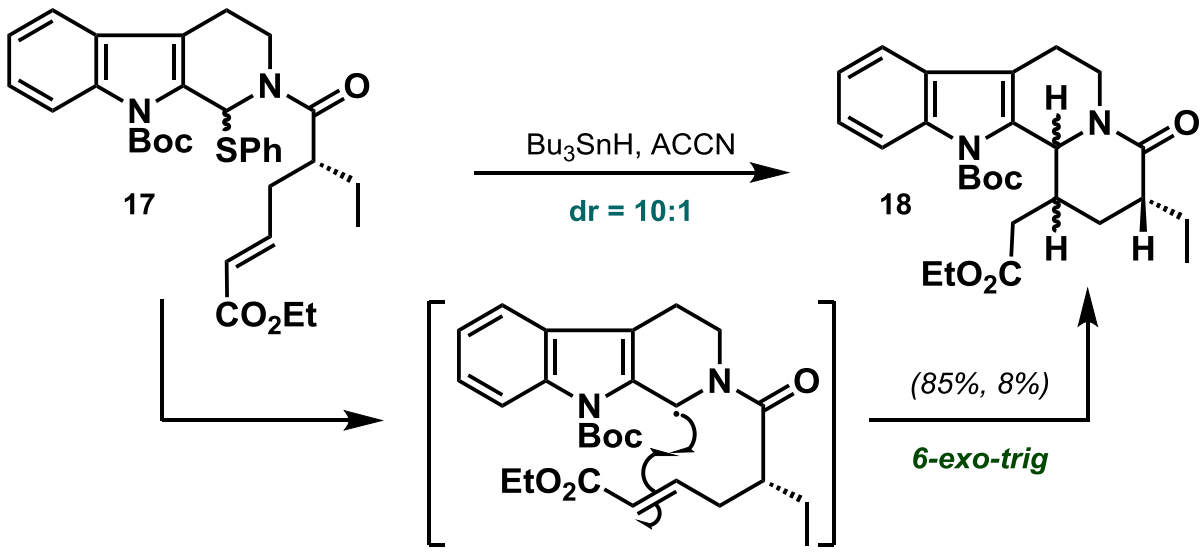

Scheme 14. *Reagents and Conditions:* Bu_3SnH (1.3 equiv), ACCN (0.1 equiv), PhMe, reflux, 3 h, 85% (major, corrected), 8% (minor, corrected), dr = 10:1.

At this point, the stereochemistries at the D/E-ring junction for the two diastereomers isolated were unknown, as indicated in Scheme 14. We therefore sought confirmation of these assignments through ^{1}H NMR spectroscopy and X-Ray analysis.

The ^{1}H NMR spectrum of the major-**18** product (with a small amount of the minor-**18** product still present, ~11%) was now much more resolved and promisingly displayed all of the requisite peaks of the desired lactam as highlighted in Figure 12. The previously vinylic H-17 proton was now seen as two overlapping doublet of doublet aliphatic resonances at 1.88 and 1.96 ppm integrating for 2H as expected. Similarly, the previously vinylic H-14 proton was observed as a multiplet in the 3.16 to 3.25 ppm range, thus overall confirming the loss of the double bond. The H-3 resonance was shielded relative to the cyclization precursor and appeared at 5.47 ppm as a broad doublet with a 3.6 Hz coupling to the adjacent H-14 proton, upfield now compared to the precursor **17** on account of having lost the phenylthio group.

In view of our previous model (Figure 3, Chapter 1), we expected that the H-3 proton should be in an axial position due to the indole moiety adopting an equatorial orientation on steric grounds. We postulated that the desired *cis* arrangement of the H-3/H-14 protons should therefore display an H_{ax}/H_{eq} coupling between H-3 and H-14. If the D-ring adopted a chair-like conformation we would expect to see an H_{ax}/H_{eq} coupling of approximately 4 Hz. In this system, however, we expected a level of distortion from the chair conformer, so a slightly lower 3.6 Hz coupling for an H_{ax}/H_{eq} relationship seemed reasonable (Figure 12). That still left the question of the H-3/H-14 to H-20 relationship, and so further analysis was carried out later on through single crystal X-ray structure determination of the pentacycle following E-ring formation, which will be presented in due course.

In addition, the ^{1}H NMR spectrum of the major lactam **18** displayed several other interesting aspects. The protons situated on the primary carbon of the ethoxy group were seen to be slightly more shielded relative to the H-18 protons and appeared as a triplet at 0.99 pm while the H-18 triplet appeared at 1.02 ppm. The diastereotopic H-15 protons were observed at 1.10 and 2.50 ppm showing a significant 1.4 ppm separation, with one of the diastereotopic protons more shielded relative to the H-19 protons. Finally, the H-5 resonances once again showed a remarkable ~2 ppm separation between its diastereotopic protons at around 2.9 and 4.9 ppm respectively.

Furthermore, at this point we should note that the H-3 signal in the ^{1}H NMR spectrum of the minor-**18** product was buried and not clearly discernible, meaning that the H-3/H-14 coupling and insight therefore into the D/E-ring junction stereochemistry could not be obtained from it. As a result of this, we pushed forward with the major-**18** product in the remaining steps and discarded trace amounts of the minor products along the way.

The identity of the minor-**18** lactam was confirmed later on through computational analysis in section 2.3.

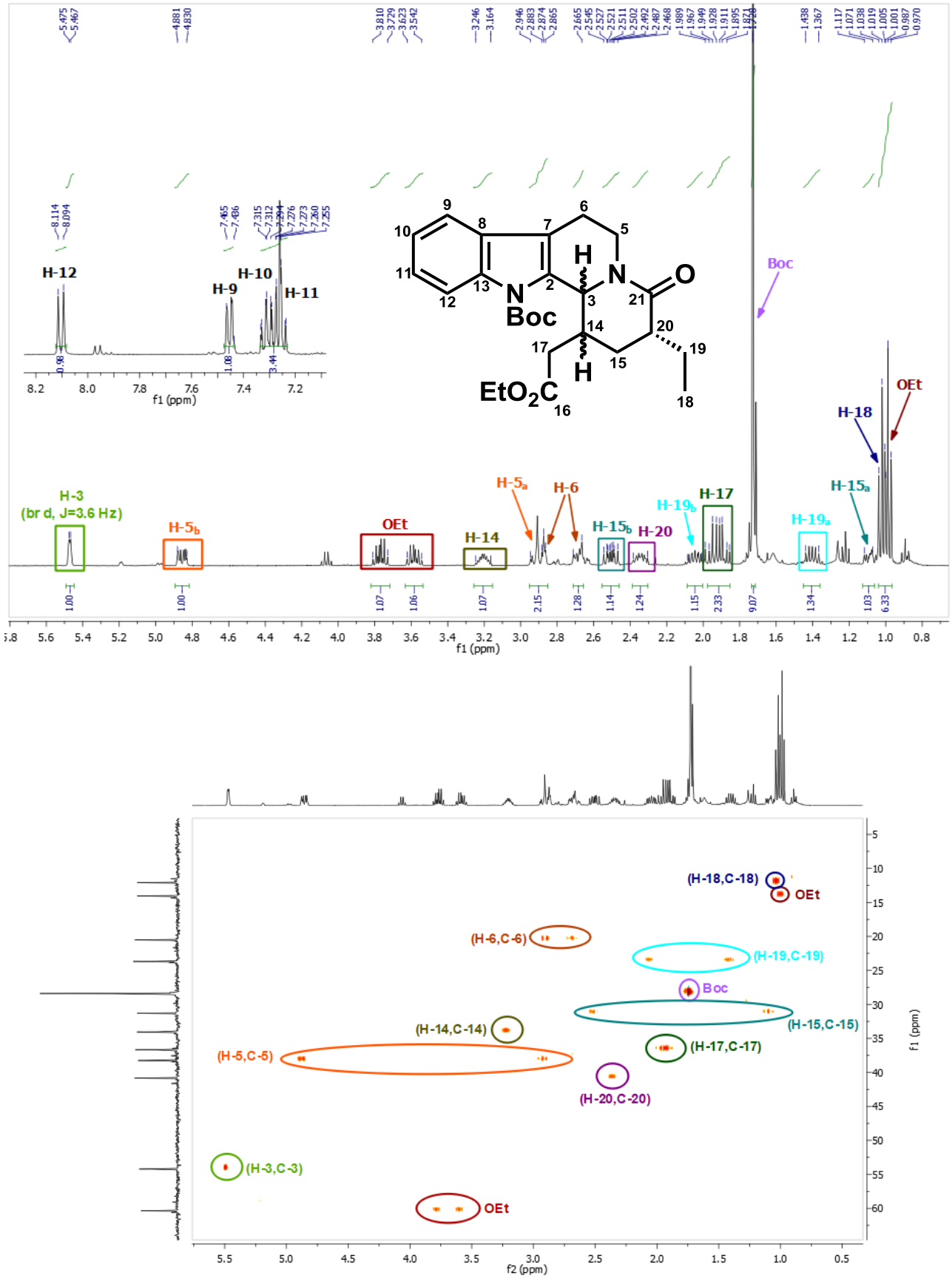

Figure 12. ^{1}H NMR (top) and HSQC (bottom) spectra of the major lactam **18**.

The ^{13}C NMR spectrum of the major lactam **18** displayed a total of 24 peaks corresponding to the requisite 24 distinct magnetically equivalent carbon environments as shown in Figure 13. C-14 and C-17 were now seen as the tertiary and secondary carbon signals at 34.1 and 36.7 ppm respectively with C-17 now shown to be deshielded relative to C-14 as expected. In addition, the C-3 signal was seen to be shielded (relative to the precursor) at 54.2 ppm, therefore providing indisputable evidence in favour of D-ring formation. Interestingly, the C-16 ester carbonyl was observed to be deshielded at 175.0 ppm relative to the C-21 lactam carbonyl at 172.1 ppm likely due to the loss of its α,β-unsaturated ester character.

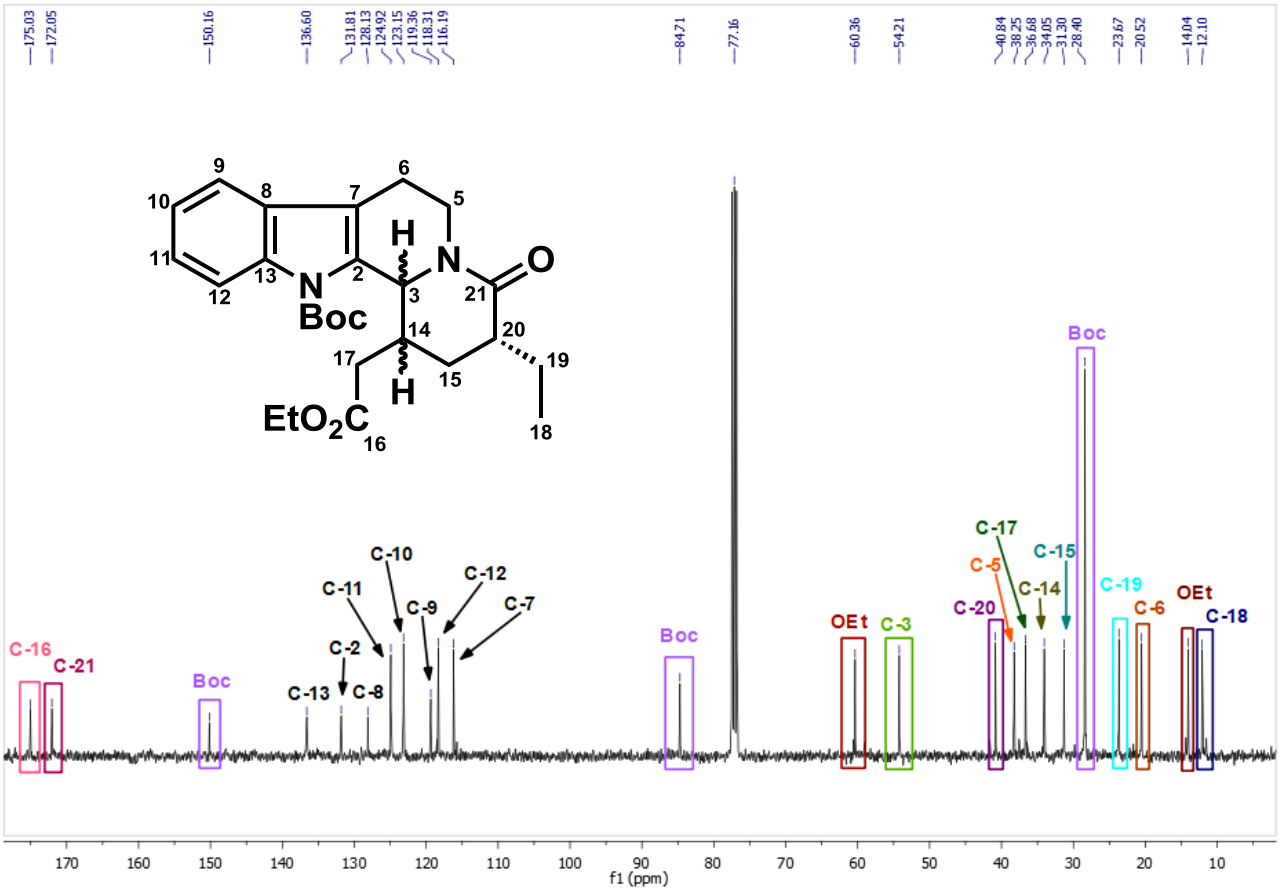

Figure 13. ^{13}C NMR spectrum of the major lactam **18**.

Finally, further evidence for the formation of the desired lactam **18** was obtained via HRMS which revealed a molecular ion $[M + H]^+$ at 455.2554 corresponding to the required 455.2548 calculated for $C_{26}H_{35}N_2O_5^+$.

2.2.4 End-Game Strategy I

With reproducible access to the desired major lactam **18** (~2 g), we then sought to tackle what remained of our route, namely, *N*-Boc deprotection, E-ring formation and chemoselective lactam reduction.

Initially we attempted to remove the *N*-Boc group of lactam **18** via the standard deprotection conditions through treatment with trifluoroacetic acid at 0 °C in the presence of anisole as the cation scavenger (Scheme 15). Unfortunately, although TLC analysis showed the consumption of the starting material, several products were formed. We postulated that the free indole was likely too sensitive under acidic conditions and that this, in conjunction with the presence of the nearby reactive ester group, could thus have resulted in partial formation of the E-ring cyclized product. In view of this, we sought an alternative methodology for the removal of the *N*-Boc group, which was found in the form of thermolytic conditions (Scheme 15).[17]

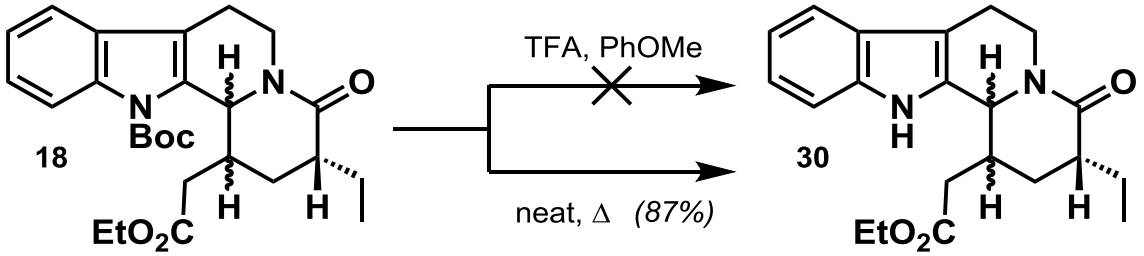

Scheme 15. *Reagents and Conditions:* neat, 180 °C, 30 min, 87% (corrected).

The method from which the desired product emerged successfully involved heating major lactam **18** (neat under argon, ~300 mg scale, still containing ~11% minor-**18**) at 180 °C for 30 minutes. Careful chromatography of the resulting residue allowed for the partial removal of the minor-**30** product, and afforded the desired deprotected major lactam **30** in 87% corrected yield. Through careful monitoring we found that heating at a higher temperature (~190 °C) or for a longer reaction time resulted in the formation of several spots on TLC and decomposition of the product, while heating at a lower temperature (~170 °C) or for a shorter reaction time (~20 min) did not allow for the reaction to go to completion.

^{1}H NMR spectroscopic analysis of the major-**30** product (with ~6% of the minor-**30** product now present) showed the disappearance of the *N*-Boc signal along with the appearance of a new NH signal, as expected (Figure 14). The H-3 and H-5 signals were seen to be slightly shielded while the H-18 resonance was now seen to be shielded relative to the primary ethoxy protons.

In addition, the H-3 doublet was now more resolved, and displayed a standard H_{ax}/H_{eq} 4.1 Hz coupling with H-14, thus providing further evidence for the formation of the desired *cis* H-3/H-14 D/E-ring junction.

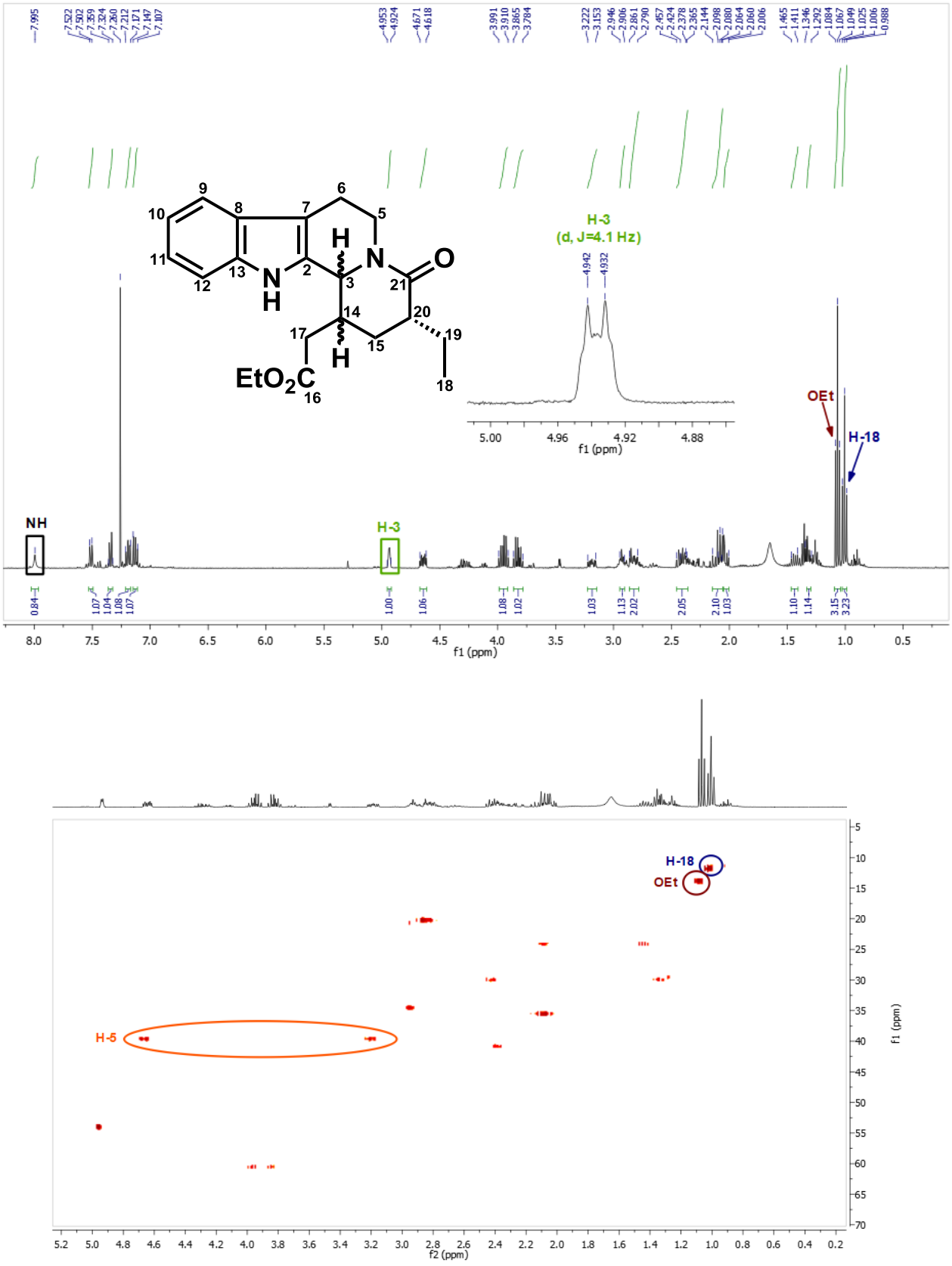

Figure 14. ^{1}H NMR (top) and HSQC (bottom) spectra of deprotected lactam **30**.

At this stage, with the deprotected lactam **30** in hand, a strategic decision to cyclize to the dilactam **19** (Scheme 16) was made, since we believed that we might be able to chemoselectively reduce the C-21 lactam in the presence of the C-16 lactam in the following step. To this end, lactam **30** was immediately cyclized to pentacycle **19** following pyrolysis owing to its instability in air (stable under argon). E-ring formation was achieved swiftly under basic conditions in near quantitative yield as shown in Scheme 16. Following extraction and purification by flash chromatography the major pentacycle **19** could be isolated cleanly as a single diastereomer, and was pleasingly obtained as a pale yellow solid (the prior lactam products **18** and **30** were both isolated as gums).

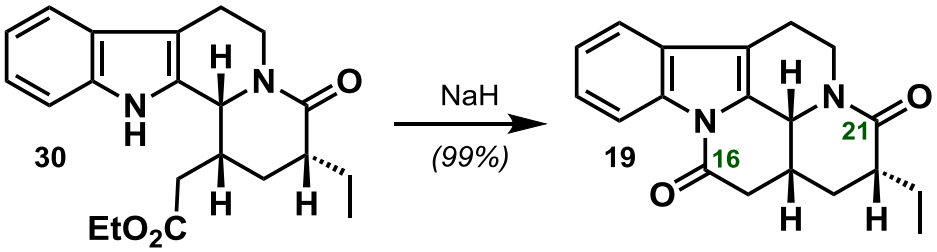

Scheme 16. *Reagents and Conditions:* NaH (1.1 equiv), THF, 0 °C, 1 h, 99%.

Given the fact that the *cis* H-3/H-14 to H-20 relationship had not yet been ascertained, we sought conclusive evidence in the form of an X-ray crystal structure determination of the pentacycle **19** following recrystallization. Much to our delight, we found that **19** did indeed display the required all *cis* H-3 to H-14 to H-20 relationship as indicated in Figure 15 below. The X-ray structure shows the C/D-ring fusion to be *cis*, in which pseudo-equatorial configurations are adopted for both the large indole moiety as well as the D-ring ethyl group, albeit that the D-ring adopts a flattened pseudo-chair due to the lactam functionality.

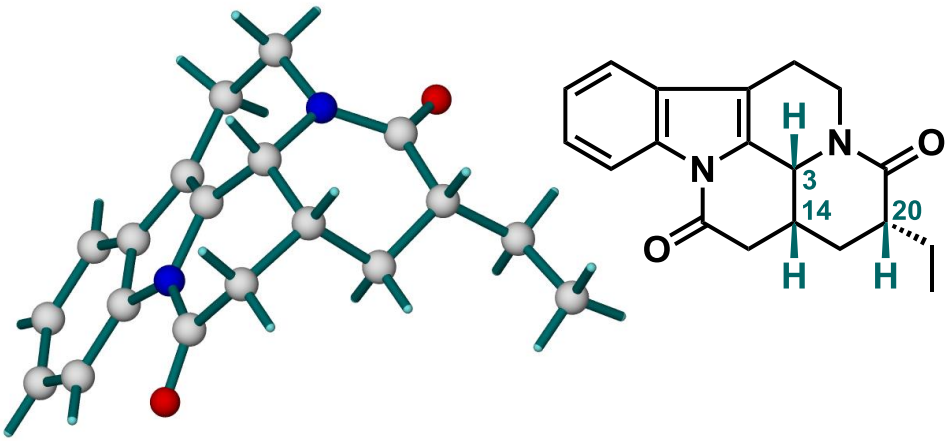

Figure 15. X-ray crystal structure of the pentacycle **19** displaying the desired all *cis* H-3 to H-14 to H-20 relationship.

With the requisite H-3, H-14 to H-20 stereochemical relationship of the pentacycle **19** fully established, we then moved on to attempt the chemoselective reduction process.

In this, we postulated that chemoselectivity differentiation might be achieved due to the C-21 lactam carbonyl oxygen being more nucleophilic and its carbonyl carbon less electrophilic compared to those atoms in the C-16 lactam, which was deemed to be less nucleophilic at oxygen but more electrophilic at carbon due to delocalization of its nitrogen lone pair into the indole π-system (see numbering in **19**, Scheme 17). In view of this, standard nucleophilic lactam reducing agents such as lithium aluminium hydride would likely result in the undesired reduction of the C-16 lactam in favour of the C-21 lactam. Thus, we went in search of other reduction strategies that would favour reduction of the C-21 lactam.

Looking through the literature, we were aware that thionation of a lactam moiety could be achieved in the presence of an ester with Lawesson's reagent due to the more nucleophilic character of an amide carbonyl oxygen over that of an ester.[18-21] Therefore, we postulated that in our system, chemoselective thionation of the more nucleophilic C-21 lactam could take place in the presence of the C-16 indole lactam. Further reduction of the thiolactam with Raney Nickel was then envisaged for the conversion of the thiolactam to the target in an overall two step thionation/reduction process (Scheme 17).

To this end dilactam **19** was subjected to the standard thionation conditions through treatment with Lawesson's reagent and refluxing in toluene.[18] Unfortunately, TLC analysis showed the formation of several product spots without full conversion of the starting material even after refluxing for several hours. Further ^{1}H NMR analysis of the products did not look promising either and suggested possible epimerization of the C-20 centre as well as dithionation of both the lactam entities.

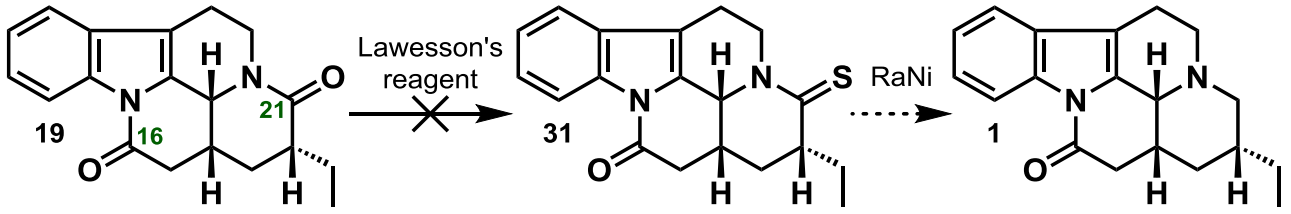

Scheme 17. Unsuccessful thionation/reduction process for the conversion of dilactam **19** to the target **1**.

As a consequence of this unfortunate outcome we were forced to review our synthetic route.

2.2.5 End-Game Strategy II

At this juncture we envisaged an alternative strategy inspired by finding the work undertaken by Schultz *et al*. in 1997, wherein they were able to generate the E-ring through an oxidation/ring-closing process in high yield in their synthesis of (-)-vincamone (Scheme 18).[22]

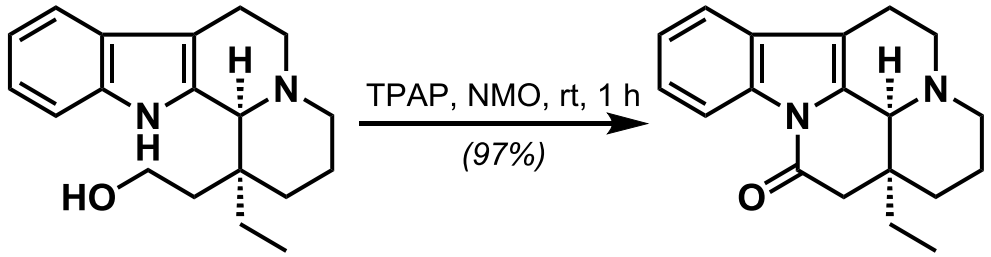

Scheme 18. Final oxidation/E-ring formation step in the Schultz *et al*. synthesis of (-)-vincamone.[22]

With this disconnection in mind we opted to revert back to the deprotected lactam **30** (Scheme 19). From this point, we then envisaged global reduction of both the amide and ester moieties followed by oxidation/closing through the method of Schultz *et al*. as shown in Scheme 19.

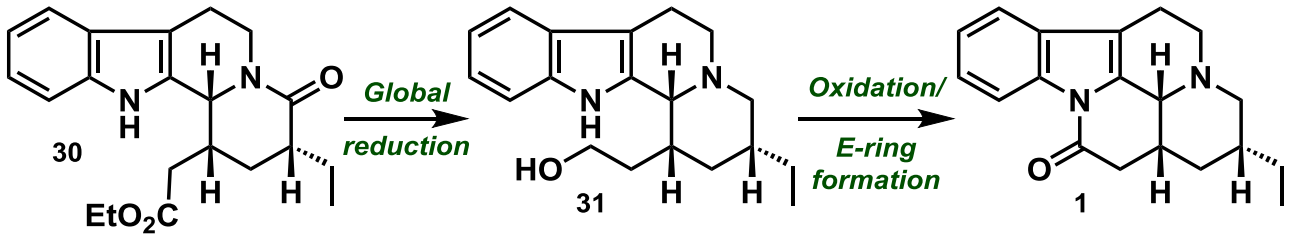

Scheme 19. Modified synthetic strategy for the conversion of the deprotected lactam **30** to the target **1**.

Naturally, we first attempted the global reduction of lactam **30** through treatment with lithium aluminium hydride at 0 °C (Scheme 20). TLC analysis showed partial conversion of the starting material likely to the reduced ester product only. Upon heating to reflux we observed the formation of the desired product along with the formation of several other products which was thus attributed to product instability at a higher temperature over longer reaction times. Several other attempts at this transformation involved varying the number of equivalents of the reagent used, lowering the temperature in an effort to control the step-wise reduction process, and varying the reaction times were all met with little success and in very low yield following isolation of the alcohol **31** (~15-30%).

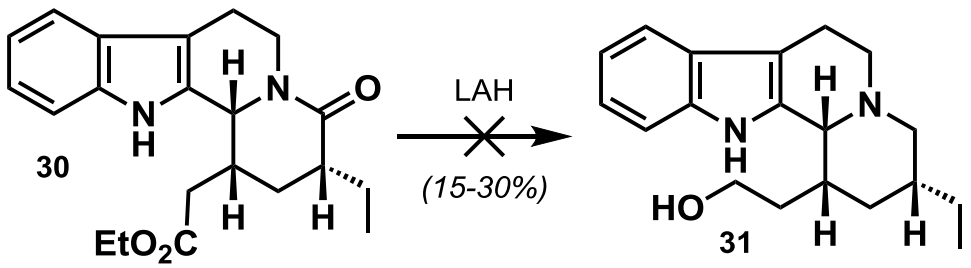

Scheme 20. Early attempts at the global reduction process.

In addition to the use of lithium aluminium hydride, various other standard reducing agents were tested including lithium borohydride, sodium borohydride/boron trifluoride diethyl etherate as well as borane dimethyl sulfide,[23] none of which led to the formation of the desired product and only achieved partial conversion of the starting material. In view of this series of disappointing results, we went in search for other lactam reducing agents that had been used in similar contexts in the literature.

In their 2016 synthesis of (-)-3-epitacamonine, Argade *et al*. used aluminium hydride (more colloquially known as alane) for the reduction of the lactam moiety bearing an adjacent C-20 ethyl group, with simultaneous removal of the pivaloyl protecting group, as shown in Scheme 21.[24]

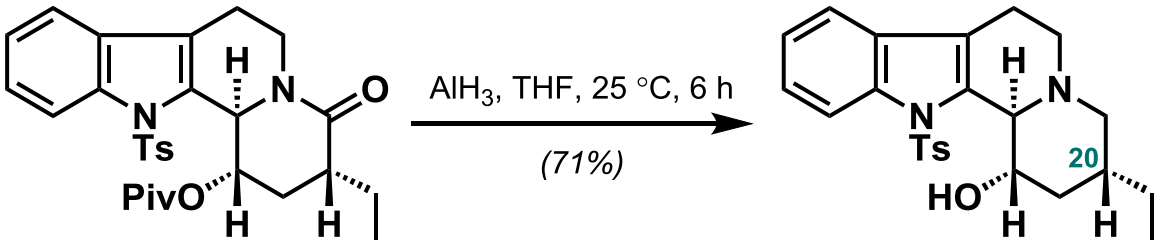

Scheme 21. Lactam reduction/pivaloyl deprotection step in the Argade *et al*. synthesis of (-)-3-epitacamonine.[24]

This method appealed to us since it indicated that both the lactam and ester functionalities could be reduced in reasonable yield and at a lower temperature without the need for reflux, since we already had cause for concern regarding the instability of our precursor at higher temperatures over longer reaction times. In addition, it confirmed that the lactam could be reduced in the presence of the adjacent C-20 ethyl group without loss of the C-20 stereogenicity. Another potential cause for concern in our case was the lack of the indole *N*-Ts protecting group used by the Argade group. Nevertheless, we proceeded to subject our lactam **30** to these conditions in the hope that we were later able to adjust the conditions to better suit our slightly more sensitive substrate.

Much to our relief, our initial efforts provided promising results. Though at this stage the reaction profile did not seem to be particularly clean by TLC analysis at room temperature, it showed complete conversion of the starting material, along with the formation of a dominant more polar spot which, up until this point, we had not observed through the use of any other reducing agent. After further optimization of the conditions (shown in Scheme 22) we were able to isolate the desired alcohol in 63% crude yield.

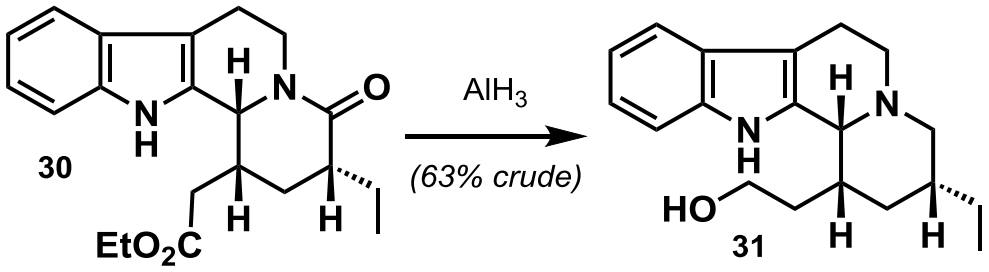

Scheme 22. *Reagents and Conditions:* AlH_3 (4 equiv), THF, –40 to 0 °C, 6 h, 63%.

In this (Scheme 22), reduction of the ester functionality was observed through low temperature treatment of the lactam **30** with aluminium hydride at –40 °C over 30 min. The reaction mixture was then stirred at this temperature for a further 30 min before being allowed to warm to 0 °C. 5 h of meticulous TLC analysis at this temperature confirmed the formation of the desired alcohol product **31**. The reaction mixture was then quenched through the careful addition of an aqueous saturated sodium sulfate solution, filtered through Celite and the filtrate concentrated *in vacuo*.

Crude ^{1}H NMR analysis of the alcohol **31** showed the loss of the ethoxycarbonyl proton resonances along with the appearance of new H-21 signals. IR spectroscopy also confirmed the loss of both the lactam and ester peaks at 1654 and 1726 cm^{-1} respectively. At this point, given the high polarity of the alcohol and our lack of material, we decided to push on to the final oxidation/closing step forgoing further purification in an effort to avoid potential losses through column chromatography.

Therefore, in the final step (Scheme 23) following the procedure of Schultz *et al*.,[22] crude alcohol **31** was treated with tetrapropylammonium perruthenate and *N*-methylmorpholine *N*-oxide at room temperature. The reaction mixture was then stirred for a further 3 h, during which time TLC analysis confirmed conversion of the alcohol to a dominant less polar spot.

Subsequent filtration, extraction and flash chromatography processes allowed for the clean isolation of the target **1** as a single diastereomer, which was obtained as long, clear, colourless needles in 45% yield over 2 steps from **30** and in 96% ee as ascertained by chiral HPLC on an OD column.

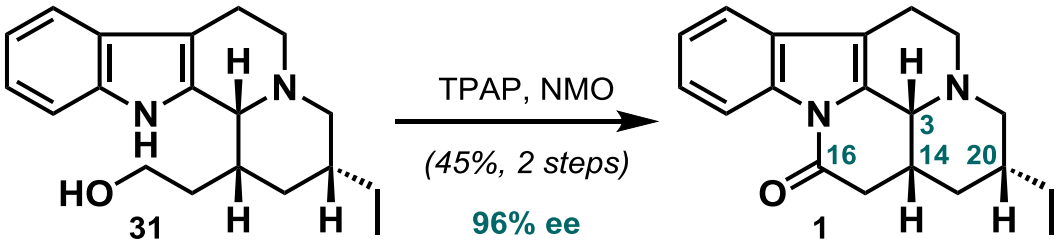

Scheme 23. *Reagents and Conditions:* TPAP (0.2 equiv), NMO (2 equiv), CH_2Cl_2 (treated with 4 Å molecular sieves), rt, 3 h, 45% (over 2 steps).

Following recrystallization from ethyl acetate/hexane, the melting point was obtained as 179 – 181 °C, in full agreement with the literature value reported by Van Beek *et al*. in their original work (180 – 181 °C).[4] ^{1}H and ^{13}C NMR data of the product obtained (shown in Figures 16 and 17) were once again in full agreement with those of the literature for (+)-tacamonine published by Van Beek *et al*.[4] and Lounasmaa *et al*.[25] respectively. A full comparison is shown in Table 1 for brevity. Furthermore, IR spectroscopy confirmed the re-appearance of the C-16 lactam signal at 1701 cm^{-1}. HMRS data gave a molecular ion $[M + H]^+$ at 295.1820 in agreement with 295.1812 calculated for $C_{19}H_{23}N_2O^+$. Finally, the optical rotation of the target **1** was found to be +117.2, in close agreement with the literature value of +122 reported by Danieli *et al*.[26]

X-ray crystal structure determination of the target **1** (Figure 18), belonging to a monoclinic crystal system and crystallizing in the P 21 space group, provided conclusive evidence for its formation. Similar to the crystal structure of the pentacycle **19** (Figure 15), it revealed the requisite *cis* H-3/H-14 to H-20 relationship, with the large indole moiety once again adopting a pseudoequatorial orientation, while the D-ring was now seen in the chair conformation owing to the loss of the sp^2 lactam system placing the C-20 ethyl group 'down' in the more stable equatorial position. Once again, the C/D-ring junction was also *cis*, to accommodate the D/E *cis* ring-junction stereochemistry.

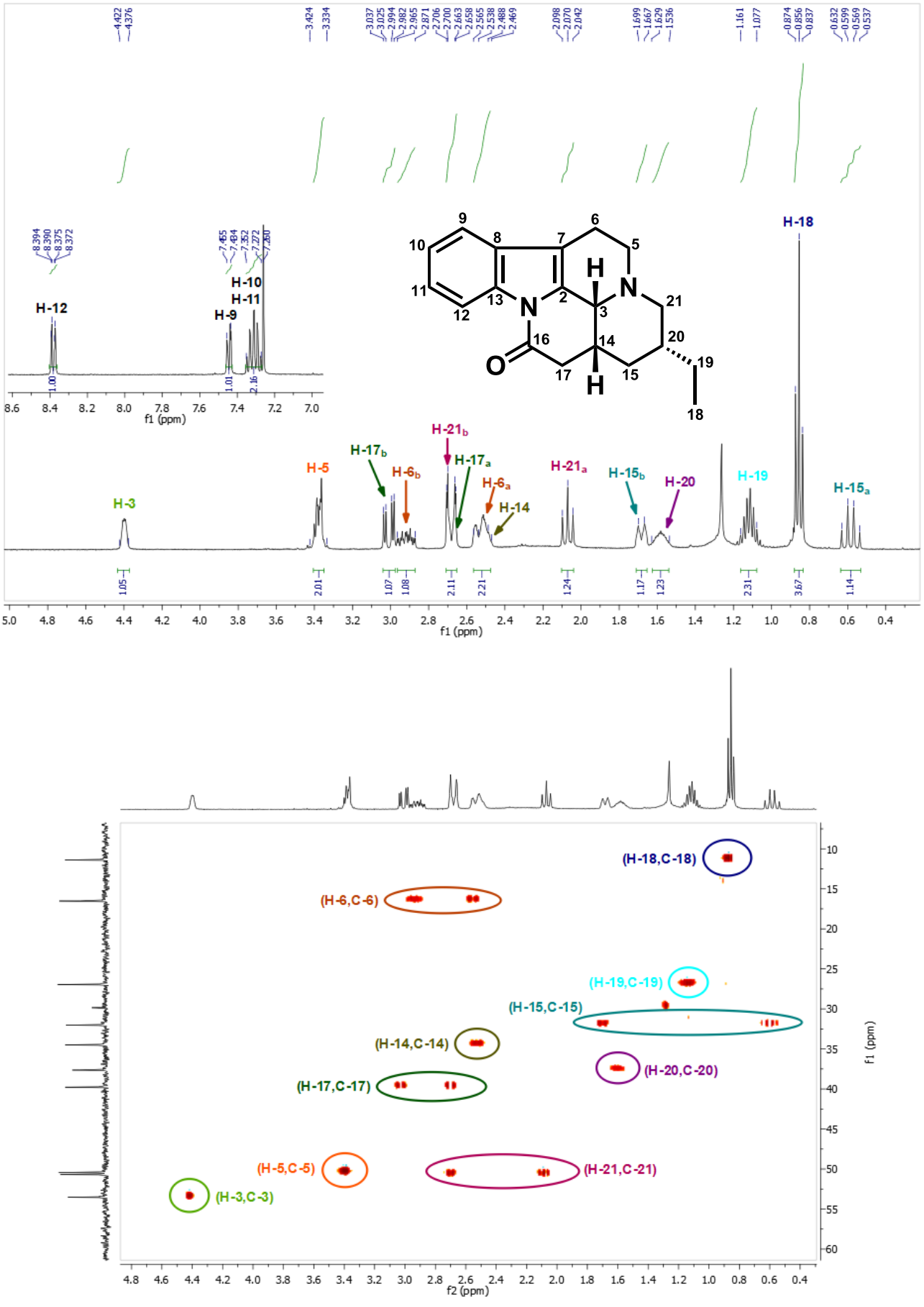

Figure 16. ^{1}H NMR (top) and HSQC (bottom) spectra of (+)-tacamonine (**1**).

Table 1. ^{1}H and ^{13}C NMR literature data comparison for (+)-tacamonine.

^{1}H NMR	**Van Beek *et al*.[4] δ (ppm)**	**Data obtained δ (ppm)**
H-3	4.33 (m, 1H)	4.42 – 4.38 (m, 1H)
$H\text{-}5_a$	3.30 (m, 1H)	3.42 – 3.33 (m, 2H)
$H\text{-}5_b$	3.38 (m, 1H)	
$H\text{-}6_a$	2.48 (br ddd, *J* = 17.0, 7.1, 3.1 Hz, 1H)	2.57 – 2.49 (m, 1H)
$H\text{-}6_b$	2.89 (m, 1H)	2.97 – 2.87 (m, 1H)
H-9	7.43 (m, 1H)	7.46 – 7.43 (m, 1H)
H-10	7.32 (ddd, *J* = 7.3, 7.3, 1.8 Hz, 1H)	7.35 – 7.27 (m, 2H)
H-11	7.28 (ddd, *J* = 7.3, 7.3, 1.8 Hz, 1H)	
H-12	8.38 (br dd, *J* = 7.3, 1.8 Hz, 1H)	8.38 (br dd, *J* = 7.3, 1.6 Hz, 1H)
H-14	2.45 (m, 1H)	2.54 – 2.47 (m, 1H)
$H\text{-}15_a$	0.56 (ddd, *J* = 12.6, 12.6, 12.6 Hz, 1H)	0.58 (ddd, *J* = 12.9, 12.8, 12.7 Hz, 1H)
$H\text{-}15_b$	1.66 (br d, *J* = 12.6 Hz, 1H)	1.71 – 1.66 (m, 1H)
$H\text{-}17_a$	2.66 (dd, *J* = 17.0, 2.3 Hz, 1H)	2.68 (dd, *J* = 17.0, 2.2 Hz, 1H)
$H\text{-}17_b$	2.99 (dd, *J* = 17.0, 4.9 Hz, 1H)	3.01 (dd, *J* = 17.0, 4.9 Hz, 1H)
H-18	0.85 (t, *J* = 7.4 Hz, 3H)	0.86 (t, *J* = 7.4 Hz, 1H)
H-19	1.10 (m, 2H)	1.16 – 1.08 (m, 2H)
H-20	1.52 (m, 1H)	1.63 – 1.54 (m, 1H)
$H\text{-}21_a$	2.03 (dd, *J* = 11.0, 10.9 Hz, 1H)	2.07 (t, *J* = 11.0 Hz, 1H)
$H\text{-}21_b$	2.64 (ddd, *J* = 10.9, 3.7, 1.7 Hz, 1H)	2.71 – 2.66 (m, 1H)
^{13}C NMR	**Lounasmaa *et al*.[25] δ (ppm)**	**Data obtained δ (ppm)**
C-2	131.5	131.4
C-3	53.2	53.5
C-5	50.2	50.4
C-6	16.3	16.5
C-7	112.7	112.9
C-8	129.8	130.0
C-9	118.0	118.3
C-10	123.7	124.1
C-11	124.3	124.7
C-12	116.2	116.5
C-13	134.3	134.7
C-14	34.3	34.5
C-15	31.9	32.0
C-16	167.3	167.4
C-17	39.6	39.8
C-18	11.3	11.4
C-19	26.8	27.0
C-20	37.6	37.6
C-21	50.5	50.7

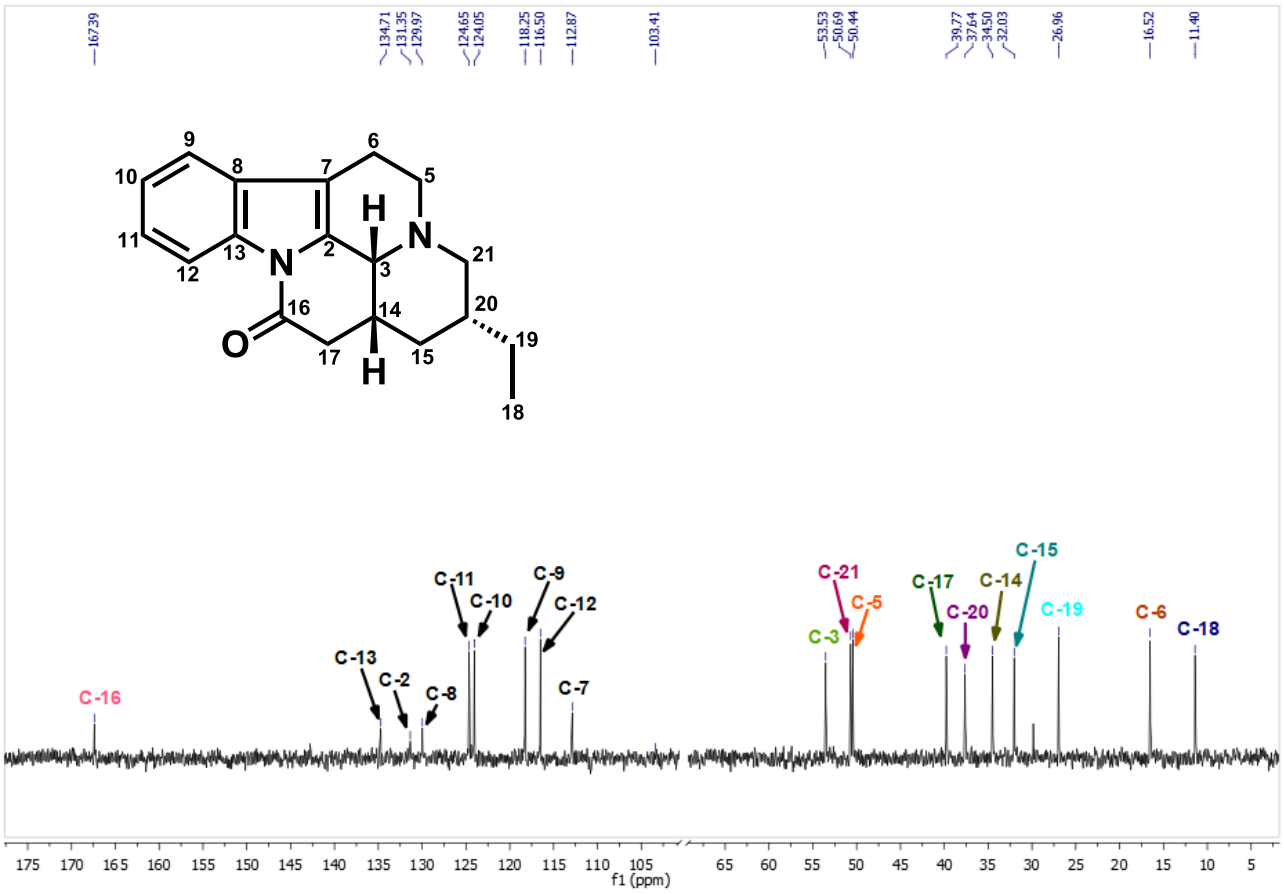

Figure 17. ^{13}C NMR spectrum of (+)-tacamonine (**1**).

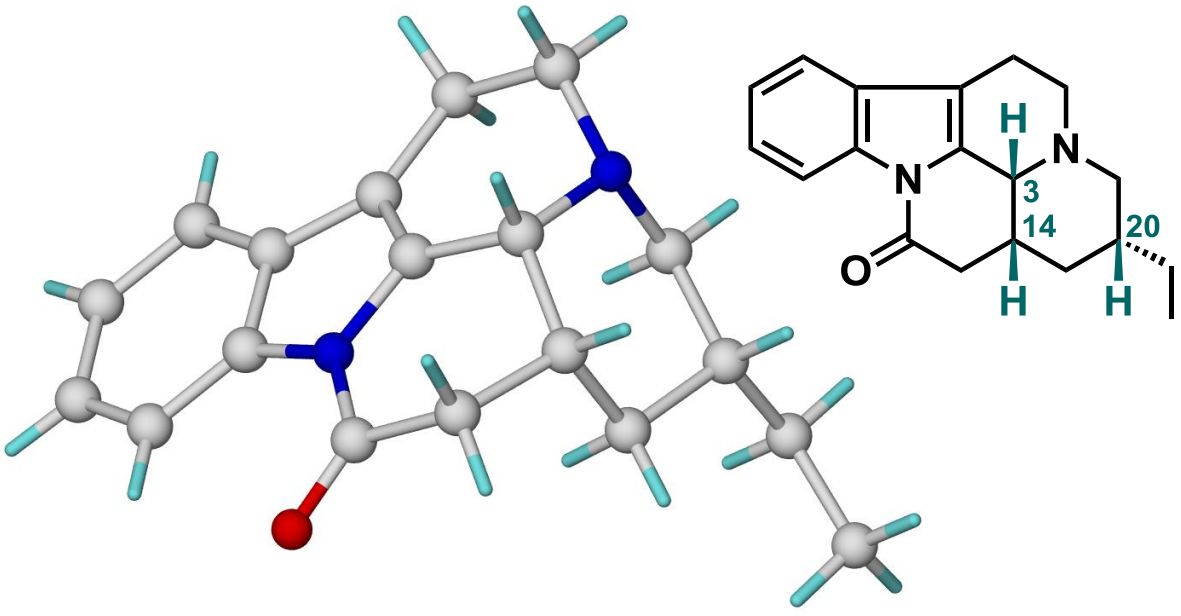

Figure 18. X-ray crystal structure of the target (+)-tacamonine (**1**) displaying the desired all *cis* H-3 to H-14 to H-20 relationship.

In summary, we were able to synthesize the target (+)-tacamonine in 8 steps over 10 distinct operations in 25% overall yield and in 96% ee. Our synthesis is thus, to the best of our knowledge, the shortest and mostly highly efficient route developed to date.

2.3 Computational Modelling of the Radical Cyclization

With our stereoselective route to (+)-tacamonine firmly in place, we then set out to investigate the diastereoselectivity of the radical cyclization which was obtained as a 10:1 diastereomeric ratio with the major-**18** product confirmed to be the all *cis* H-3 to H-14 to H-20 diastereomer as shown in Scheme 24. At this stage, however, we had not yet confirmed the minor-**18** products D/E *cis*/*trans* ring-junction as well as the relative H-3/H-14 to H-20 stereochemistry.

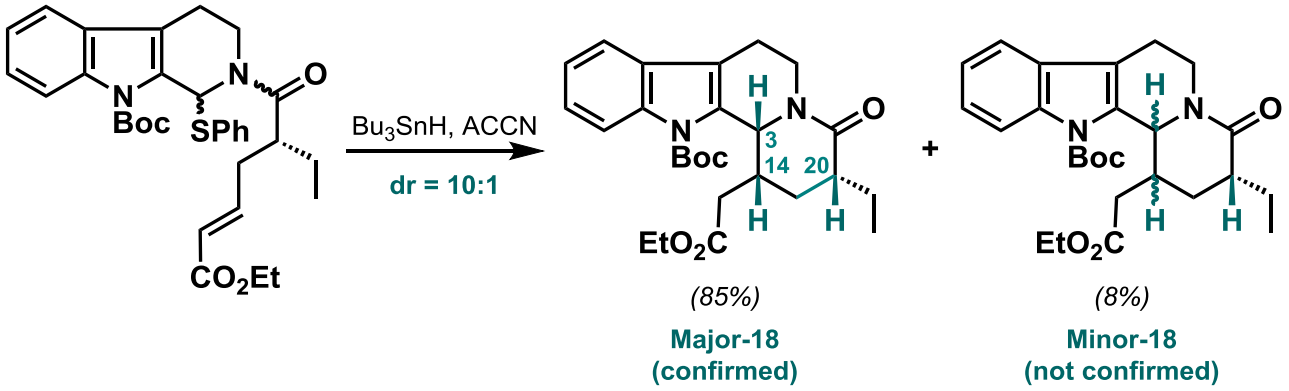

Scheme 24. A review of the radical cyclization diastereoselectivity.

In order to address this issue, we first noted that the radical cyclization step could lead to the formation of four possible products as shown in Figure 19. For convenience these were labelled the **up/up**, **down/down**, **down/up** and **up/down** products respectively.

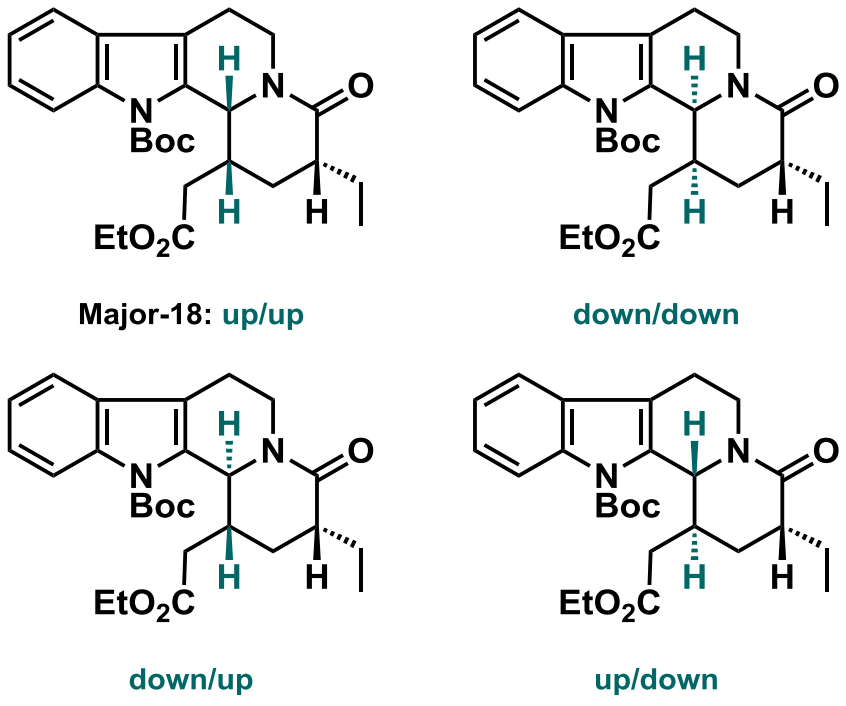

Figure 19. A depiction of the four possible radical cyclization products.

Since we had already established that the major-**18** product was indeed the **up/up** product, we assumed that it had the lowest energy transition state relative to the other products. Therefore, we postulated that the second lowest energy transition state would thus lead to the formation of the minor-**18** product. With this in mind, we set out to calculate the relative transition state energies leading to the four possible products shown in Figure 19, in order to confirm the identity of the minor-**18** product.

To this end, we opted to model the transformation from the radical reactant to each of the radical products as shown in Scheme 25 through computational methods (see Chapter 3 section 3.3 for further details).

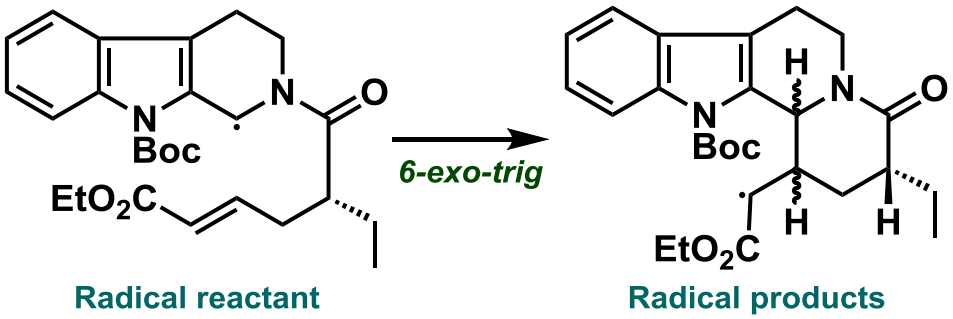

Scheme 25. An illustration of the radical reactant and radical products used in the computational modelling of the radical cyclization step.

In this, we began by calculating the minimum energy conformation of the radical reactant, as well as the energies of the radical products. The four radical transition states were then found in a separate calculation. This was done by first starting with each radical product structure and scanning the bond being formed from its product bond length in 20 steps of +0.1 Å. The maximum energy point along the resultant path was then used as a starting point for the transition state optimization, which was based on the same mechanics as the regular procedure, and adjusted to search for a first order saddle point. Once the transition states had been found and optimized, the activation energies from the radical reactant leading to each of the four possible transition states were computed.

Through our experimental observations and X-Ray analysis, we already knew that the **up/up** transition state was likely the lowest in activation energy, unless thermodynamic control were to be operating which was considered to be unlikely (see rationale later in Scheme 26). Therefore, we opted to assign the **up/up** transition state an activation energy value of 0 $kJ.mol^{-1}$, from which the relative activation energies of the three other transition states were calculated. A summary of the relative activation energies obtained for each of the four possible radical transition states labelled **TS-1**, **TS-2**, **TS-3** and **TS-4** (in order to those shown in Figure 19) are in turn shown in Figure 20.

The results of our calculations (Figure 20) reinforced our experimental observations. Indeed, **TS-1**, leading to the major *cis* **up/up** diastereomer, was found to have the lowest relative activation energy as expected. Moreover, the transition state with the second lowest relative activation energy was higher by +11.3 kJ.mol^{-1} and traced to **TS-3**, corresponding to the minor-**18** product (Scheme 24) as the *trans* **down/up** diastereomer as shown in Figure 19. The relative activation energies of the *cis* **down/down** (via **TS-2**) and *trans* **up/down** (via **TS-4**) diastereomers were also found to be +16.6 kJ.mol^{-1} and +35.0 kJ.mol^{-1} respectively.

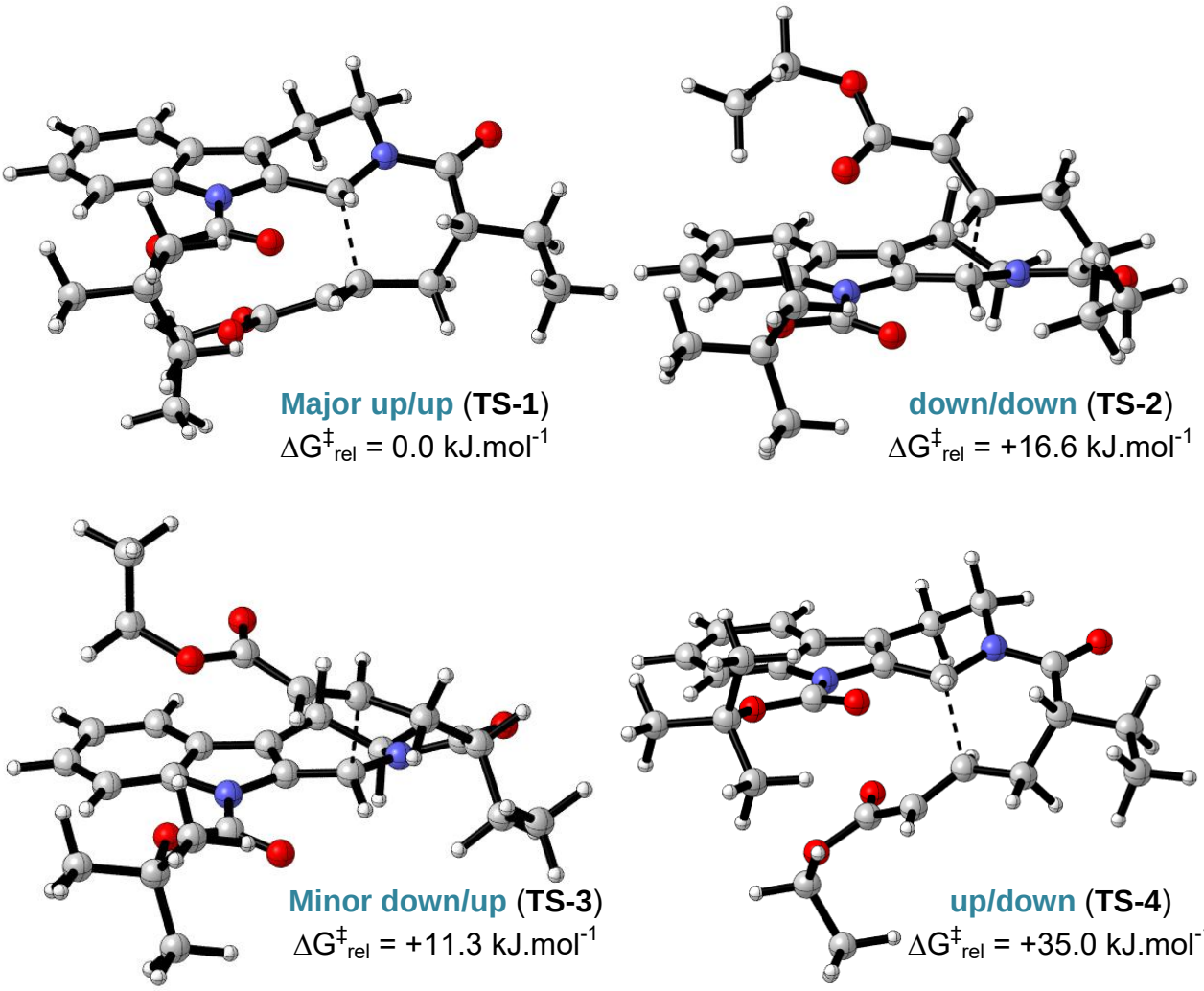

Figure 20. A depiction of the four possible radical cyclization transition states with their associated relative transition state energies. *Calculations done using PW6B95–D3/def2–QZVP//TPSS–D3/def2–TZVP. Toluene solvent included using SMD. RRHO correction to free energy obtained from vibrational frequency analysis at TPSS–D3/def2–TZVP*.

At this stage, however, we should note that the radical cyclization is a two-step process overall, the first of which is the formation of the cyclized radical, followed by hydrogen addition to form the product as shown in Scheme 26.

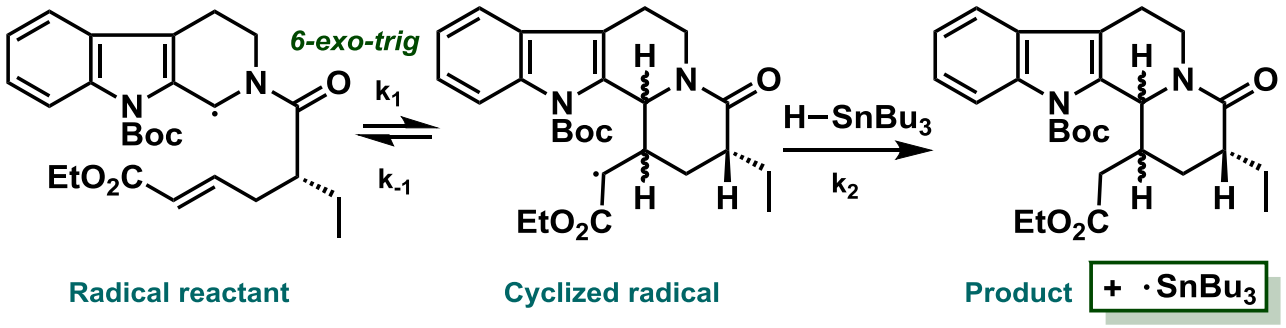

Scheme 26. Delineation of the two step radical process from the radical reactant to the products.

In the second step of this process (Scheme 26), we should note the formation of the strong C-H bond (452 kJ.mol^{-1}) at the expense of the much weaker H-Sn bond (267 kJ.mol^{-1}).[27] This large difference in bond strengths meant that the second step (k_2) would likely happen much more rapidly compared to equilibration in the first (k_{-1}), implying that the rate of the reaction is dependent on the rate of the initial cyclization, and thus, that there is no appreciable equilibration in the first cyclization step ($k_2 > k_{-1}$).

In view of this, we looked to model the rate-determining cyclization in the form of a reaction energy diagram. With the computed the minimum energy of the radical reactant, the activation energies of each of the transition states, and the energies of the four possible radical products in hand, we were able to construct the reaction energy profile shown in Figure 21.

The reaction energy diagram obtained highlighted several interesting aspects (Figure 21). Firstly, it indicated that both the **up/up TS-1** as well as the **up/up** radical product were lowest in relative energy, in full agreement with our experimental observations. Secondly, it indicated that the radical to radical cyclization is endergonic ($\Delta G>0$, non-spontaneous), meaning that the cyclized radical products are higher in energy than the radical reactant.

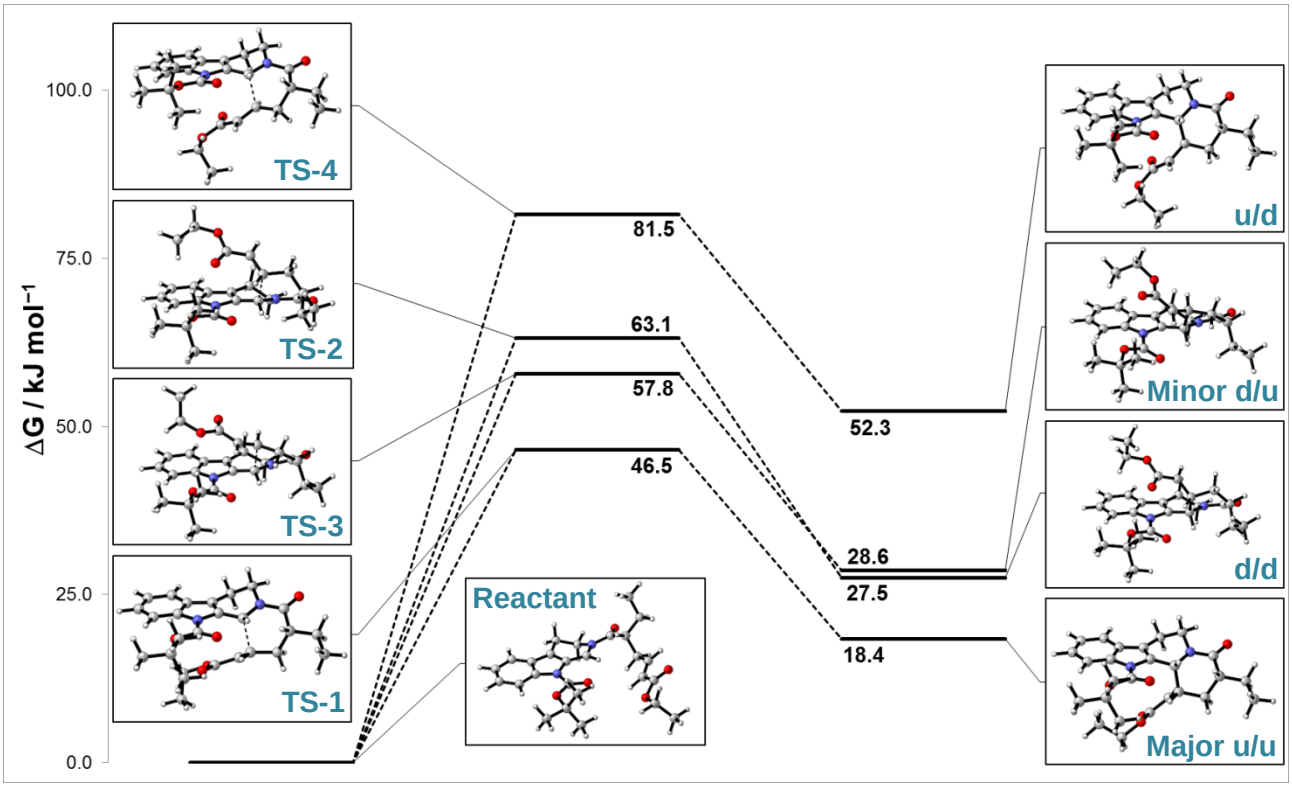

Figure 21. Reaction energy profile of the radical to radical cyclization step (Scheme 25). *Calculations done using PW6B95–D3/def2–QZVP//TPSS–D3/def2–TZVP. Toluene solvent included using SMD. RRHO correction to free energy obtained from vibrational frequency analysis at TPSS–D3/def2–TZVP*.

This can be rationalized by the loss of entropy (due to loss of degrees of freedom) as well as an increase in enthalpy (due to increased non-bonding interactions as well as π- to σ-bond formation) going from the radical reactant to the radical product, resulting in an overall $\Delta G>0$ according to $\Delta G = \Delta H - T\Delta S$. This also implied a degree of reversibility, which would in turn depend on the rate of the second hydrogen reduction. Since we had already postulated that the rate of the second step (k_2) would be much faster (higher), we assumed that the degree of reversibility would thus be negligible. These insights indicate that the reaction overall likely proceeds under kinetic control, which in turn meant that the relative activation energies calculated for each of the transition states (Figure 20) would determine the diastereomeric ratio as reflected in the products.

Furthermore, the exact nature of the interplay of non-bonded interactions and conformational aspects determining the relative order of activation energies leading to **TS1-4** is complex and somewhat beyond the scope of this dissertation. The nature of the enoate ester stacking relative to the indole ring, the configurational preference of the C-20 ethyl group, as well as the nature of the D-ring as it folds as either chair- or boat-like, no doubt all play their roles

2.4 Conclusions

As detailed in the previous sections, we have developed a novel strategy for the asymmetric synthesis of (+)-tacamonine proceeding over 8 steps from commercially available materials in 10 distinct operations, making it the shortest known route developed to date (summarized in Scheme 27).

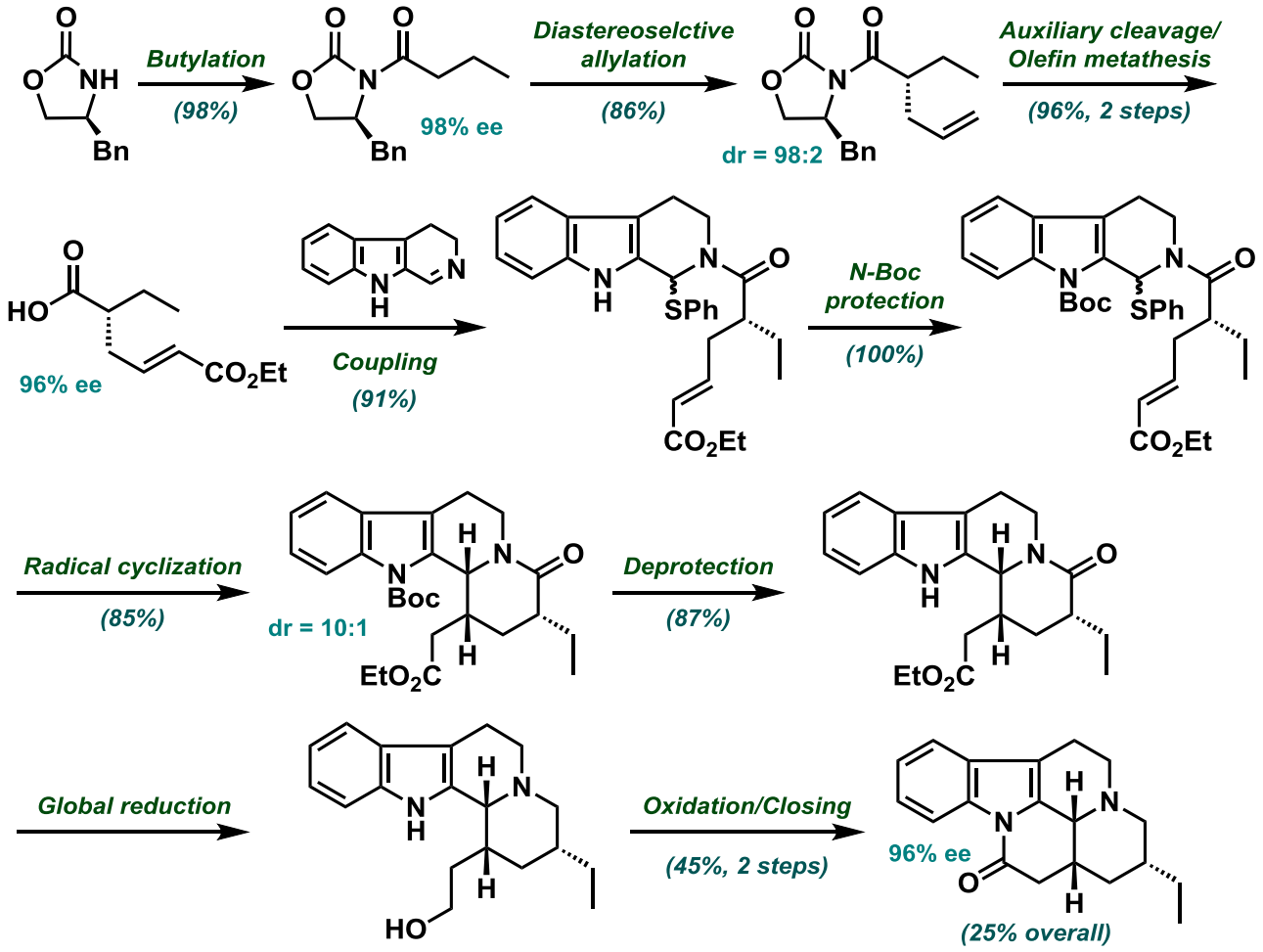

Scheme 27. A summary of our route to the target (+)-tacamonine.

Our highly-efficient strategy allowed for the synthesis of the target in 25% overall yield and in 96% enantiomeric access. Furthermore, computational investigation of the kinetically controlled diastereoselective radical cyclization procedure suggested the formation of a major product coinciding with our experimental observations. This novel route along with our computational calculations will be published in due course.

2.5 References

1. R. Clauss and R. Hunter, *J. Chem. Soc., Perkin Trans. 1*, **1997**, 71-76.
2. R. Hunter and P. Richards, *Tetrahedron Lett.*, 2000, **41**, 3755-3758.
3. M. W. Smith, R. Hunter, D. J. Patten and W. Hinz, 2009, **50**, 6342-6346.
4. T. A. van Beek, R. Verpoorte and A. B. Svendsen, *Tetrahedron*, 1984, **40**, 737-748.
5. N. Whittaker, *J. Chem. Soc.* (*C*), **1969**, 85-89.
6. C. Szántay, L. Tõke, M. B. Bárczai and G. Kalaus, *Period. Polytech. Chem. Eng.*, 1965, **9**, 231-236.
7. B. Pal, P. Jaisankar, V. S. Giri, S. Mondal and M. Mukherjee, *Tetrahedron Lett.*, 2004, **45**, 6489-6492.
8. D. A. Evans, J. S. Tedrow, J. T. Shaw and C. W. Downey, *J. Am. Chem. Soc.*, 2002, **124**, 392-393.
9. D. Balamurugan and K. M. Muraleedharan, *Tetrahedron*, 2009, **65**, 10074-10082.
10. D. A. Evans, M. D. Ennis and D. J. Mathre, *J. Am. Chem. Soc.*, 1982, **104**, 1737-1739.
11. D. A. Evans, D. L. Rieger, T. K. Jones and S. W. Kaldor, *J. Org. Chem.*, 1990, **55**, 6260-6268.
12. D. A. Evans, T. C. Britton and J. A. Ellman, *Tetrahedron Lett.*, 1987, **28**, 6141-6144.
13. S. B. Garber, J. S. Kingsbury, B. L. Gray and A. H. Hoveyda, *J. Am. Chem. Soc.*, 2000, **122**, 8168-8179.
14. A. A. Waghmare, R. M. Hindupur and H. N. Pati, *Rev. J. Chem.*, 2014, **4**, 53-131.
15. E. Valeur and M. Bradley, *Chem. Soc. Rev.*, 2009, **38**, 606-631.
16. D. X. Hu, P. Grice and S. V. Ley, *J. Org. Chem.*, 2012, **77**, 5198-5202.
17. V. H. Rawal and M. P. Cava, *Tetrahedron Lett.*, 1985, **26**, 6141-6142.
18. A. A. El-Barbary, S. Carlsson and S-O. Lawesson, *Tetrahedron*, 1982, **38**, 405-412.
19. T. J. Curphey, *J. Org. Chem.*, 2002, **67**, 6461-6473.
20. M. Jesberger, T. P. Davis and L. Barner, *Synthesis*, 2003, **13**, 1929-1958.
21. T. Ozturk, E. Ertas and O. Mert, *Chem. Rev.*, 2007, **107**, 5210-5278.

22. A. G. Schultz and L. Pettus, *J. Org. Chem.*, 1997, **62**, 6855-6861.

23. I. Moldvai, T. Gáti, C. Szántay Jr. and C. Szántay, *J. Org. Chem.*, 2006, **71**, 3768-3772.

24. P. Mondal and N. P. Argade, *Org. Biomol. Chem.*, 2016, **14**, 10394-10406.

25. M. Lounasmaa, K. Karinen, D. Din Belle and A. Tolvanen, *Tetrahedron*, 1998, **54**, 157-164.

26. B. Danieli, G. Lesma, D. Passarella, A. Sacchetti and A. Silvani, *Tetrahedron Lett.*, 2001, **42**, 7237-7240.

27. T. L. Cottrell, *The Strengths of Chemical Bonds*, Butterworths Scientific Publications, London, 1958.

C H A P T E R 3

Experimental

3.1 General Procedures

All reagents were purchased from Sigma-Aldrich or Merck at the highest commercial quality and used without further purification. All dry solvents used were freshly distilled. Dichloromethane was distilled under nitrogen from phosphorus pentoxide. Tetrahydrofuran was distilled under nitrogen from sodium wire with benzophenone. Toluene was distilled under nitrogen from calcium hydride. All reactions were carried out under an argon atmosphere with dry solvents under anhydrous conditions unless otherwise stated. Low temperature reactions were carried out in an acetone bath cooled by liquid nitrogen to –78 °C unless otherwise stated. Reactions were magnetically stirred and monitored by thin-layer chromatography (TLC) carried out on aluminium-backed Merck silica-gel 60 F_{254} plates using UV light, iodine vapour and/or spraying with a 2.5% solution of anisaldehyde in a 10% sulfuric acid/ethanol mixture followed by heating as visualizing agents. Column chromatography was performed using Merck silica-gel (pore size 60 Å, 230 mesh). The enantiomeric excess (ee) and diastereomeric ratio (dr) values were calculated from peak area percentages obtained via high performance liquid chromatography (HPLC) using an Agilent Technologies 1220 Infinity LC instrument equipped with a UV detector. Specific rotations ($[\alpha]_D^{20}$) of optically active compounds were obtained using a Perkin Elmer 343 polarimeter at 20 °C and λ = 589 nm. The concentrations (*c*) of the samples used are given in g/100ml. Electron-ionization high resolution mass spectrometry (HRMS) was performed using a Direct Probe JEOL GCmate II instrument. Melting points were obtained using a Reichert Jung Thermovar hot-stage microscope and are uncorrected. Infrared (IR) absorptions were measured using a Bruker Tensor27 platinum ATR instrument. Nuclear magnetic resonance (NMR) spectra were recorded on either Bruker Ultrashield 400 Plus or Bruker 300 instruments and were carried out in chloroform-d unless otherwise stated. Chemical shifts (δ) were recorded in ppm relative to residual chloroform resonances at 7.26 and 77.16 in ^{1}H NMR and ^{13}C NMR respectively unless otherwise stated. All the structures are numbered relative to the natural (+)-tacamonine numbering convention.[1]

N-Formyltryptamine 24[2]

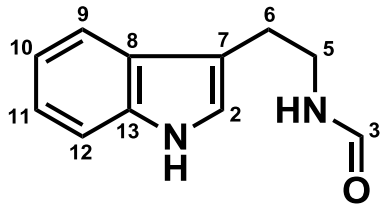

Excess ethyl formate (80 mL) was added to a flask containing tryptamine (10.0 g, 62.4 mmol, 1.0 equiv) and the stirred suspension immediately heated to 60 °C for 1 h then left to stir overnight at 70 °C. After 17 h the solution was allowed to cool to room temperature and the remaining ethyl formate was removed *in vacuo* to yield crude **24** (12.7 g) as a brown oil[2] that was used immediately in the next step.

3,4-Dihydro-β-carboline 8[3]

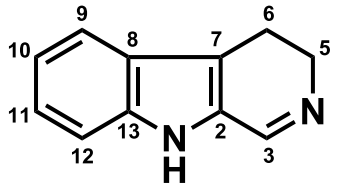

Excess phosphoryl chloride (55 mL, 590. mmol, 8.7 equiv) was slowly added to a flask containing the crude **24** (12.7 g, 67.5 mmol, 1.0 equiv) at 0 °C over 15 min and then left to stir at room temperature. After 1.5 h the excess phosphoryl chloride was removed by distillation and H_2O (1000 mL) was slowly added to the crude residue at 0 °C with stirring, after which the aqueous mixture was filtered to remove a black solid precipitate that formed during the addition. The filtrate was then basified with concentrated aqueous ammonia from which 3,4-dihydro-β-carboline **8** separated as a pale yellow micro-crystalline solid[3] (10.2 g, 96% yield over 2 steps). The resulting crude product was deemed pure enough by ^{1}H NMR spectroscopy to be used in the following coupling step without further purification.

Mp = 173 – 176 °C (Literature[3] = 175 – 176 °C); ^{1}H NMR (300 MHz, $CDCl_3$) δ 8.71 (br s, 1H, N-**H**), 8.38 (br s, 1H, H-3), 7.59 (d, *J* = 8.0 Hz, 1H, H-12), 7.39 (d, *J* = 8.2 Hz, 1H, H-9), 7.28 (t, *J* = 7.1 Hz, 1H, H-10), 7.15 (t, *J* = 7.1 Hz, 1H, H-11), 3.89 (m, 2H, H-5), 2.90 (t, *J* = 8.3 Hz, 2H, H-6).

Butyryl oxazolidinone 21[4]

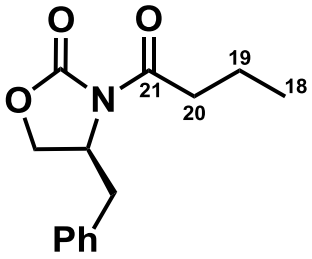

(*S*)-4-Benzyl-2-oxazolidinone (863 mg, 4.87 mmol, 1.0 equiv) was dissolved in THF (20 mL) and cooled to –78 °C before *n*-BuLi (1.6 M solution in hexanes, 3.35 mL, 5.36 mmol, 1.1 equiv) was added dropwise over 5 min. After stirring for a further 30 min at –78 °C, freshly distilled butyryl chloride (0.71 mL, 6.82 mmol, 1.4 equiv) was added dropwise and the mixture left to warm to room temperature slowly over 4 h. At this point saturated aqueous NH_4Cl (20 mL) was added and the reaction contents transferred to a separatory funnel, diluting with water (30 mL) and CH_2Cl_2 (50 mL). The layers were separated and the aqueous layer extracted a further two times with CH_2Cl_2 (50 mL). The combined organic layers were dried with $MgSO_4$, filtered and concentrated *in vacuo*. The resulting product was purified by flash chromatography (silica gel, EtOAc/hexanes, 0% to 15%) to give **21** (1.177 g, 98%) as a colourless syrup. The data given below is in agreement with the literature data.[4]

$[\alpha]_D^{20}$ = +53.8 (Literature[4] = +52.4, *c* = 1, $CHCl_3$); ee found as 98% by HPLC (Daicel Chiralcel OD column, 0.46 cm × 25 cm, 10% *i*-PrOH/hexane, 1 mL/min, τ_{major} = 11.2 min, τ_{minor} = 14.1 min); IR (neat) ν_{max} 1774 (carbamate, C=O), 1696 (C-21, C=O) cm^{-1}; ^1H NMR (400 MHz, $CDCl_3$) δ 7.34 – 7.31 (m, 2H, Ph-**H**), 7.29 – 7.26 (m, 1H, Ph-**H**), 7.21 (d, *J* = 6.9 Hz, 2H, Ph-**H**), 4.70 – 4.66 (m, 1H, ($PhCH_2$)C**H**), 4.21 – 4.15 (m, 2H, ($PhCH_2$)CH(C$\mathbf{H}_2$O-)), 3.30 (dd, *J* = 13.4, 3.2 Hz, 1H, ($PhCH_a\mathbf{H_b}$)CH), 2.98 – 2.93 (m, 1H, H-20_b), 2.91 – 2.85 (m, 1H, H-20_a), 2.77 (dd, *J* = 13.4, 9.6 Hz, 1H, (PhC$\mathbf{H_a}H_b$)CH), 1.77 – 1.70 (m, 2H, H-19), 1.01 (t, *J* = 7.4 Hz, 3H, H-18); ^{13}C NMR (101 MHz, $CDCl_3$) δ 173.4 (C-21), 153.6 (-O(**C**=O)N-), 135.5 (C-arom), 129.6 (2C-arom), 129.1 (2C-arom), 127.5 (C-arom), 66.3 (($PhCH_2$)CH(**C**H_2O-)), 55.3 (($PhCH_2$)**C**H(CH_2O-)), 38.1 (($Ph\mathbf{C}H_2$)CH(CH_2O-)), 37.5 (C-20), 17.9 (C-19), 13.8 (C-18); HRMS (ESI) calcd for $C_{14}H_{17}NO_3Na^+$ $[M + Na]^+$ requires 270.1105, found 270.1105.

Allylated oxazolidinone 22[5]

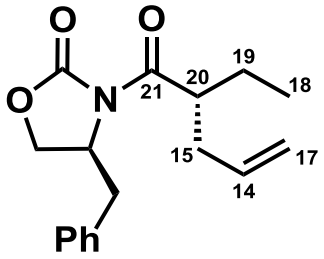

NaHMDS (1.0 M solution in THF, 5.24 mL, 5.24 mmol, 1.1 equiv) was added to a solution of **21** (1.177 g, 4.76 mmol, 1.0 equiv) in THF (20 mL) at –78 °C dropwise over 15 min with stirring. After stirring for a further 30 min, allyl bromide (1.03 mL, 11.9 mmol, 2.5 equiv) was added to the reaction mixture at –78 °C over 5 min, and the reaction mixture allowed to warm to –20 °C slowly over 5 h. The reaction mixture was quenched with saturated aqueous NH_4Cl (20 mL) and transferred to a separatory funnel, diluting with water (30 mL) and CH_2Cl_2 (50 mL). The layers were separated and the aqueous layer extracted a further two times with CH_2Cl_2 (50 mL). The combined organic layers were dried with $MgSO_4$, filtered and concentrated *in vacuo*. The resulting product was purified by flash chromatography (silica gel, EtOAc/hexanes, 0% to 10%) to give **22** (1.177 g, 86%) as a clear, colourless oil. The data that follows is in agreement with the literature data.[5]

$[\alpha]_D^{20}$ = +57.9 (*c* = 1, $CHCl_3$); dr found as 98:2 by HPLC (Zorbax Eclipse Plus C18 column, 0.46 cm × 15 cm, 50% H_2O/acetonitrile, 1 mL/min, τ_{major} = 19.1 min, τ_{minor} = 26.8 min); IR (neat) v_{max} 1785 (carbamate, C=O), 1697 (C-21, C=O) cm^{-1}; ^1H NMR (400 MHz, $CDCl_3$) δ 7.34 – 7.32 (m, 2H, Ph-**H**), 7.28 – 7.26 (m, 1H, Ph-**H**), 7.22 (d, *J* = 7.0 Hz, 2H, Ph-**H**), 5.83 (ddt, *J* = 17.1, 10.0, 7.0 Hz, 1H, H-14), 5.09 (dd, *J* = 17.1, 1.7 Hz, 1H, H-17_b), 5.04 (dd, *J* = 10.0, 1.7 Hz, 1H, H-17_a), 4.72 – 4.68 (m, 1H, ($PhCH_2$)C**H**), 4.16 (dd, *J* = 9.1, 7.4 Hz, 1H, ($PhCH_2$)CH(CH_a**H**$_b$O-)), 4.14 (dd, *J* = 9.1, 3.0 Hz, 1H, ($PhCH_2$)CH(C**H**$_a$$H_b$O-)), 3.86 (tt, *J* = 7.9, 5.7 Hz, 1H, H-20), 3.30 (dd, *J* = 13.4, 3.3 Hz, 1H, ($PhCH_a$**H**$_b$)CH), 2.68 (dd, *J* = 13.4, 10.0 Hz, 1H, (PhC**H**$_a$$H_b$)CH), 2.51 – 2.46 (m, 1H, H-15_b), 2.35 – 2.31 (m, 1H, H-15_a), 1.79 – 1.72 (m, 1H, H-19_b), 1.60 – 1.55 (m, 1H, H-19_a), 0.93 (t, *J* = 7.4 Hz, 3H, H-18); ^{13}C NMR (101 MHz, $CDCl_3$) δ 176.1 (C-21), 153.3 (-O(**C**=O)N-), 135.6 (C-arom), 135.5 (C-14), 129.6 (2C-arom), 129.1 (2C-arom), 127.5 (C-arom), 117.2 (C-17), 66.1 (($PhCH_2$)CH(**C**H_2O-)), 55.7 (($PhCH_2$)**C**H(CH_2O-)), 43.9 (C-20), 38.3 ((Ph**C**H_2)CH(CH_2O-)), 36.4 (C-15), 24.7 (C-19), 11.7 (C-18); HRMS (ESI) calcd for $C_{17}H_{21}NO_3Na^+$ $[M + Na]^+$ requires 310.1418, found 310.1419.

Free acid 23[6]

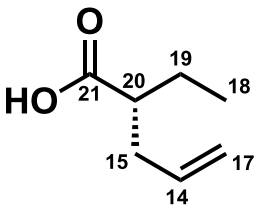

LiOH monohydrate (329 mg, 7.83 mmol, 2.0 equiv) followed by H_2O_2 (30% solution, 8.82 M, 2.23 mL, 19.6 mmol, 5.0 equiv) was added to a solution of **22** (1.126 g, 3.92 mmol, 1.0 equiv) in THF/H_2O 5:1 (10 mL) at 0 °C with stirring. After 2 h saturated aqueous Na_2SO_3 was added (10 mL), the excess THF was removed under reduced pressure and the contents transferred to a separatory funnel. The aqueous layer was diluted with water (10 mL) and washed with CH_2Cl_2 (3 x 20 mL) to remove free chiral auxiliary (96% recovery) and then acidified to pH ~ 1. The acidic solution was extracted with CH_2Cl_2 (3 x 20 mL), the organic extracts combined, dried over $MgSO_4$ and concentrated *in vacuo* to give crude **23** in quantitative yield as a clear, colourless oil.

$[\alpha]_D^{20}$ = +3.3 (*c* = 1, $CHCl_3$); IR (neat) ν_{max} 1702 (C-21, C=O) cm^{-1}; ^1H NMR (400 MHz, $CDCl_3$) δ 5.77 (ddt, *J* = 17.0, 10.1, 6.9 Hz, 1H, H-14), 5.09 (dd, *J* = 17.0, 1.7 Hz, 1H, H-17_b), 5.04 (dd, *J* = 10.1, 1.7 Hz, 1H, H-17_a), 2.42 – 2.37 (m, 2H, H-15), 2.29 – 2.23 (m, 1H, H-20), 1.69 – 1.64 (m, 1H, H-19_b), 1.61 – 1.56 (m, 1H, H-19_a), 0.95 (t, *J* = 7.4 Hz, 3H, H-18); ^{13}C NMR (101 MHz, $CDCl_3$) δ 182.1 (C-21), 135.4 (C-14), 117.1 (C-17), 46.8 (C-20), 35.8 (C-15), 24.7 (C-19), 11.7 (C-18); HRMS (ESI) calcd for $C_7H_{11}O_2^-$ $[M - H]^-$ requires 127.0757, found 127.0761.

Acid ester 15

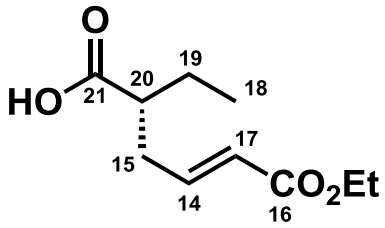

Excess ethyl acrylate (4.35 mL, 39.9 mmol, 5.0 equiv) followed by the Hoveyda-Grubbs 2nd generation catalyst (50.0 mg, 0.080 mmol, 0.01 equiv) was added to a solution of crude free acid **23** (1.023 g, 7.98 mmol, 1.0 equiv) in dry, degassed (by 15 min argon purge) CH_2Cl_2 (40 mL) at room temperature with stirring. The resulting suspension was then immediately heated to reflux at 50 °C. After 2 h the reaction mixture was removed from heat and left to cool before being concentrated *in vacuo*. The dark red-brown residue was then purified directly by flash chromatography (silica gel, EtOAc/hexanes, 0% to 20%) to give acid ester **15** (1.527 g, 96%) as a clear, pale brown oil.

$[\alpha]_D^{20}$ = –11.2 (*c* = 1, $CHCl_3$); ee found as 96% by HPLC (Daicel Chiralpak IC column, 0.46 cm × 25 cm, 5% *i*-PrOH/hexane, 0.75 mL/min, τ_{major} = 19.3 min, τ_{minor} = 16.8 min); IR (neat) ν_{max} 1713 (C-16, C=O), 1702 (C-21, C=O), 1651 (C=C) cm^{-1}; ^1H NMR (400 MHz, $CDCl_3$) δ 6.89 (dt, *J* = 15.6, 7.0 Hz, 1H, H-14), 5.87 (d, *J* = 15.6 Hz, 1H, H-17), 4.18 (q, *J* = 7.1 Hz, 2H, -OC**H**$_2$CH$_3$), 2.60 – 2.45 (m, 2H, H-15), 2.42 – 2.35 (m, 1H, H-20), 1.73 – 1.59 (m, 2H, H-19), 1.28 (t, *J* = 7.1 Hz, 3H, -OCH$_2$C**H**$_3$), 0.96 (t, *J* = 7.4 Hz, 3H, H-18); ^{13}C NMR (101 MHz, $CDCl_3$) δ 180.7 (C-21), 166.5 (C-16), 145.4 (C-14), 123.6 (C-17), 60.5 (C-20), 45.7 (-O**C**H$_2$CH$_3$), 33.7 (C-15), 24.8 (C-19), 14.4 (-OCH$_2$**C**H$_3$), 11.5 (C-18); HRMS (ESI) calcd for $C_{10}H_{16}O_4Na^+$ $[M + Na]^+$ requires 223.0946, found 223.0941.

Sulfanyl amides 16[7]

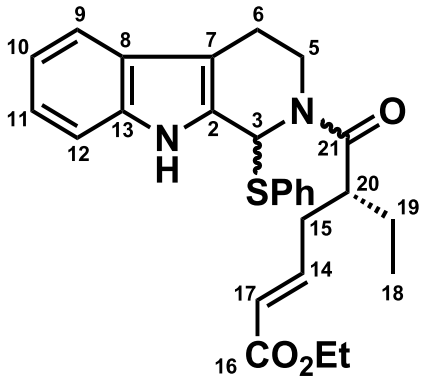

Acid ester **15** (940 mg, 4.70 mmol, 1.0 equiv) was dissolved in CH_2Cl_2 (90 mL) and cooled to 0 °C before a sequence of *N*,*N*′-dicyclohexylcarbodiimide (1.065 g, 5.16 mmol, 1.1 equiv), 1-hydroxybenzotriazole (698 mg, 5.16 mmol, 1.1 equiv) and 3,4-dihydro-β-carboline (959 mg, 5.63 mmol, 1.2 equiv) was added to the solution with stirring. After 1 h the reaction mixture was cooled to –78 °C and $BF_3{\cdot}OEt_2$ (0.77 mL, 6.10 mmol, 1.3 equiv) was added followed by the addition of thiophenol (0.63 mL, 6.10 mmol, 1.3 equiv) and the mixture slowly left to warm to –50 °C over a 1 h period. The reaction mixture was then quenched by the addition of saturated aqueous $NaHCO_3$ (50 mL) before the contents were transferred into a separatory funnel and diluted with another 50 mL of aqueous $NaHCO_3$ and 100 mL CH_2Cl_2. The organic layer was extracted and the aqueous layer washed a further three times with CH_2Cl_2 (100 mL). The combined organic layers were dried with $MgSO_4$, filtered and concentrated *in vacuo*. Cold Et_2O (100 mL) was then added to the grainy residue before being filtered through a pad of Celite and concentrated in order to remove the thiourea by-product. This cold filtration process was then repeated a further two times. The resulting residue was purified carefully by flash chromatography (silica gel, EtOAc/hexanes, 0% to 20%) to give a mixture of diastereomers with two amide rotamers each (1.985 g, 91%) as a clear, colourless foam **16**.

$[\alpha]_D^{20}$ = –8.9 (*c* = 1, $CHCl_3$); IR (neat) ν_{max} 2969 (N-H), 1781 (C-16, C=O), 1701 (C-21, C=O) cm^{-1}; ^1H NMR (400 MHz, $CDCl_3$) δ 8.32, 8.23, 8.17, 8.11 (s, 1H, N-**H**), 7.54 – 7.21 (m, 5H, SPh-**H**), 7.48 – 7.45, 7.33 – 7.29, 7.22 – 7.19, 7.16 – 7.09 (m, 4H, {H-9 to H-12}), 7.42, 7.38, 6.44, 6.34 (s, 1H, H-3), 6.85, 6.81, 6.64, 6.51 (dt, *J* = 15.6, 7.4 Hz, 1H, H-14), 5.85, 5.76, 5.71, 5.57 (d, *J* = 15.6 Hz, 1H, H-17), 4.96 – 4.89, 4.11 – 4.08, 3.83 – 3.78, 3.31 – 3.22 (m, 2H, H-5), 4.23 – 4.19, 4.00 – 3.95, 3.90 – 3.85, 3.61 – 3.55 (m, 2H, -OC**H**$_2$CH$_3$), 2.85 – 2.75 (m, 2H, H-6), 2.82 – 2.78, 2.24 – 2.18 (m, 1H, H-20), 2.55 – 2.50, 2.41 – 2.36, 2.32 – 2.27, 2.24 – 2.19, 1.97 – 1.92 (m, 2H, H-15), 1.71 – 1.64, 1.63 – 1.57, 1.52 – 1.45, 1.35 – 1.31 (m, 2H, H-19), 1.31, 1.30, 1.06, 0.92 (t, *J* = 7.1 Hz, 3H, -

$OCH_2C\mathbf{H}_3$), 0.81, 0.77, 0.65, 0.55 (t, *J* = 7.4 Hz, 3H, H-18); ^{13}C NMR (101 MHz, $CDCl_3$) δ {174.0, 173.8, 173.6, 173.5 (C-21)}, {166.6, 166.4, 166.2, 165.7 (C-16)}, {146.8, 145.9, 145.9, 144.3 (C-14)}, 136.7, 136.5, 136.5, 136.3, 136.2, 134.3, 133.9, 132.5, 132.5, 131.5, 131.5, 130.6, 130.4, 129.9, 129.8, 129.7, 129.4, 129.3, 129.0, 128.5, 128.4, 126.5, 126.5, 126.4, 126.4, {123.8, 123.5, 123.5, 123.2 (C-17)}, 123.3, 123.1, 122.9, 122.9, 120.2, 119.9, 119.9, 119.0, 118.9, 118.6, 118.5, 111.5, 111.4, 110.2, 110.2, {62.6, 62.6, 58.0, 57.9 (C-3)}, {60.5, 60.3, 60.3, 60.2 (-O**C**H_2CH_3)}, {42.9, 42.6, 42.6, 41.5 (C-20)}, {40.2, 40.2, 36.6, 36.4 (C-5)}, {35.2, 34.6, 33.7 (C-15)}, {25.8, 25.3, 25.2, 25.1, (C-19)}, {22.6, 22.6, 21.3, 21.1 (C-6)}, {14.4, 14.2, 14.0 (-OCH_2**C**H_3)}, {11.8, 11.3, 10.8 (C-18)}; HRMS (ESI) calcd for $C_{21}H_{25}N_2O_3^+$ $[M - SPh]^+$ requires 353.1865, found 353.1875.

_N_-Boc protected sulfanyl amides 17[7]

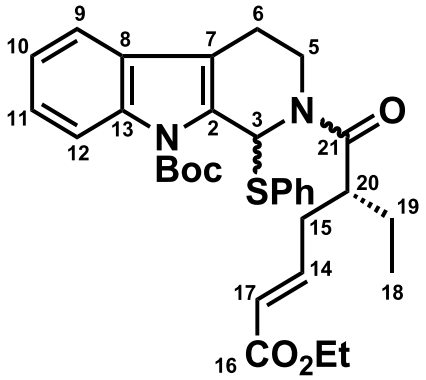

Di-*tert*-butyl dicarbonate (1.492 g, 6.83 mmol, 1.3 equiv) followed by 4-dimethylaminopyridine (32 mg, 0.263 mmol, 0.05 equiv) was added to a solution of sulfanyl amides **16** (2.432 g, 5.26 mmol, 1.0 equiv) in THF (30 mL) at room temperature with stirring. After 2 h the reaction mixture was concentrated *in vacuo* and the residue purified by flash chromatography (silica gel, EtOAc/hexanes, 0% to 25%) to give a mixture of diastereomers and amide rotamers **17** in quantitative yield (2.957 g) as a white paste.

$[\alpha]_D^{20}$ = +10.1 (*c* = 1, $CHCl_3$); IR (neat) ν_{max} 1737 (Boc, C=O), 1721 (C-16, C=O), 1648 (C-21, C=O) cm^{-1}; ^{1}H NMR (400 MHz, $CDCl_3$) δ 8.20 – 8.18, 8.03 – 8.00, 7.68 – 7.66, 7.50 – 7.30, 7.28 – 7.20 (m, 9H, {H-9 to H-12, SPh-**H**}), 8.03, 8.00, 7.26, 7.23 (s, 1H, H-3), 6.83 – 6.76, 6.69 – 6.64, 6.41 – 6.36 (m, 1H, H-14), 5.78, 5.77, 5.64, 5.56 (d, *J* = 15.6 Hz, 1H, H-17), 4.96 – 4.89, 4.14 – 4.08, 4.04 – 4.01, 3.74 – 3.66 (m, 2H, H-5), 4.22 – 4.16, 4.00 – 3.94, 3.87 – 3.81, 3.44 – 3.39, 3.17 – 3.11 (m, 2H, -OC$\mathbf{H}_2CH_3$), 2.83 – 2.74 (m, 2H, H-6), 2.82 – 2.72, 2.25 – 2.19, 2.15 – 2.08 (m, 1H, H-20), 2.55 – 2.49, 2.33 – 2.08,

1.85 – 1.81 (m, 2H, H-15), 1.81, 1.79, 1.70, 1.69 (s, 3H, -OC(C**H**$_3$)$_3$), 1.72 – 1.14 (m, 2H, H-19), 1.32, 1.28, 1.07, 0.89 (t, *J* = 7.1 Hz, 3H, -OCH$_2$C**H**$_3$), 0.82, 0.69, 0.64, 0.39 (t, *J* = 7.4 Hz, 3H, H-18); ^{13}C NMR (101 MHz, $CDCl_3$) δ {173.7, 173.7, 173.4 (C-21)}, {166.6, 166.4, 166.3, 165.3 (C-16)}, {150.1, 150.0, 149.6 (-**C**O$_2$^{t}Bu)}, {147.0, 146.0, 145.9, 144.5 (C-14)}, 136.7, 136.7, 136.4, 136.3, 136.2, 136.0, 133.7, 133.6, 132.9, 132.8, 132.3, 131.9, 131.3, 131.2, 131.0, 129.6, 129.6, 129.5, 129.3, 128.9, 128.3, 128.1, 128.1, 127.6, 127.5, 125.3, 125.2, 125.1, 123.7, 123.4, 123.4, 123.1, 123.0, 123.0, 122.9, 122.8, 118.9, 118.7, 118.5, 118.5, 118.3, 118.2, 116.5, 116.4, 116.0, 115.9, 115.8, 115.7, {84.8, 84.7, 84.5 (-O**C**(CH$_3$)$_3$)}, {64.6, 64.4, 58.1, 58.0 (C-3)}, {60.4, 60.3, 59.7 (-O**C**H$_2$CH$_3$)}, {42.7, 42.7, 42.6, 41.4 (C-20)}, {38.6, 35.6, 35.1, 34.7 (C-5)}, {34.8, 34.6, 33.8 (C-15)}, {28.5, 28.5, 28.4, 28.3 (-OC(**C**H$_3$)$_3$)}, {25.8, 25.2, 25.0 (C-19)}, {22.3, 22.3, 20.8, 20.7 (C-6)}, {14.5, 14.4, 14.2, 14.1 (-OCH$_2$**C**H$_3$)}, {12.0, 11.5, 11.3, 10.8 (C-18)}; HRMS (ESI) calcd for $C_{26}H_{33}N_2O_5^+$ [M – SPh]$^+$ requires 453.2389, found 453.2396.

Lactam major-18[7]

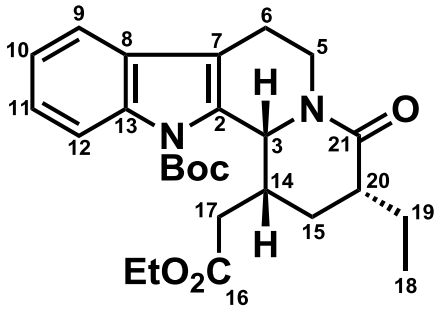

To a solution of *N*-Boc protected sulfanyl amides **17** (2.824 g, 5.02 mmol, 1.0 equiv) in dry, degassed (by 30 min argon purge) toluene (220 mL) was added *n*-Bu$_3$SnH (1.75 mL, 6.52 mmol, 1.3 equiv) and the mixture immediately heated to reflux. Once the reaction mixture was refluxing vigorously a solution of 1,1'-azobis(cyclohexanecarbonitrile) (123 mg, 0.502 mmol, 0.1 equiv) in dry, degassed (by 30 min argon purge) toluene (30 mL) was slowly added over 1 h. After refluxing for a further 2 h the reaction mixture was left to cool to room temperature before being concentrated *in vacuo*. The resulting residue was very carefully chromatographed (silica gel, EtOAc/hexanes, 0% to 20%) to give major *cis*-**18** (2.052 g, 85% corrected yield) and minor *trans*-**18** (144 mg, 8% corrected yield) diastereomers as clear, colourless gums (dr = 10:1). The data that follows is for the major *cis*-**18** diastereomer which was isolated with ~11% of the minor *trans*-**18** diastereomer present.

$[\alpha]_D^{20}$ = +159.9 (*c* = 1, $CHCl_3$); IR (neat) ν_{max} 1732 (Boc, C=O), 1722 (C-16, C=O), 1665 (C-21, C=O) cm^{-1}; ^1H NMR (400 MHz, $CDCl_3$) δ 8.10 (d, *J* = 8.2 Hz, 1H, H-12), 7.47 – 7.44 (m, 1H, H-9), 7.31 (td, *J* = 7.4, 1.4 Hz, 1H, H-10), 7.26 (td, *J* = 7.4, 1.2 Hz, 1H, H-11), 5.47 (br d, *J* = 3.6 Hz, 1H, H-3), 4.88 – 4.83 (m, 1H, H-5_b), 3.81 – 3.72 (m, 1H, -OC**H**$_2$$CH_3$), 3.62 – 3.54 (m, 1H, -OC**H**$_2$$CH_3$), 3.25 – 3.16 (m, 1H, H-14), 2.95 – 2.87 (m, 1H, H-5_a), 2.88 – 2.87 (m, 1H, H-6_b), 2.71 – 2.67 (m, 1H, H-6_a), 2.50 (ddd, *J* = 13.7, 9.6, 7.5 Hz, 1H, H-15_b), 2.38 – 2.31 (m, 1H, H-20), 2.08 – 2.01 (m, 1H, H-19_b), 1.96 (dd, *J* = 15.9, 8.6 Hz, 1H, H-17_b), 1.88 (dd, *J* = 15.9, 6.1 Hz, 1H, H-17_a), 1.73 (br s, 9H, -OC(C**H**$_3$)$_3$), 1.44 – 1.37 (m, 1H, H-19_a), 1.12 – 1.07 (m, 1H, H-15_a), 1.02 (t, *J* = 7.5 Hz, 3H, H-18), 0.99 (t, *J* = 7.1 Hz, 3H, -OCH_2C**H**$_3$); ^{13}C NMR (101 MHz, $CDCl_3$) δ 175.0 (C-16), 172.1 (C-21), 150.2 (-**C**O_2^{t}Bu), 136.6 (C-13), 131.8 (C-2), 128.1 (C-8), 124.9 (C-11), 123.2 (C-10), 119.4 (C-9), 118.3 (C-12), 116.2 (C-7), 84.7 (-O**C**$(CH_3)_3$), 60.4 (-O**C**H_2CH_3), 54.2 (C-3), 40.8 (C-20), 38.3 (C-5), 36.7 (C-17), 34.1 (C-14), 31.3 (C-15), 28.4 (-OC(**C**$H_3)_3$), 23.7 (C-19), 20.5 (C-6), 14.0 (-OCH_2**C**H_3), 12.1 (C-18); HRMS (ESI) calcd for $C_{26}H_{35}N_2O_5^+$ $[M + H]^+$ requires 455.2548, found 455.2554.

Deprotected lactam 30[8]

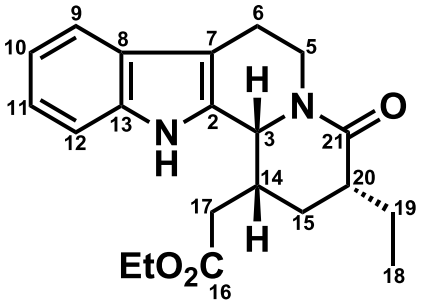

Neat lactam *cis*-**18** (101 mg, 0.222 mmol, 1.0 equiv) containing a small amount of minor *trans*-**18** was heated at a temperature of 180 °C for a period of 30 min, after which the deprotection reaction was shown to be complete by TLC analysis. The residue was then left to cool to room temperature and purified immediately by flash chromatography (silica gel, EtOAc/hexanes, 0% to 40%) to give deprotected major lactam *cis*-**30** (73 mg, 87% corrected yield) as a clear, pale yellow gum. The presence of trace amounts of minor deprotected lactam *trans*-**30** still allowed for the clean isolation of (+)-tacamonine later on.

$[\alpha]_D^{20}$ = +83.1 (*c* = 1, $CHCl_3$); IR (neat) ν_{max} 1726 (C-16, C=O), 1654 (C-21, C=O) cm^{-1}; ^1H NMR (400 MHz, $CDCl_3$) δ 7.96 (br s, 1H, N-**H**), 7.51 (d, *J* = 8.4 Hz, 1H, H-12), 7.36 – 7.32 (m, 1H, H-9), 7.21 – 7.17 (m, 1H, H-10), 7.15 – 7.11 (m, 1H, H-11), 4.93 (d, *J* = 4.1 Hz, 1H, H-3), 4.67 – 4.62 (m, 1H, H-5_b), 3.99 – 3.91 (m, 1H, -OC**H**$_2$$CH_3$), 3.87 – 3.78 (m, 1H, -OC**H**$_2$$CH_3$), 3.22 – 3.15 (m, 1H, H-5_a), 2.95 – 2.91 (m, 1H, H-14), 2.86 – 2.79 (m, 2H, H-6), 2.46 – 2.38 (m, 1H, H-15_b), 2.42 – 2.37 (m, 1H, H-20), 2.14 – 2.08 (m, 1H, H-17_b), 2.10 – 2.06 (m, 1H, H-19_b), 2.06 – 2.01 (m, 1H, H-17_a), 1.47 – 1.41 (m, 1H, H-19_a), 1.35 – 1.29 (m, 1H, H-15_a), 1.07 (t, *J* = 7.1 Hz, 3H, -OCH_2C**H**$_3$), 1.01 (t, *J* = 7.2 Hz, 3H, H-18); ^{13}C NMR (101 MHz, $CDCl_3$) δ 174.6 (C-16), 172.8 (C-21), 136.8 (C-13), 130.4 (C-2), 126.7 (C-8), 122.6 (C-11), 120.1 (C-10), 118.5 (C-9), 112.2 (C-12), 111.3 (C-7), 60.8 (-O**C**H_2CH_3), 54.2 (C-3), 41.1 (C-20), 39.9 (C-5), 35.8 (C-17), 34.8 (C-14), 30.2 (C-15), 24.4 (C-19), 20.5 (C-6), 14.1 (-OCH_2**C**H_3), 12.2 (C-18); HRMS (ESI) calcd for $C_{21}H_{27}N_2O_3^+$ [M + H]$^+$ requires 355.2023, found 355.2025.

Alcohol 31[9]

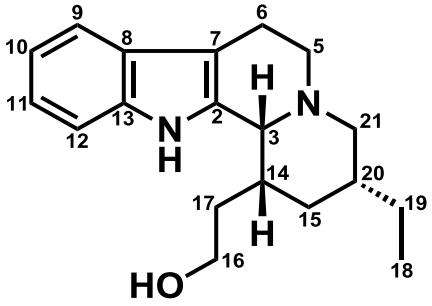

To a solution of deprotected lactam **30** (91 mg, 0.257 mmol, 1.0 equiv) in THF (10 mL) at –40 °C was added alane *N*,*N*-dimethylethylamine complex (0.5 M solution in toluene, 2.05 mL, 1.03 mmol, 4.0 equiv) dropwise over 30 min. The reaction mixture was left to stir at this temperature for 30 min before being allowed to warm to 0 °C. After stirring for a further 5 h at this temperature the reaction mixture was quenched by the careful addition of saturated Na_2SO_4 (2 mL) and filtered through a pad of Celite. The solid residue was washed with a large amount of 5% MeOH/CH_2Cl_2. The filtrate was then dried over $MgSO_4$ and concentrated *in vacuo* to give alcohol **31** (48 mg, 63% crude) as a yellowish residue that was used in the next step without further purification.

IR (neat) ν_{max} 3353 (O-H stretching), 1415 (O-H bending), 1054 (C-O stretching) cm^{-1}.

(+)-Tacamonine (1)[10]

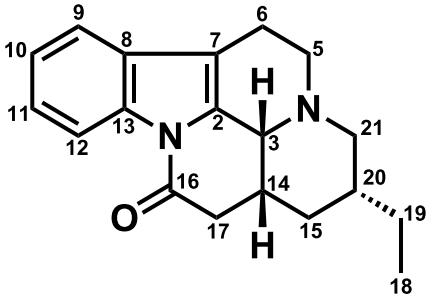

To a solution of crude **31** (48 mg, 0.161 mmol, 1.0 equiv) and a small amount of 4 Å molecular sieves (15 mg) in CH_2Cl_2 (5 mL) was added *N*-methylmorpholine *N*-oxide (38 mg, 0.322 mmol, 2.0 equiv) followed by tetrapropylammonium perruthenate (11 mg, 0.032 mmol, 0.2 equiv) 10 min later with stirring at room temperature. After 3 h the resulting mixture was filtered through a small pad of Celite and washed with a large amount of CH_2Cl_2. The filtrate was transferred to a separatory funnel and washed with saturated Na_2SO_3 (5 mL), brine (5 mL), and saturated $CuSO_4$ (5 mL). The organic layer was separated, dried and concentrated. The dark brown residue was purified by flash chromatography (silica gel, MeOH/CH_2Cl_2, 0% to 5%) to afford (+)-tacamonine (34 mg, 45% yield over 2 steps) as colourless needles. The data given below is in agreement with literature reports.[1,11,12]

Mp = 179 – 181 °C (Literature[1] = 180 – 181 °C); $[\alpha]_D^{20}$ = +117.2 (Literature[11] = +122, *c* = 0.2, $CHCl_3$); ee found as 96% by HPLC (Daicel Chiralcel OD column, 0.46 cm × 25 cm, 50% *i*-PrOH/hexane, 0.5 mL/min, τ_{major} = 22.6 min, τ_{minor} = 25.0 min); IR (neat) ν_{max} 1701 (C-16, C=O) cm^{-1}; ^{1}H NMR (400 MHz, $CDCl_3$) δ 8.38 (br dd, *J* = 7.3, 1.6 Hz, 1H, H-12), 7.46 – 7.43 (m, 1H, H-9), 7.35 – 7.27 (m, 2H, H-10 and H-11), 4.42 – 4.38 (m, 1H, H-3), 3.42 – 3.33 (m, 2H, H-5), 3.01 (dd, *J* = 17.0, 4.9 Hz, 1H, H-17$_b$), 2.97 – 2.87 (m, 1H, H-6$_b$), 2.71 – 2.66 (m, 1H, H-21$_b$), 2.68 (dd, *J* = 17.0, 2.2 Hz, 1H, H-17$_a$), 2.57 – 2.49 (m, 1H, H-6$_a$), 2.54 – 2.47 (m, 1H, H-14), 2.07 (t, *J* = 11.0 Hz, 1H, H-21$_a$), 1.71 – 1.66 (m, 1H, H-15$_b$), 1.63 – 1.54 (m, 1H, H-20), 1.16 – 1.08 (m, 2H, H-19), 0.86 (t, *J* = 7.4 Hz, 3H, H-18), 0.58 (ddd, *J* = 12.9, 12.8, 12.7 Hz, 1H, H-15$_a$); ^{13}C NMR (101 MHz, $CDCl_3$) δ 167.4 (C-16), 134.7 (C-13), 131.4 (C-2), 130.0 (C-8), 124.7 (C-11), 124.1 (C-10), 118.3 (C-9), 116.5 (C-12), 112.9 (C-7), 53.5 (C-3), 50.7 (C-21), 50.4 (C-5), 39.8 (C-17), 37.6 (C-20), 34.5 (C-14), 32.0 (C-15), 27.0 (C-19), 16.5 (C-6), 11.4 (C-18); HRMS (ESI) calcd for $C_{19}H_{23}N_2O^+$ [M + H]$^+$ requires 295.1812, found 295.1820.

3.2 X-Ray Crystal Structure Determination

Single crystal X-ray analysis of the pentacycle **19** and the target **1** was carried out in collaboration with Dr. Hong Su who is a scientific officer in the Centre for Supramolecular Chemistry Research at the University of Cape Town.

A single crystal of the pentacycle **19** and the target **1** were covered in a small amount of paratone oil and mounted on a glass fibre. Single-crystal X-ray diffraction data were collected on a Bruker KAPPA APEX II DUO diffractometer using graphite-monochromated Mo-Kα radiation (χ = 0.71073 Å). Data collection was carried out at 173(2) K. Temperature was controlled by an Oxford Cryostream cooling system (Oxford Cryostat). Cell refinement and data reduction were performed using the program SAINT.[13] The data were scaled and absorption correction performed using SADABS.[14] The structure was solved by direct methods using SHELXS-97[14] and refined by full-matrix least-squares methods based on F^2 using SHELXL-2014[14] and using the graphics interface program X-Seed.[15] The programs X-Seed and POV-Ray were both used to prepare molecular graphic images. All non-hydrogen atoms were refined anisotropically. All hydrogen atoms were placed in idealised positions and refined in riding models with U_{iso} assigned 1.2 or 1.5 times U_{eq} of their parent atoms and the bond distances were constrained from 0.95 to 1.00 Å. The structure was refined to R factor of 0.0368. Flack x = 0.217(999) by classical fit to all intensities; -0.701(660) from 1418 selected quotients (Parsons' method). Absolute structure cannot be determined reliably. The parameters for crystal data collection and structure refinements, the bond lengths, angles, torsion angles are beyond the scope of this work and have thus not been included for brevity.

3.3 Computational Methods

Computational modelling of the radical cyclization step was carried out in collaboration with Dr. Gerhard Venter who is an assistant director in the Scientific Computing Research Unit as well as a senior lecturer in the Department of Chemistry at the University of Cape Town.

The DFT calculations were done with the Gaussian 16 software package.[16] The conformational search was done with the confab module[17] as implemented in OpenBabel,[18] using the MMFF94 force field.[19] The structures were optimized using the TPSS DFT functional[20] and the def2-TZVP basis set.[21] The D3 dispersion correction of Grimme *et al.*, with the Becke-Johnson damping function,[22] was added. This level of theory is denoted as TPSS-D3(BJ)/def2-TZVP. Solvent affects were taken into account using the SMD model with default parameters for toluene.[23] Following the geometry optimization, single point energies were computed using the PW6B95 functional[24] and the larger def2-QZVP basis set,[21] again adding the D3 dispersion correction of Grimme *et al.*[22] (i.e. PW6B95-D3(BJ)/def2-QZVP). Thermal corrections to the energy were added using the standard rigid-rotor harmonic-oscillator (RRHO) approximations with frequencies computed at the TPSS-D3/def2-TZVP level of theory. All stationary points were characterized as either minima (no imaginary frequencies) or saddle-points (a single imaginary frequency). It was visually confirmed that the saddle-points are connected to the expected reactants and products by animating the normal mode associated with the imaginary frequency. All calculations were run using computational resources provided by the Centre for High Performance Computing (CHPC), South Africa.

3.4 References

1. T. A. van Beek, R. Verpoorte and A. B. Svendsen, *Tetrahedron*, 1984, **40**, 737-748.
2. González-Gómez, G. Domínguez and J. Pérez-Castells, *Tetrahedron*, 2009, **65**, 3378-3391.
3. (a) N. Whittaker, *J. Chem. Soc.* (*C*), **1969**, 85-89; (b) C. Szántay, L. Tõke, M. B. Bárczai and G. Kalaus, *Period. Polytech. Chem. Eng.*, 1965, **9**, 231-236.
4. D. A. Evans, J. S. Tedrow, J. T. Shaw and C. W. Downey, *J. Am. Chem. Soc.*, 2002, **124**, 392-393.
5. D. A. Evans, D. L. Rieger, T. K. Jones and S. W. Kaldor, *J. Org. Chem.*, 1990, **55**, 6260-6268.
6. D. A. Evans, T. C. Britton and J. A. Ellman, *Tetrahedron Lett.*, 1987, **28**, 6141-6144.
7. M. W. Smith, R. Hunter, D. J. Patten and W. Hinz, 2009, **50**, 6342-6346.
8. V. H. Rawal and M. P. Cava, *Tetrahedron Lett.*, 1985, **26**, 6141-6142.
9. P. Mondal and N. P. Argade, *Org. Biomol. Chem.*, 2016, **14**, 10394-10406.
10. A. G. Schultz and L. Pettus, *J. Org. Chem.*, 1997, **62**, 6855-6861.
11. B. Danieli, G. Lesma, D. Passarella, A. Sacchetti and Alessandra Silvani, *Tetrahedron Lett.*, 2001, **42**, 7237-7240.
12. D. Din Belle, A. Tolvanen and M. Lounasmaa, *Tetrahedron*, 1996, **52**, 11361-11378.
13. SAINT (Version 7.60a), Bruker AXS Inc., Madison, WI, USA, 2006.
14. G. M. Sheldrick, SHELXS-97, SHELXL-2014 and SADABS version 2.05, University of Göttingen, Germany, 1997.
15. (a) L. J. Barbour, *J. Supramol. Chem.*, 2001, **1**, 189-191; (b) J. L. Atwood and L. J. Barbour, *Cryst. Growth Des*., 2003, **3**, 3-8.
16. Gaussian 16 (Revision B.01), Gaussian Inc., Wallingford, CT, 2016.
17. N. M. O'Boyle, T. Vandermeersch, C. J. Flynn, A. R. Maguire and G. R. Hutchison, *J. Cheminf.*, 2011, **3**, 1-9.
18. N. M. O'Boyle, M. Banck, C. A. James, C. Morley, T. Vandermeersch and G. R. Hutchison, *J. Cheminf.*, 2011, **3**, 1-14.

19. T. A. Halgren, *J. Comput. Chem.*, 1996, **17**, 490-519.

20. J. Tao, J. P. Perdew, V. N. Staroverov and G. E. Scuseria, *Phys. Rev. Lett.*, 2003, **91**, 146401.

21. F. Weigend and R. Ahlrichs, *Phys. Chem. Chem. Phys.*, 2005, **7**, 3297-3305.

22. (a) S. Grimme, J. Antony, S. Ehrlich and H. Krieg, *J. Chem. Phys.*, 2010, **132**, 154104; (b) S. Grimme, S. Ehrlich and L. Goerigk, *J. Comput. Chem.*, 2011, **32**, 1456-1465.

23. A. V. Marenich, C. J. Cramer and D. G. Truhlar, *J. Phys. Chem. B*, 2009, **113**, 6378-6396.

24. Y. Zhao and D. G. Truhlar, *J. Phys. Chem. A*, 2005, **109**, 5656-5667.